University of Alberta
Department of Civil Engineering

Structural Engineering Report No. 53

Web Slenderness Limits for Non-Compact Beam-Columns

by

D.S. Nash

and

G.L. Kulak

March, 1976

WEB SLENDERNESS LIMITS FOR NON-COMPACT BEAM-COLUMNS

by

D. S. NASH

and

G. L. KULAK

DEPARTMENT OF CIVIL ENGINEERING

THE UNIVERSITY OF ALBERTA

EDMONTON, ALBERTA

MARCH, 1976

ABSTRACT

This investigation was established in an attempt to determine more rational web slenderness limitations for non-compact beam-columns. The present limits, as set forth in the CSA S16.1 and S16.2 Standards, distinguish between compact and non-compact cross-sections only in the range of beam-column design of $0 \leq P/Py \leq 0.15$. This results in a limit which is too conservative, as non-compact sections are not required to deform to the same extent as compact sections.

The results of six beam-column tests, along with the test results from another investigation on non-compact beams are presented. Utilizing these results, this study indicates a safe limit to which the web slenderness limitation for non-compact beam-columns may be raised.

ACKNOWLEDGEMENTS

This study was carried out in the Department of Civil Engineering at the University of Alberta. It was conducted with the financial assistance of the Canadian Steel Industries Construction Council.

The authors wish to express their thanks also to the technical staff of the Department of Civil Engineering for their assistance during the testing program.

TABLE OF CONTENTS

CHAPTER I

INTRODUCTION

1.1 General

According to the Canadian Standards Association Specification S16-1969[1], members subjected to combined axial load and bending moment (beam-columns), are classified as either non-compact, compact, or suitable for plastic design. The web and flange slenderness limitations set forth have been chosen so that a non-compact section can just reach the yield moment, a compact section can just reach the plastic moment, and a section suitable for plastic design can both reach the plastic moment and undergo sufficient rotation so that the moments can be redistributed before local buckling occurs. These requirements are shown in Figure 1.1.

It has been well established that the critical buckling stress of a plate loaded in uniform edge compression is a function of its width-to-thickness ratio[2],

$$\sigma_{cr} = \frac{K \pi^2 E}{12 (1 - \nu^2) (h/w)^2}$$

It follows, therefore, that the flange and web plate components of a beam or a beam-column must become progressively stockier in order that buckling be precluded as the

deformation demands on the cross-section increase. Thus, in order to prevent the possibility of local buckling, the limiting flange and web slenderness ratios must be decreased for a given grade of steel as the member classification goes from non-compact to compact to plastic design.

Deformation requirements increase also as the yield strength of the material increases. More member deformation is required to develop the higher critical buckling stress. As a result, the critical plate slenderness ratios for higher strength steels must be less than those for lower strength steels. The present CSA requirements take this into account (Figures 1.2 and 1.3).

1.2 Definition of the Problem

The CSA S16-1969 Standard used one set of critical web slenderness limitations for all three classifications: non-compact, compact, and suitable for plastic design. The only difference in design is that non-compact sections involve a factor of safety against reaching the yield moment (reduced for axial load) and the compact and suitable for plastic design sections involve a factor of safety against reaching the plastic moment (reduced for axial load). If the stipulated web slenderness limitation is satisfactory for plastically designed members, then it must be conservative for compact members, and even more conservative for

non-compact members where the deformation and strength requirements are less severe.

According to the web slenderness limits in CSA S16-1969, for values of P/Py (ratio of actual load to yield load) less than 0.28, the critical web slenderness ratio for a beam-column is linearly reduced as the applied axial load increases. For all values of P/Py greater than or equal to 0.28, the critical web slenderness ratio is constant for a given grade of steel. This is illustrated in Figure 1.3.

Both the CSA S16-1969 Standard and the American Institute of Steel Construction Specification[3] have based their web slenderness limitations primarily on a series of tests conducted by Haaijer[4] in 1956 on stub columns and short beam specimens of ASTM-A7 steel. In only three of the tests was failure associated with web buckling, and each of these occurred in the stub column (pure compresion) tests.

Recently, Perlynn and Kulak[5] have shown that a substantial relaxation of the web slenderness requirements can safely be implemented for compact beam-columns, and their recommendations for both non-compact and compact beam-columns have been introduced into the CSA Standard S16.1[6] on limit states design and S16.2[7] on working stress design (Figure 1.3).

1.3 Objectives of the Research Proposal

The objectives of this investigation are threefold:

1. To examine the present and proposed web slenderness limitations for non-compact beam-columns by means of a suitable testing program,
2. To examine existing theories, and to develop, if necessary, additional theories to describe the behaviour of web plate buckling under combined axial load and bending,
3. To suggest revisions for the web slenderness limitations for non-compact beam-columns, if appropriate.

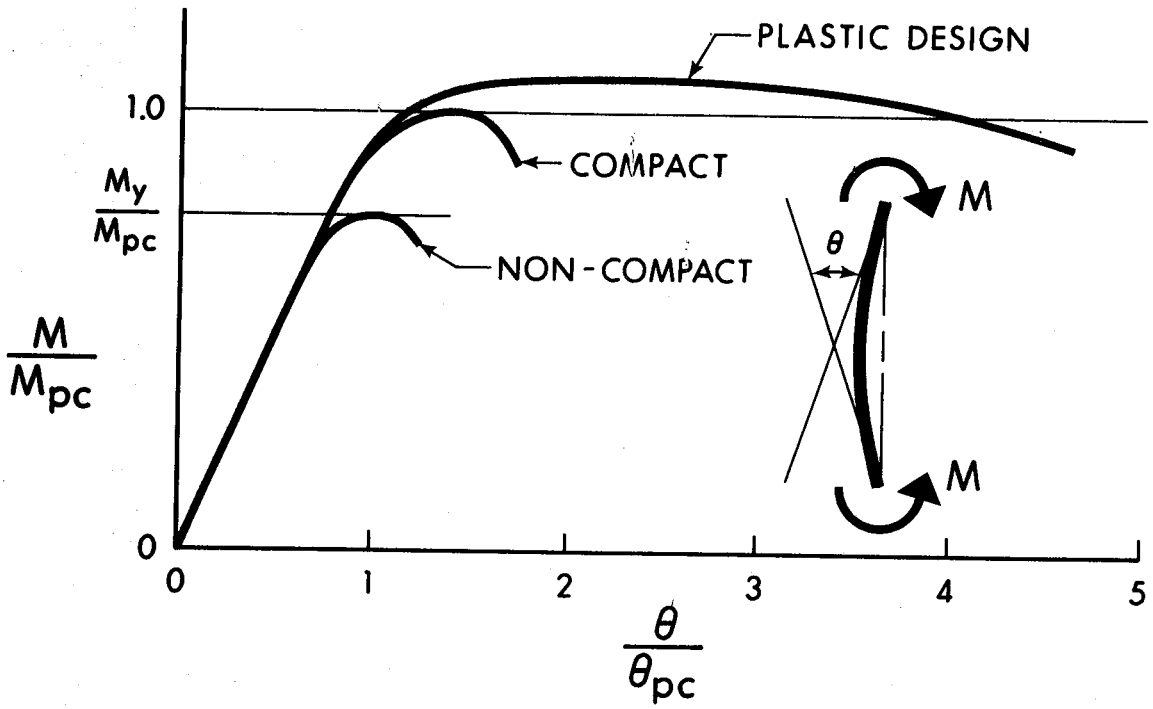

FIGURE 1.1

MOMENT-ROTATION BEHAVIOUR OF BEAM-COLUMNS

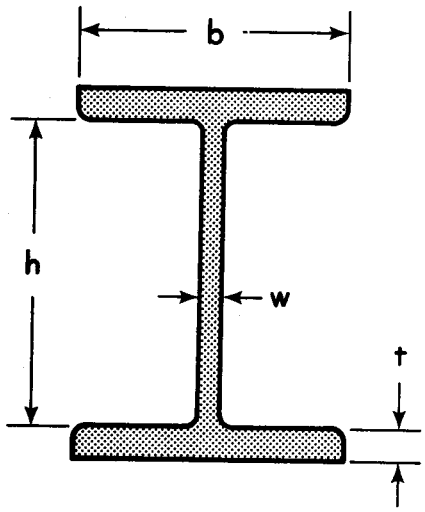

NON-COMPACT $\frac{b}{2t} \leq \frac{100}{\sqrt{F_y}}$

COMPACT $\frac{b}{2t} \leq \frac{64}{\sqrt{F_y}}$

PLASTIC DESIGN $\frac{b}{2t} \leq \frac{54}{\sqrt{F_y}}$

FIGURE 1.2

PRESENT CSA S16-1969 FLANGE SLENDERNESS REQUIREMENTS

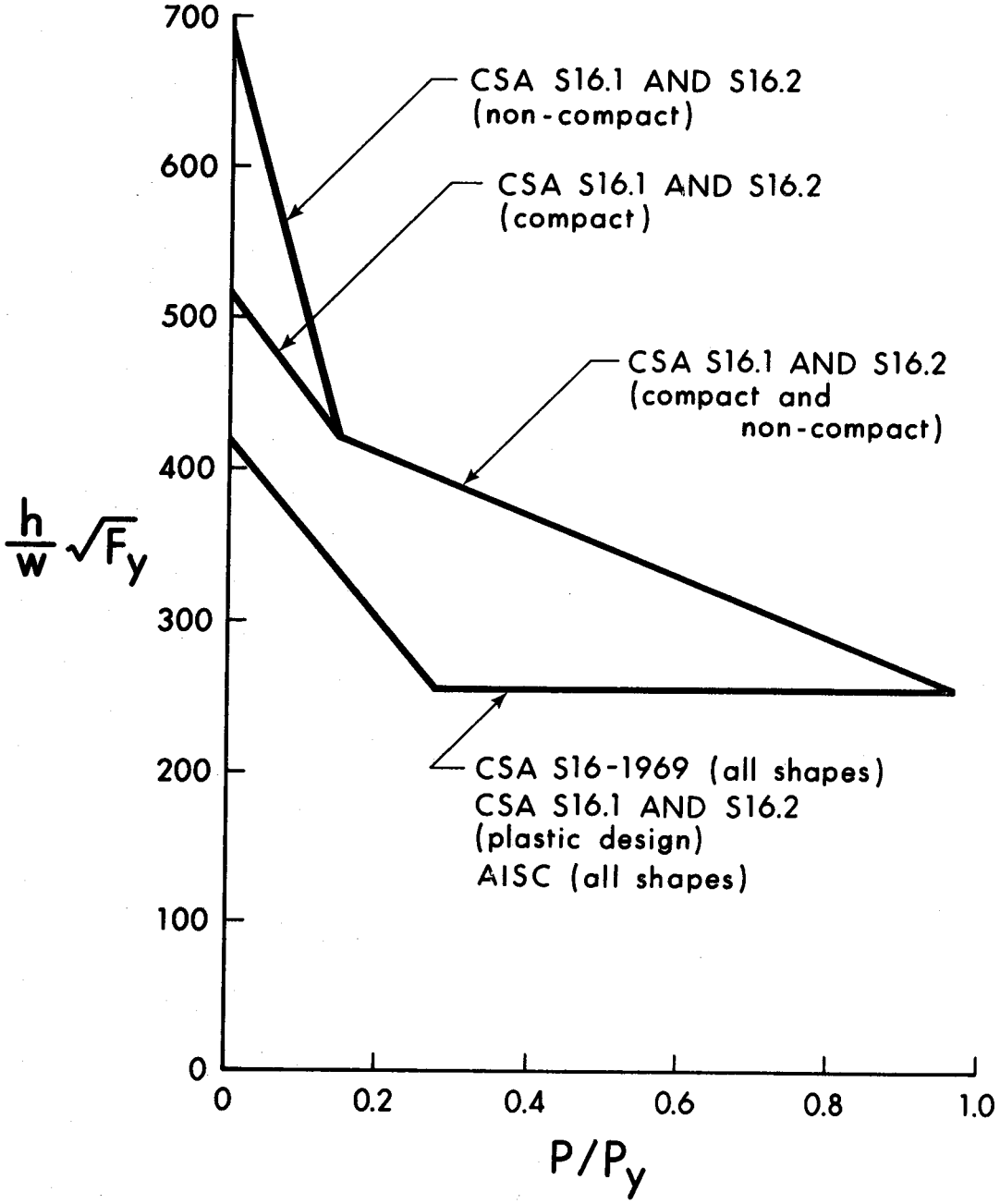

FIGURE 1.3

PRESENT WEB SLENDERNESS REQUIREMENTS

CHAPTER II

LITERATURE SURVEY

2.1 Previous Investigations

Comparatively only a small amount of research has been conducted into the problem of web buckling in beam-columns. Although buckling problems in general have been investigated over a long period of time, and plate buckling problems for the past half-century, it is only relatively recently that web buckling problems have been examined.

From the following fourth-order partial differential equation

$$\frac{\partial^4 u}{\partial x^4} + 2\frac{\partial^4 u}{\partial x^2 \partial y^2} + \frac{\partial^4 u}{\partial y^4} = -\frac{w}{D}\sigma_x \frac{\partial^2 u}{\partial x^2} \qquad (2.1)$$

Timoshenko[2] derived the solution for the critical buckling stress in an isotropic simply-supported flat rectangular plate acting elastically under uniform edge loading in the longitudinal direction as

$$\sigma_{cr} = \frac{K \pi^2 E}{12 (1 - \nu^2) (h/w)^2} \qquad (2.2)$$

where: σ_{cr} = elastic critical buckling stress,

E = Young's modulus,

ν = Poisson's ratio,

h = width of plate,

w = thickness of plate,

$D = EI/(1-\nu^2)$,

K = plate buckling coefficient.

The plate buckling coefficient, "K", was introduced into the equation to account for various ratios of length to width (the aspect ratio). Timoshenko showed that the minimum critical buckling stress for a plate simply-supported on all four sides could be found using $K = 4.0$ in Equation 2.2. This he showed to be valid for all length-to-width ratios.

This major development by Timoshenko opened the field of plate buckling to investigation by others. Of the many plate buckling models developed, some are concerned with plates subjected to loading conditions similar to those for web plates in a wide-flange member. The work by Haaijer[4] and by Haaijer and Thurlimann[8] is of particular interest and is discussed below.

2.2 Development of the CSA S16-1969 Code Requirements

It was not until 1956 that a specific study into inelastic plate buckling was carried out[4]. Prior to this it was generally accepted that when the yield stress of the material was reached, the element (column or plate) would buckle[8]. Haaijer[4] investigated both flange and web plate buckling, accounting for both the inelastic behaviour of the material and the restraint against rotation provided at the web-to-flange junction. Good correlation was found to exist between Haaijer's web buckling theory and the results of his pure bending and pure compression tests on ASTM-A7 steel (σ_y=33ksi) wide-flange shapes. Some of the pure compression tests established that both web and flange plates were capable of reaching strain-hardening before the occurrence of buckling. Haaijer did not, however, consider the effects of residual stresses or the combined loading of in-plane bending and axial compression on web plates.

In 1958, Haaijer and Thurlimann[8] proposed a plate buckling relationship (Figure 2.1) which included an empirical transition curve for the inelastic range between the proportional limit and the point of strain-hardening. For prediction of web buckling, they also developed a web plate buckling equation based on Timoshenko's elastic plate buckling equation (Equation 2.2) for combined axial compression and in-plane bending. The result was an expression:

$$\alpha = \frac{h}{\pi w}\sqrt{\frac{12\ \sigma_y\ (1 - \nu^2)}{K\ E}} \qquad (2.3)$$

where: α = plate buckling modulus,

$\frac{1}{\alpha^2} = \frac{\sigma_{cr}}{\sigma_y}$

σ_{cr}= elastic critical buckling stress,

σ_y = yield strength of the material,

K = plate buckling coefficient for a fully-plastified wide-flange section.

They used this modified "K", the plate buckling coefficient, to account for inelastic plate behaviour, and showed that this procedure adequately described their three test results of failure due to web buckling in stub columns.

For a member that may be required to deform plastically, the following assumptions were made to develop a web buckling curve for design purposes:

1. A/Aw=2.0 (ratio of total area of wide-flange section to total area of web)

2. $h_t/h=1.05$ (ratio of total depth of wide-flange to clear depth of web)

3. $\varepsilon_m/\varepsilon_y=4.0$ (ratio of maximum strain in compression flange to yield strain)

Using these assumptions (taken as valid for an average wide-flange section), it followed that the neutral axis in a beam-column subjected to Mpc (plastic moment reduced for axial load) and P/Py=0.28, would have just reached the tension flange. Thus the whole web would be in compression, but not necessarily in uniform compression.

A theoretical design curve was first established, then approximated by two straight lines. The design curve has since been modified to make the web slenderness limitations applicable to steels of various yield strengths, and it is this representation that forms the basis for all cross-sections in the AISC Specification and CSA S16-1969 as well as for plastic design sections in CSA S16.1 and S16.2. Figure 1.3 shows this limit.

It should be noted that no tests on specimens subjected to combined axial load and bending were done by Haaijer and Thurlimann, hence the theory was not experimentally verified for this mode of loading.

2.3 Recent Code Revisions

Perlynn and Kulak[5] conducted tests on nine beam-column specimens under different combinations of axial load and moment, and showed that the previously-used web slenderness limitations[1,3] for compact beam-columns were too conservative. For their tests, they chose flanges which just met the S16-1969 requirements for compact flanges (Figure 1.2). By testing specimens with this flange proportion, it was known that if the flange buckled, the web was too stocky to be on the limit of web slenderness for a compact section. Similarly, if the web buckled, it was too slender. By testing more than one specimen at each value of P/Py, they were able to determine quite closely the limit where simultaneous flange and web buckling would occur. This limit would then be the maximum web slenderness a compact beam-column should have in order to guarantee that web buckling will not occur before flange buckling.

Perlynn and Kulak, however, were not able to satisfactorily correlate their results with Haaijer and Thurlimann's web buckling theory. Consequently, they developed two methods for predicting web buckling. In these, the effects of residual stresses were included. Comparison between their methods and the results from three other testing programs (including Haaijer's) showed both methods capable of giving valid predictions of the occurrence of web buckling.

Using the limit of simultaneous web and flange failure which they established experimentally, Perlynn and Kulak developed a theoretical limit for maximum web slenderness ratios as a function of P/Py for compact beam-columns. The equation for the curve is:

$$\frac{h}{w}\sqrt{Fy} = 520\ \sqrt{1 - 0.695(P/Py)^{0.3846}} \qquad (2.4)$$

where: P = axial load,

Py= yield load of section,

Fy= yield stress of material,

h = clear web height,

w = web thickness.

This theoretical limit was then approximated for design purposes by a bi-linear expression:

(a) For $P/Py \leq 0.15$

$$\frac{h}{w}\sqrt{Fy} = 520\ [1 - 1.28(P/Py)]$$

(b) For $P/Py > 0.15$

$$\frac{h}{w}\sqrt{Fy} = 450\ [1 - 0.43(P/Py)]$$

These expressions have been incorporated into the CSA Standard S16.1 on limit states design and S16.2 on working stress design. Using the results of a testing program of non-compact beams[9], Perlynn and Kulak have also recommended the following bi-linear approximation to be used for the design of non-compact beam-columns:

(a) For $P/Py \leq 0.15$

$$\frac{h}{w}\sqrt{Fy} = 690\,[1 - 2.60(P/Py)]$$

(b) For $P/Py > 0.15$

$$\frac{h}{w}\sqrt{Fy} = 450\,[1 - 0.43(P/Py)]$$

where $\frac{h}{w}\sqrt{Fy} = 690$ was found to be a reasonable web slenderness limit for non-compact beams. This bi-linear approximation is different from that for compact beam-columns only in the region $0 \leq P/Py \leq 0.15$. It was felt that since non-compact beam-columns do not have to undergo the same degree of deformation as compact beam-columns, a safe approximation would be to linearly reduce the slenderness limit from $\frac{h}{w}\sqrt{Fy} = 690$ at $P/Py = 0$ to the junction of the linear approximations for compact members at $P/Py = 0.15$. For $P/Py \geq 0.15$, the web slenderness limitation for non-compact members was set at the same value as those for compact members pending a study into the possible limit to

which the web slenderness of non-compact beam-columns may be raised. Figure 1.3 illustrates this approximation.

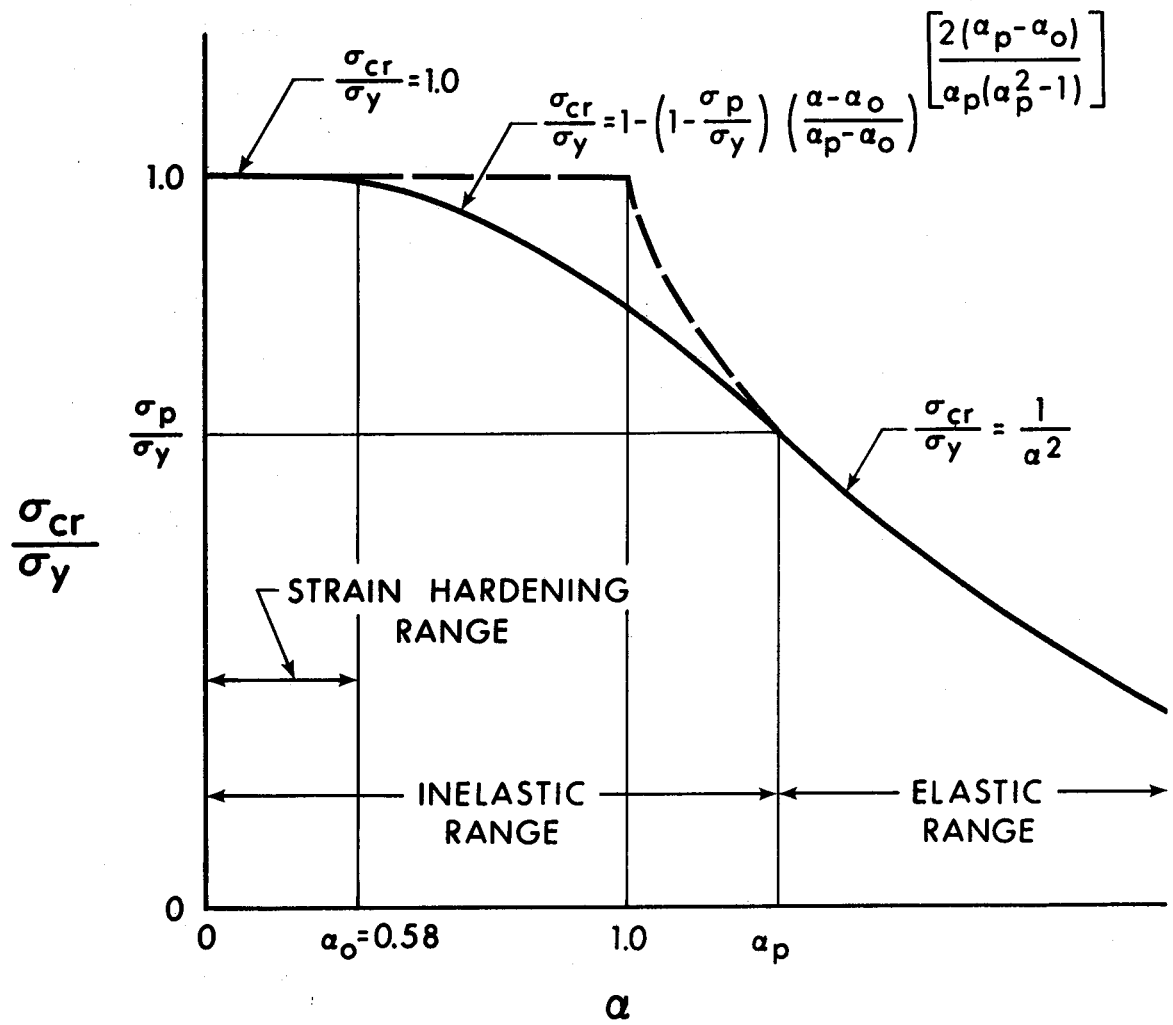

FIGURE 2.1

HAAIJER AND THURLIMANN'S INELASTIC PLATE BUCKLING CURVE

CHAPTER III

EXPERIMENTAL PROGRAM

3.1 Scope

For the purpose of examining the present non-compact web slenderness limitations (Figure 1.3), a total of six wide-flange specimens subjected to combined axial load and moment were tested. A flange shape common to all the specimens was established that just met the non-compact limitation of the CSA Standard S16 (i.e., $b/2t = 100/\sqrt{Fy}$). The webs of all the specimens were more slender than that allowed by the present CSA Standards[6, 7] for non-compact members. The web depth (h) of the specimen was varied to produce the different web slenderness ratios desired (Table 3.1). For the six specimens tested, all had similar cross-sectional shapes with webs of the same thickness (Figure 3.1).

Tests were conducted at P/Py ratios of 0.15, 0.3, and 0.7 in order to obtain results representative of a wide range of beam-column design. Two tests were conducted at each ratio of P/Py. The location of the test specimens relative to the various currently-used web slenderness limits is indicated in Figure 3.2 and their design is discussed in Appendix I.

It was hoped that observation of the failure modes of the specimens would help to determine the web slenderness limit at which simultaneous web and flange buckling would occur. This limit would then be the maximum web slenderness that a non-compact beam-column could have in order to preclude local web buckling as the mode of member failure for loads up to the yield moment (reduced for axial load).

3.2 Specimen Description

The specimens were tested while simply-supported at their ends and with the moment applied by means of a concentrated load (P_2) placed eccentrically (Figure 3.3). A second axial load (P_1) was applied in such a way as to uniformly load the specimen over its cross-section. Thus the total axial load (P) acting on the specimen was the sum of the two individual loads and the applied moment (M) was the product of the eccentric load (P_2) and its eccentricity (e) from the centreline of the specimen. Because of the manner in which the concentrated loads were applied, the beam-column was essentially subjected to uniform compression and constant moment throughout its length, without the presence of shear. It was, therefore, theoretically possible that buckling could occur at any point along the length of the specimen. If the strong-axis deflections became significant during testing, however, the axial load acting

through the deflection might increase the moment at mid-height enough to initiate buckling at this location.

The moment produced by the eccentrically placed concentrated load was transmitted to the beam-column specimen by means of reusable arms fabricated from back-to-back channels and cover plates. These arms were bolted to the cap plates at the ends of the specimens (Figure 3.3). It was felt that the connection would be stronger than the specimen, and buckling would not occur at either end of the specimen because of the presence of the cap plate. The arms were designed to withstand the maximum moment (Specimen 1), and the maximum load P (Specimen 5). They were checked against premature failure in bending, shear, and web crippling. It was considered that potential lateral-torsional buckling of the specimen, and lateral buckling of the moment arms would be resisted because the eccentric load would be acting against any deflections caused by twisting of the specimen or moment arms.

The webs of the specimens were fabricated from 1/4 inch thick CSA G40.21 Grade 44W steel plate[10]. The flanges and webs had been designed on the basis of a yield stress of 44 ksi, the nominal yield stress of G40.21 Grade 44W steel plate less than 1-1/2 in. thick. Because of supply difficulties, the flanges were made from a particular piece of ASTM A36[11] plate that had a yield point approximately equal to that specified for G40.21 Grade 44W, that is,

44ksi. The flanges of all the beam-column specimens had dimensions of 5/16in. by 9-1/2in., and all were fabricated from the same mill rolling in an effort to have constant material properties. These flange dimensions give a width-to-thickness ratio of 15.20, comparable to the non-compact limitation of 15.08 as established by the CSA Standard S16 for 44 ksi yield strength steel. It was also specified that the individual web plates be all taken from the same piece.

The clear length of the beam-column was established at 45 inches. This length provided adequate room for the placement of gauges and recording equipment and also provided sufficient span over which the local buckling could occur without being restricted by the boundary effects at the ends. However, the length was short enough to prevent premature overall member buckling about the strong axis during testing.

To prevent member buckling about the weak axis, lateral bracing was provided for the tension and compression flanges of each of the beam-columns. A bracing arrangement based upon Watt's straight line mechanism[12] was attached by threaded pins welded at mid-height to the centreline of the flanges. This produced a short beam in the weak axis direction which met the bracing requirements for plastic design.

Although the lateral bracing prevented movement perpendicular to the weak axis, no other movement was restricted. The beam-column was, however, torsionally restrained at its mid-height by the manner in which the braces were attached. The bracing did not interfere with lateral movements perpendicular to the weak axis, nor did it interfere significantly with the local buckling of the flanges and webs. Since the beam-column itself was torsionally stable, the torsional restraint offered by the bracing system was not expected to affect the test results. Perlynn and Kulak did note, however, with their similar testing arrangement, that because the threaded pins were welded at the mid-height of the specimen in the middle of the flange, the local buckle did not occur there[5].

The proportions of the beam-column test specimens, as received, are shown in Table 3.1.

3.3 Test Arrangement

The concentric concentrated load (P_1) was applied using an MTS (Material Testing System 908.14) testing machine, capable of applying 1400 kips in compression (Figure 3.4). The magnitudes of the concentric load were measured from an electronic transducer connected to an oil pressure line located within the compression head of the testing machine. The accuracy of this system of measurement

is considered to be ±0.5%.

The eccentric load (P_2) was applied using a hydraulic centrehole jack rated at 120 kips maximum capacity (Figure 3.5). A 1-1/8 in. diameter high-strength steel rod, threaded at the ends was passed upward through the upper arm and the centrehole jack and downward through the lower arm and a load cell capable of measuring up to 100 kips. With the centrehole jack applying a tensile load to the rod, the resulting reactions tended to pull the arms towards each other.

Steel rockers were provided at reaction points of the concentric load (i.e., at the top and bottom of the specimen). These seven inch radius rockers acted as simple supports. Rockers 1-1/2 in. thick and with a radius of curvature of 4-1/2 in. were provided at the reaction points of the eccentric load. These were drilled to provide passage of the tension rod.

As a result of the precautions taken as to the physical assembly, no overall instability problems of the setup were encountered during the testing program.

Rotations of the specimen were recorded by means of an apparatus consisting of two light channel sections securely clamped to small plates welded to the cap plates at the top and bottom of the specimen, where the specimen was bolted to the moment arms. Three rod-and-plunger type trans-

ducers were placed between the channel sections. Two of these were mounted at 21 inches and 42 inches respectively from the centreline of the beam-column. From the readings of these two transducers, an average rotation could be determined. The third transducer was mounted coincident with the beam-column centreline and recorded the axial shortening due to the loads. This was applied as a correction to determine the actual rotations.

Out-of-plane web and compression flange deflections were measured using a device which was originally developed to measure the depth of a stream bed in a hydraulics testing flume. This apparatus was modified so it would measure semi-automatically a series of web deflections on a predetermined grid size. This was done by means of a motorized trolley running along the tension flange which moved a depth-measuring probe over the flange and web of the specimen. The probe itself operates on optical principles and nothing physically touches the surface being monitored. This device is illustrated in Figure 3.6 in position to measure one vertical line of web deflections. It is also shown in Figure 3.7 in position to measure the compression flange deflections which were taken about 1/2 in. from the outer edge of the flange. The accuracy of the readings taken by this device was considered to be about ±0.002 inch. The apparatus is discussed in greater detail in Appendix II.

The strong axis deflections of the specimen were measured by six rod-and-plunger type transducers (Figure 3.5). Five of these were connected at approximately equal increments along the 45 inch length of the specimen. Because the bottom rocker support, unlike the top one, tended to travel as it rotated, the sixth transducer was mounted so as to monitor its translation. These readings were taken in case the buckle appeared at mid-height of the specimen, so that P-Δ effects could be incorporated into the analysis.

The strain distribution at the mid-height of the specimen was measured by means of a set of fourteen electric resistance strain gauges placed at the mid-height of the specimen. Four of these were placed on the inside face of the flanges, 1-3/4 in. from the flange edges. The remaining ten gauges were placed on the web, four 1-1/4 in. from the inside flange faces, and six at the three locations that divide the web into four equal increments. At each of the web locations, one gauge was placed on either side of the web in order to obtain an average reading. If web buckling was occurring at this location, (i.e., at the mid-height of the specimen) it would be noticed before any visual observation because of the marked increase in difference between the two strain readings. The four gauges closest to the inside flange faces were placed near the two positions along the web where the assumed residual strain distribution was zero.

All measurements were recorded on a Data General Nova 2 minicomputer serving as a data acquisition device. The minicomputer made it possible to take many readings effortlessly, and hence very comprehensive web and flange deflection readings were taken during the tests.

Prior to testing, each specimen was whitewashed on the side not used for deflection measurements in order to aid in the observation of yield patterns. The other surfaces were painted flat white to enable the optical deflection apparatus to operate properly.

3.4 Testing Procedure

Although the top and bottom ends of the specimen were to be prepared square and true, imperfections were considered inevitable. As a result, before a specimen could be tested, it had to be aligned[13]. The specimen was first centered between the head of the testing machine and the floor roller. Alignment was then accomplished by loading the specimen concentrically to 4 kips, and then to 50 kips with the testing machine, and reading the four strain gauges mounted near the flange tips for each load. Care was taken not to exceed the proportional limit of the material and cause premature yielding. The minicomputer was programmed to calculate the net eccentricities in the two directions of the horizontal plane for each of the testing machine loads.

The specimen was then unloaded, and shims were placed between the head of the testing machine and the top of the specimen and the process repeated such that the eccentricities were reduced to less than 0.25 in. from the specimen cross-sectional centroid in both directions.

Once the specimen had been aligned, the concentric load was reduced to 4 kips to hold the specimen in position and all initial readings were taken.

To begin testing, the concentric load was applied in increments of approximately one-fifth of the total axial load P, with some readings taken after each increment. Upon reaching the total axial load P, moment application was started. Because the moment was applied by means of the eccentric load, an increase in moment was accompanied by an increase in eccentric load. To keep the total axial load constant, it was necessary to reduce the axial load applied by the testing machine by the same amount as the eccentric load was increased. The net effect was to apply moment to the specimen while the axial load remained constant. No attempt was made to lower the MTS load and increase the eccentric load simultaneously. This was not expected to affect the test results.

After each increment, and while holding the loads constant, all deformations were allowed to stabilize before a set of readings was taken. When failure was imminent,

however, it became difficult to maintain the eccentric load at the value desired. Hence it was allowed to drop off, and when the readings were stable, they were recorded. The maximum drop in a particular test was typically 2% of the maximum eccentric load, and hence was not expected to affect the readings significantly.

Strain gauge, rotation meter, strong-axis deflection readings, and the load readings were taken every load increment. Web and flange deflection readings were taken at intervals depending upon the slope of the moment-rotation curve and the amount of load present at that increment. These readings were taken at least every third increment, and as failure was pending, they were taken more often. Throughout the test the behaviour of the specimen was monitored by plotting the moment-rotation relationship.

Prior to the start of the beam-column tests, two series of standard coupon tests were conducted to determine the material behaviour and strength. Eight coupon tests were performed on the flange plate material, and six were performed on the web plate material. These were done on pieces of plate supplied by the specimen fabricator and taken from the same rollings as the web and flange materials.

SPECIMEN	P/Py	h (inches)	(h/w) $\sqrt{Fy}$
1	0.15	24.01	639.4
2	0.15	20.06	534.2
3	0.30	22.18	590.7
4	0.30	18.33	488.2
5	0.70	18.82	501.2
6	0.70	15.06	401.1

TABLE 3.1

PROPORTIONS OF TEST SPECIMENS

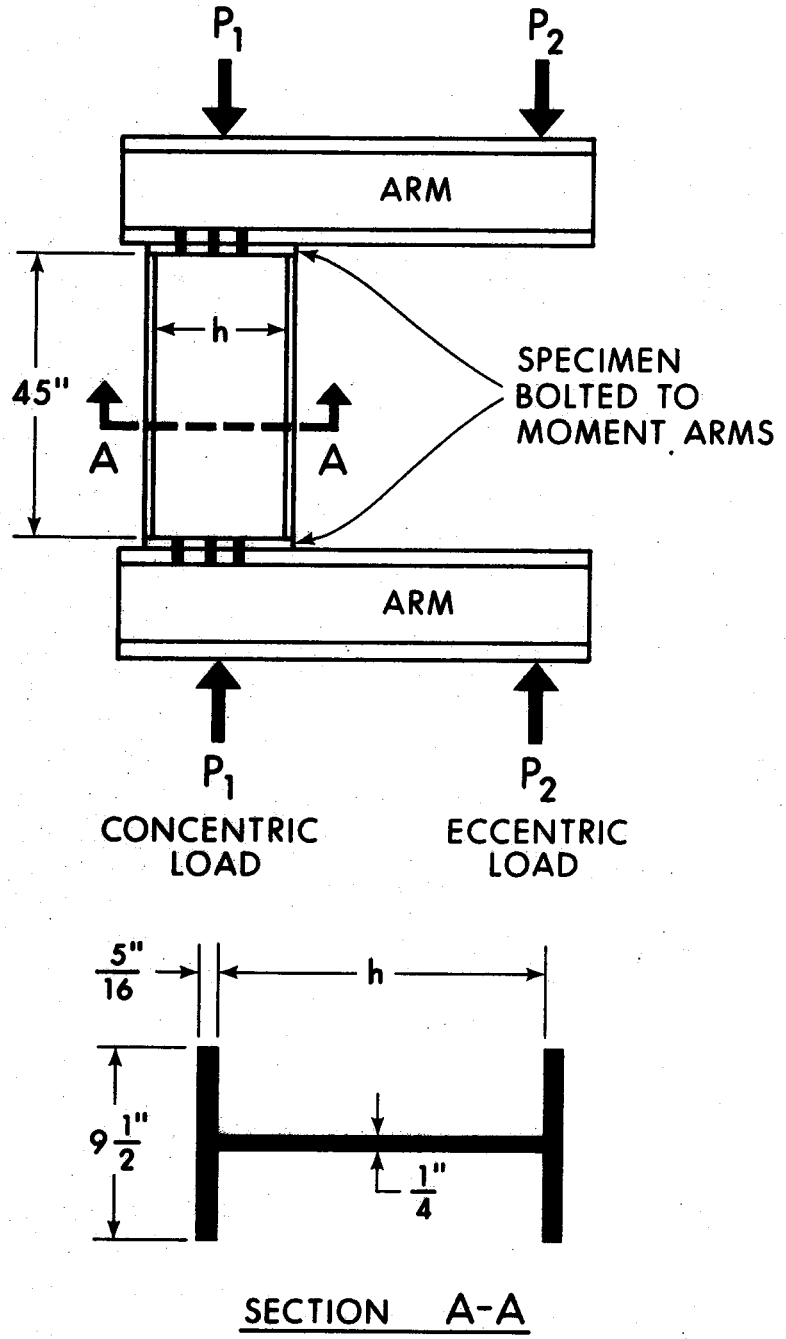

FIGURE 3.1

DETAILS OF BEAM-COLUMN TEST SPECIMENS

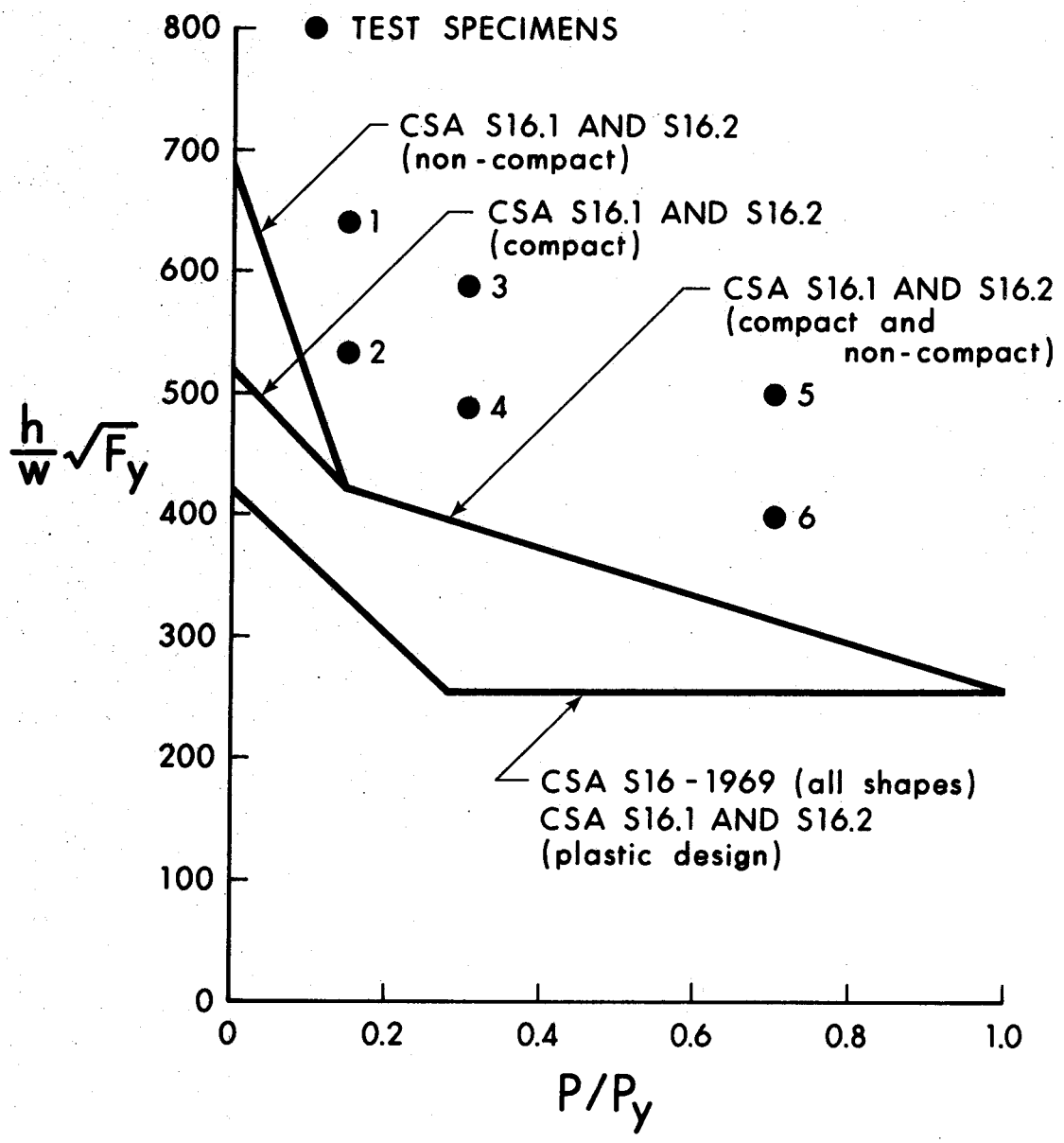

FIGURE 3.2

THE VARIOUS CURRENTLY-USED WEB SLENDERNESS LIMITATIONS AND THE TEST SPECIMENS

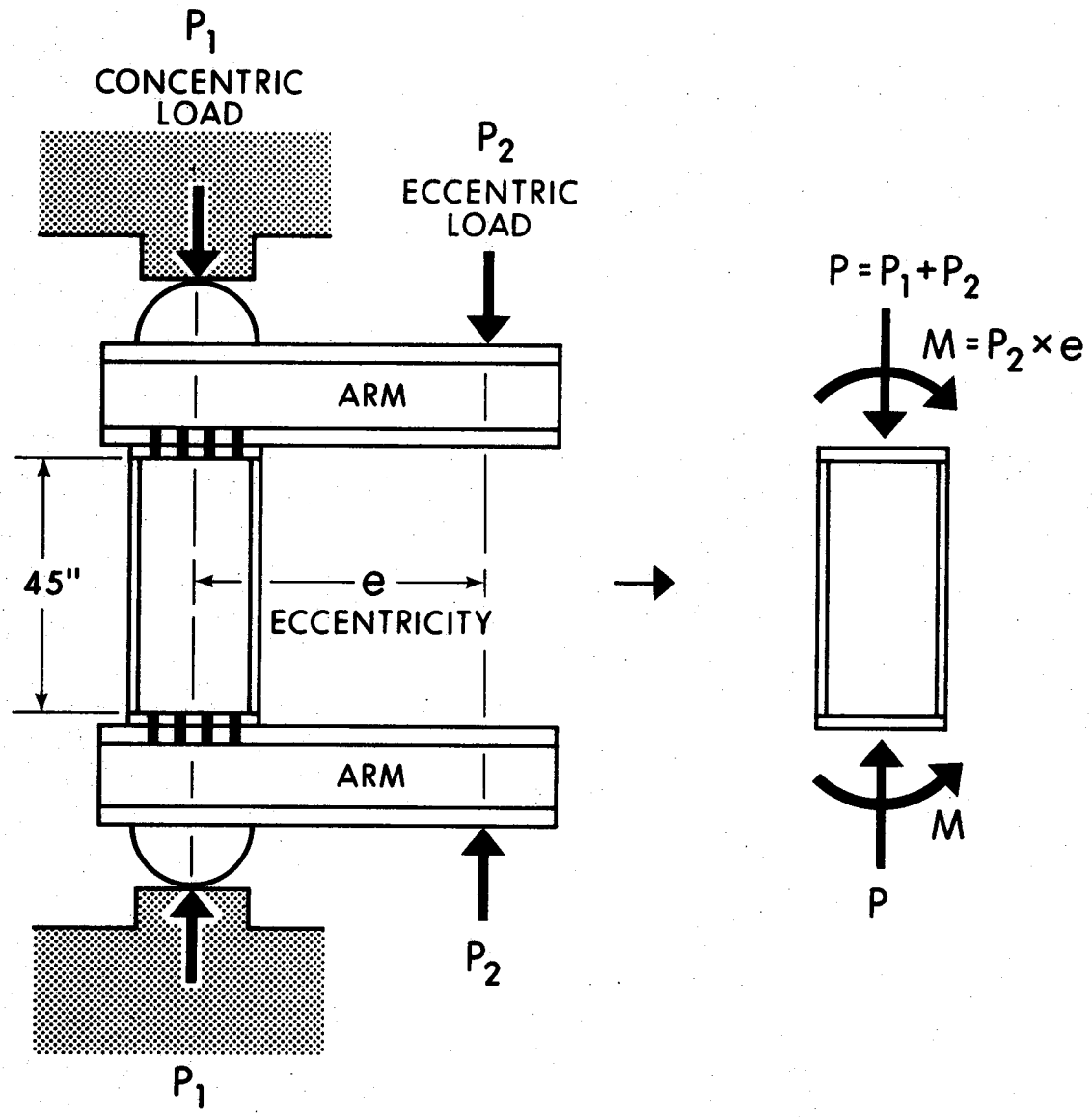

FIGURE 3.3

IDEALIZED TEST SETUP

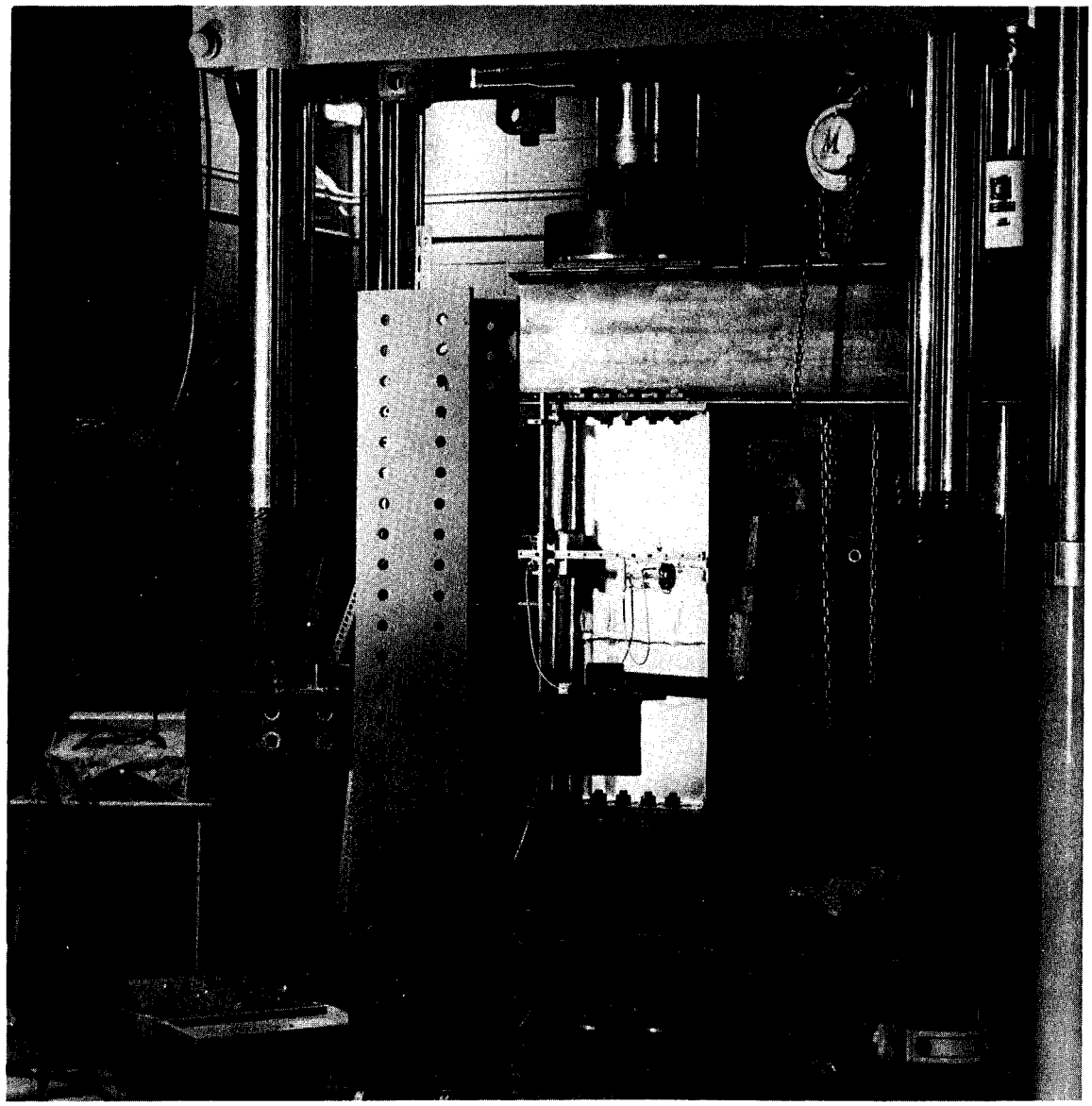

FIGURE 3.4

TEST SETUP

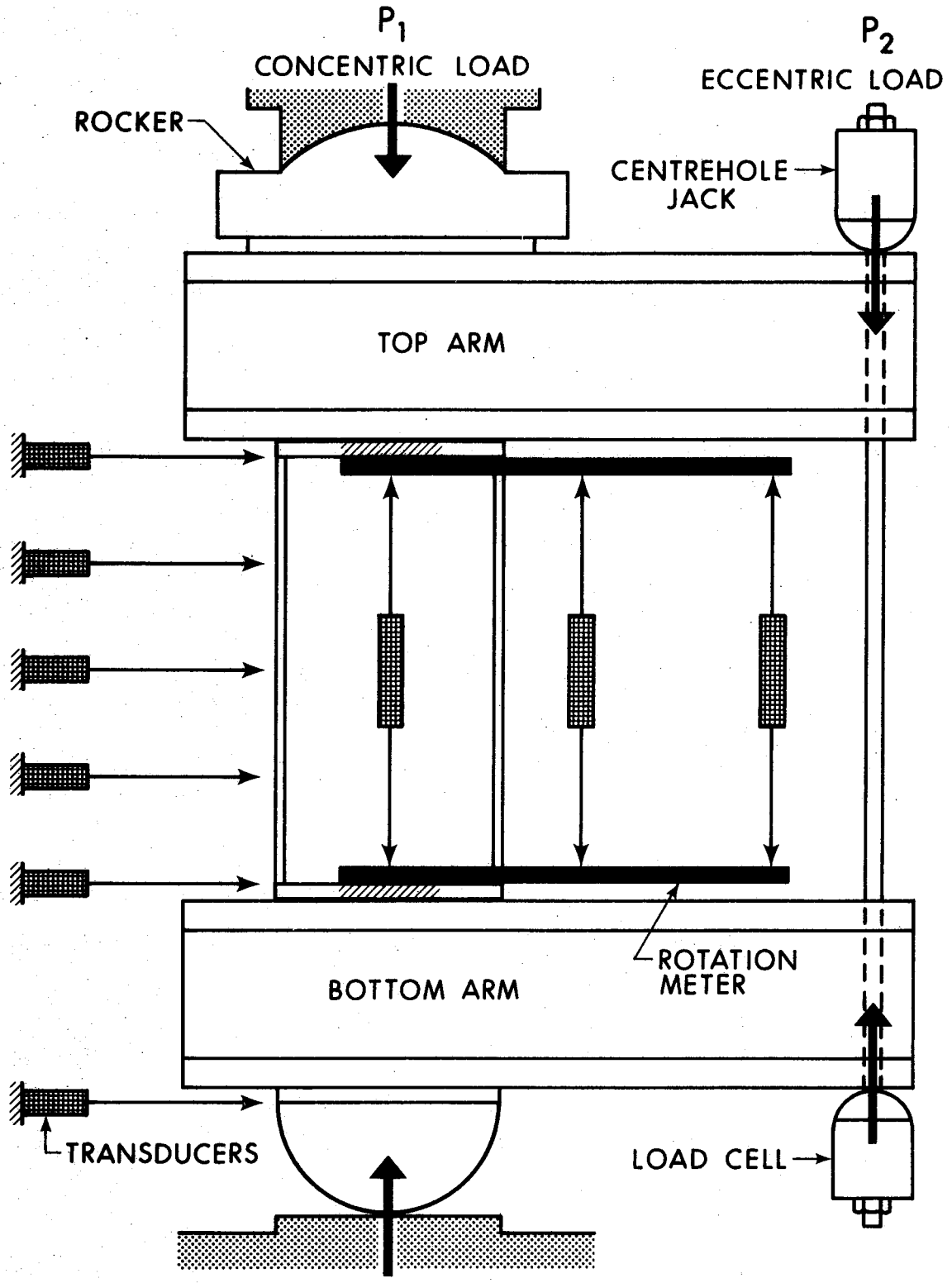

FIGURE 3.5

INSTRUMENTATION

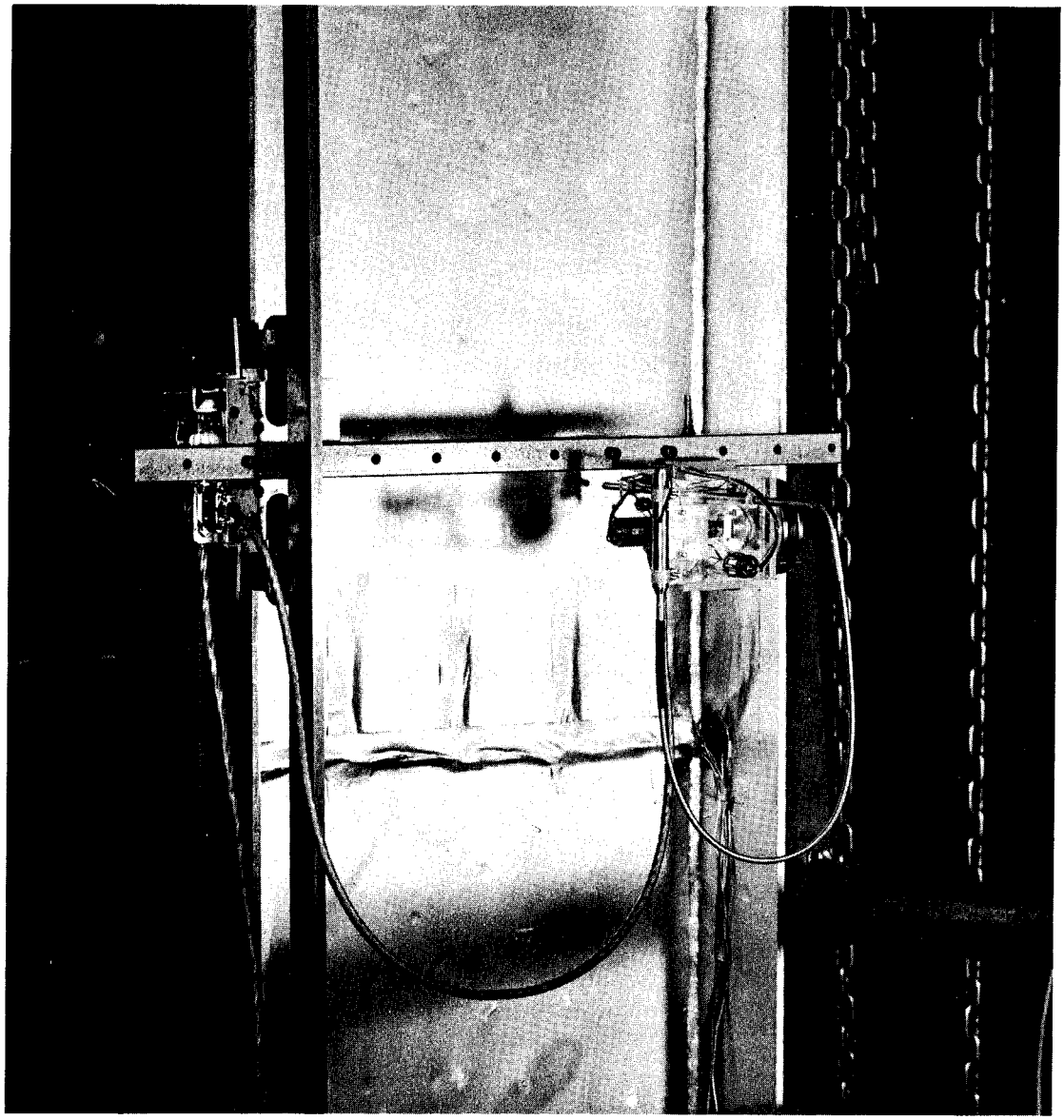

FIGURE 3.6

DEFLECTION DEVICE MEASURING WEB

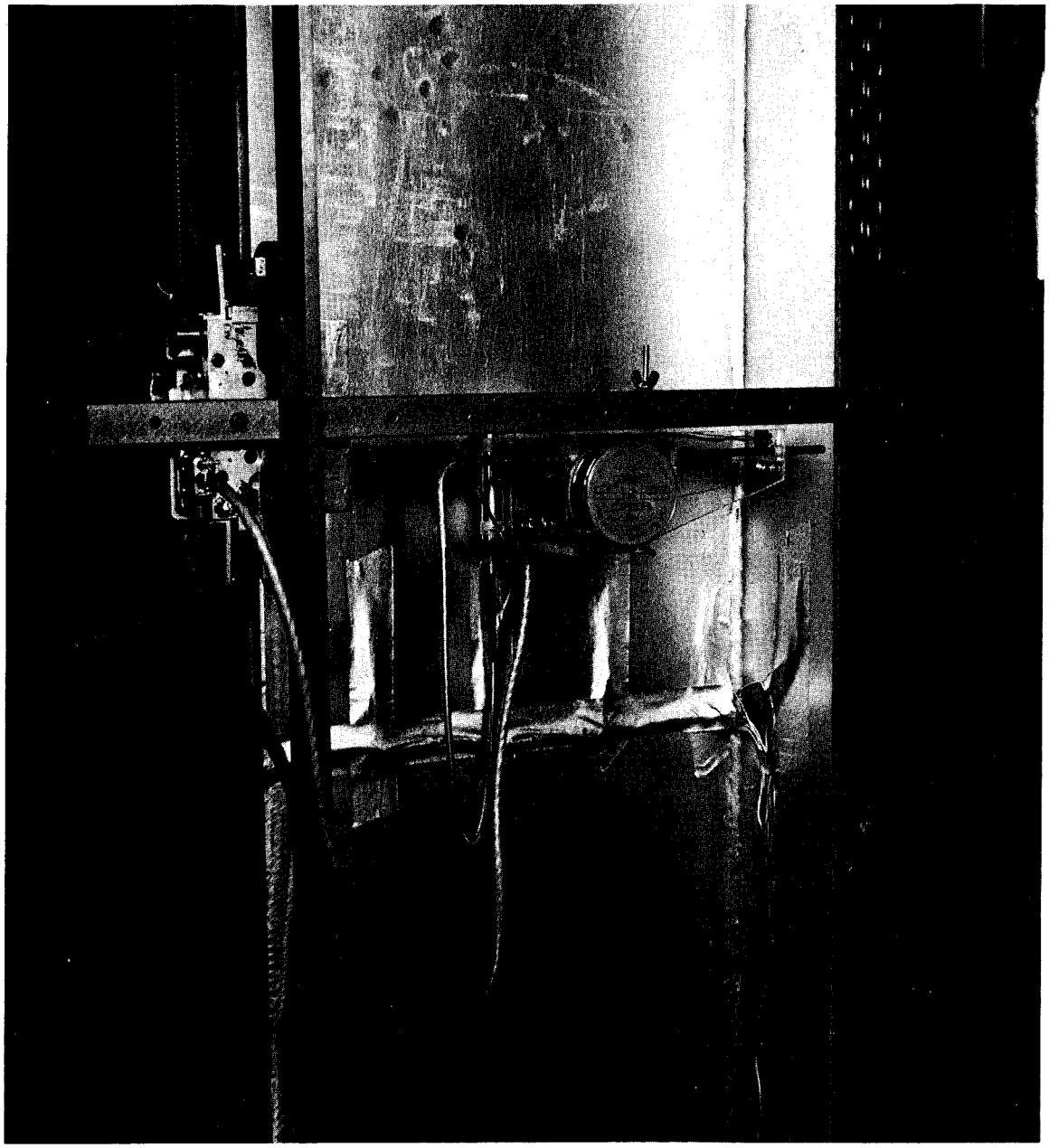

FIGURE 3.7

DEFLECTION DEVICE MEASURING FLANGE

CHAPTER IV

TEST RESULTS

4.1 Coupon Tests

From two series of tension tests done on standard coupons it was determined that the average static yield strength of the flange material was 44.53 ksi, and that of the web was 44.33 ksi. These values corresponded very closely to the nominal yield stress of 44.00 ksi, on which the specimen design was based. This was convenient for the analysis, and made easier the prediction of specimen behaviour before the tests were performed.

In all, fourteen coupon tests were performed. Six of these were on the web plate material, and the other eight on the flange plate material. Since the flange plate material was A36 steel, it was felt that the two extra tests would make any major differences between it and G40.21 Grade 44W steel more noticeable. The steel behaved satisfactorily, and its yield point was found to be very close to that specified for G40.21 Grade 44W steel.

4.2 Specimen Moment-Rotation Behaviour

The specimens were loaded at least until the ultimate moment was reached. This was indicated by either a

zero or a negative slope of the moment-rotation curve. The moment-rotation curves for the specimens are shown in Figures 4.1(a) through 4.1(f). These curves were adjusted to account for initial curvatures that were present under full axial load only.

All but two of the specimens reached the expected yield moment, reduced for axial load, before failure. Specimen 2 reached 99% of its yield moment, and specimen 5 reached 79% of its yield moment. These data are tabulated in Table 4.1.

In general, the form of the moment-rotation curves is consistent with what was expected. In particular, the specimens with low axial load were able to withstand substantially larger rotations before failure than did the specimens with higher axial load. Furthermore, the specimens under high axial load tended to fail much more suddenly than did the specimens under lower axial load.

Specimen 1 appears to have behaved more like a plastic design section than a non-compact section. It underwent large rotations before failure, while sustaining a moment approximately equal to the plastic moment. This specimen was the only one not to have shown a decrease in moment capacity within the range of data taken. It was tested until the rotation was approximately seven times that at yield. The moment-rotation plot was still horizontal when

the test was stopped.

Specimen 2 also underwent a large rotation before failure occurred, although the moment was not as great. Because it is more likely for a stocky specimen to fail at a larger moment relative to its yield moment (i. e., a larger Mu/My ratio) than a slender section, it was expected that specimen 2 would fail at a higher Mu/My ratio than specimen 1. This, however, was not the case and no apparent reason seems to exist for this discrepancy.

Specimen 3 exceeded the yield moment and exhibited a more sudden failure than either specimens 1 or 2. The specimen rotation at failure was less than the failure rotations exhibited by either specimens 1 or 2.

Specimen 4 behaved in much the same way as specimen 3. It was noted for specimens 3 and 4, that the stockier one (specimen 4) failed at the larger Mu/My ratio.

Specimen 5 failed suddenly at a moment considerably less than the yield moment, and had a smaller rotation at failure than did any of the other specimens. It is possible that the high axial load caused the specimen to fail prematurely as it interacted with initial deflections in the flange and the web.

Specimen 6 also failed suddenly, although it had the largest Mu/My ratio of all the specimens. Its failure

rotation was greater than that of specimen 5.

4.3 Specimen Buckling Behaviour

In the investigation conducted by Perlynn and Kulak[5] the identification of which plate element (web or flange) buckled first had been very helpful in the analysis of the test results. Unfortunately, and in spite of the large amount of data on web and flange movements collected in the present tests, it was frequently not apparent which plate element buckled first.

Because the deflection readings of the web were taken at grid points whose locations were known and constant (having been adjusted for specimen curvature and shortening), it was possible to plot contours of the deflections of the web, and a single line graph of compression flange deflections for each load increment. Because of the varying reflectivity of the paint and the variance of the ambient light at the different grid points, changes in deflections were plotted rather than absolute values as contour intervals. Using changes in deflections would cancel out any undesired effects due to these variations.

Deflection readings on specimen 1 were taken with a grid size of 4 in. by 4 in. on the web, and linearly every

4 in. on the flange. For the remaining specimens, a grid size of 2 in. by 2 in. was used for the web and readings every 2 in. were taken along the flange.

All the specimens had deflection measurements taken over the central 32 in. length of the beam-columns. This meant that no deflection data were taken for the top and bottom 6-1/2 in. of the specimen (Figure 4.2). In the case of specimen 2 this was unfortunate because the web movements which eventually caused specimen failure occurred very close to the cap plate of the specimen. Other specimens also had yield lines and significant deflections near the cap plates where no deflection readings were taken. Because the total grid size was an integral number of 2 in. or 4 in. grid points, the portion of the web monitored for deflections varied from specimen to specimen and did not encompass the entire distance "h" between the flanges (Figure 4.2).

The contour values used in plotting the web deflections were chosen on the basis of the intervals that would encompass most of the greatest deflection changes for all the load increments of a particular specimen. In the end, ten contour values were chosen for each specimen. Often, not all of the ten contour values existed for a particular load increment plot. This was deliberate. If, in a later load increment plot in a test, a new contour value of a larger deflection change is plotted, the web is known

to be moving. The flange deflections were plotted as a straight line graph of deflections over the flange length.

Determination of the web buckling behaviour was accomplished by superimposing three contour plots on a graph, each having a reduced number of contour values. A similar procedure was followed for the flange plots. By noting the movement of a particular section of the flange or a contour value over the web, it is possible to gain insight into the buckling of the plate element. Comparison between web and flange plate movements helped determine how the specimens failed.

The contour and deflection plots are shown in Figure 4.3. The load increments and the respective contour values for each load increment are indicated on the plots for each specimen. The solid lines represent the web contours and the flange deflections at the first load increment plotted; the dashed lines, the intermediate load increment; and the dotted lines, the highest load increment. A negative contour value or flange deflection value indicates that the plate element is moving away from its initial position. The contour plots in these figures are drawn to an approximate scale of 1:5.33. The load increments plotted were chosen so that one would be at a low load in order to provide a basis for web and flange plate movements at the higher load increments. The other two load increments plotted are at high loads, usually one at the load increment

nearest the failure load for which the web and compression flange deflection readings were taken, and the other load increment immediately preceeding it for which these deflections were taken.

Since it was not definitely clear in most cases whether the first plate element to buckle was the web or the flange, judgement was used to provide a decision. In view of the uncertainties this was generally such that the most conservative prediction of behaviour would result.

Figure 4.3(a) shows that specimen 1 underwent a substantial amount of movement in the web as the load was increasing, while the flange movements were much smaller. In fact, the flange appears to be almost straight except for part near mid-height where the deflections are noticeable. It appears that this specimen failed by web buckling. The strain gauge readings (not presented) do not indicate a web buckle, but the contour plots show that the largest movements do not occur at mid-height, where the strain gauges were located.

It was more difficult to determine the failure mode for specimen 2 (Figure 4.3(b)). Substantial flange movements occurred near the bottom of the specimen at the higher load increments. The web was also moving, both at the top and the bottom of the specimen, and hence appears as if it could have caused the failure. It apparently had twisted;

the top is closer and the bottom farther away than at the first load increment. It was judged that the web caused the specimen failure. Unfortunately, the buckle of this specimen formed very close to the cap plate at one end of the specimen, and no deflection readings were taken in the immediate vicinity of the buckle. Hence the determination of which plate element caused this specimen to fail was difficult. At the higher load increments, the strain gauges indicate some web movement, but, as was the case for specimen 1, the large deflections did not occur where the strain gauges were located.

As shown in Figure 4.3(c), specimen 3 showed substantial movements of both the flange and the web. It was apparent that as one plate element failed, the other one was close to failure itself. It appears as though the flange was deflecting more at the first load increment, but the web deflected as much as the flange did as the loads were increased. The buckle formed just above mid-height, and appears to have been caused by a simultaneous web and flange failure. The strain gauges indicate some web movement.

Specimen 4 had substantial web movements at the top and bottom with the mid-height remaining relatively stable. Figure 4.3(d) shows that the flange exhibited large movements at the same heights as the web deflections were occurring. The flange moved a substantial amount more than the web, so it appears as if the specimen failed by flange

buckling. The strain gauge readings indicate some movement of the web.

Specimen 5 appears to have substantial movement of both the web and the flange. In Figure 4.3(e), it can be seen that, for low load, the web and flange moved approximately the same amount. Because of the high axial load involved, it was noticed that the tension flange was beginning to twist before the application of moment was started. Hence, the deflection readings for the intermediate load increments were not considered to be accurate, and could not be used. For the higher load increments, the flange appeared to be moving a very large amount while the web was not moving to such a great extent. The strain gauges showed, however, that a web buckle was forming. Hence it appears as if the specimen failed by simultaneous web and flange buckling.

Figure 4.3(f) shows that specimen 6 had reasonably large movements at the low load increment for both the web and the flange. However, for the higher load increments, it appears as if the flange moved more than the web. Hence, it was concluded that this specimen failed by flange buckling. The strain gauges do not indicate any substantial movement of the web at mid-height.

It was also noted that specimens 1, 2, and 4 had substantial movements of the web and flange near the top and

bottom of the specimen, but much smaller deflections at the mid-height of the specimen. This is thought to be due to the presence of the studs welded to the specimens for the lateral bracing system.

A web and flange buckle (shown well after the ultimate moment had been attained) is given in Figure 4.4, and a summary of how each specimen is considered to have failed is included in Table 4.1.

4.4 Initial Deflections and their Effects

Relatively light steel plate was used in order to fabricate reasonable cross-sectional shapes for testing. It is probable that, as a result of residual stresses resulting from the welding of these thin plates and from normal shop fabrication procedures, initial deflections of both the flanges and web were present.

From the initial web deflection measurements, it was determined that the maximum relative out-of-straightness (δ/h) for these specimens was 0.005 (Specimen 2). This is 74.7% of the allowable limit according to CSA Standard W59.1[14]. The out-of-straightness of the compression flange was measured only relative to the tension flange. Because of the uncertainty of the straightness of the datum, these values are not presented here.

The effects of initial out-of-straightness of the plate elements are not obvious from the tests. However, it may be reasonably assumed that if the compression flange has an large initial out-of-straightness compared to the web any axial load or moment application will tend to increase this out-of-straightness. A similar situation exists for the web. For non-compact beam-columns, the effect of the initial out-of-straight of the flanges has perhaps as profound an effect as that of the web, because the flanges are so slender.

It was noted that the high axial load specimens were more susceptible to out-of-straightness effects, and hence sudden failures.

4.5 Second-Order Considerations

It was noted that the maximum second-order moment due to the interaction between strong-axis deflections and axial load at ultimate moment was 3% (Specimen 5). Hence it appears to be reasonable to neglect these second-order P-Δ effects.

SPECIMEN	P/Py	$\frac{h}{w}\sqrt{Fy}$	Mu/My	FAILURE
1	0.15	639.4	1.16	W
2	0.15	534.2	0.99	W
3	0.30	590.7	1.12	W&F
4	0.30	488.2	1.20	F
5	0.70	501.2	0.79	W&F
6	0.70	401.1	1.53	F

TABLE 4.1

SPECIMEN MOMENT AND FAILURE DATA

SPECIMEN	HEIGHT (in)	δ (WEB) (in)	δ/h (WEB)	% (all.)
1	24.01	0.061	0.0025	37.5
2	20.06	0.100	0.0050	74.7
3	22.18	0.041	0.0018	27.0
4	18.33	0.071•	0.0038	57.0
5	18.82	0.081•	0.0043	64.5
6	15.06	0.057•	0.0038	57.0

•ESTIMATE ONLY

TABLE 4.2

INITIAL WEB DEFLECTION DATA

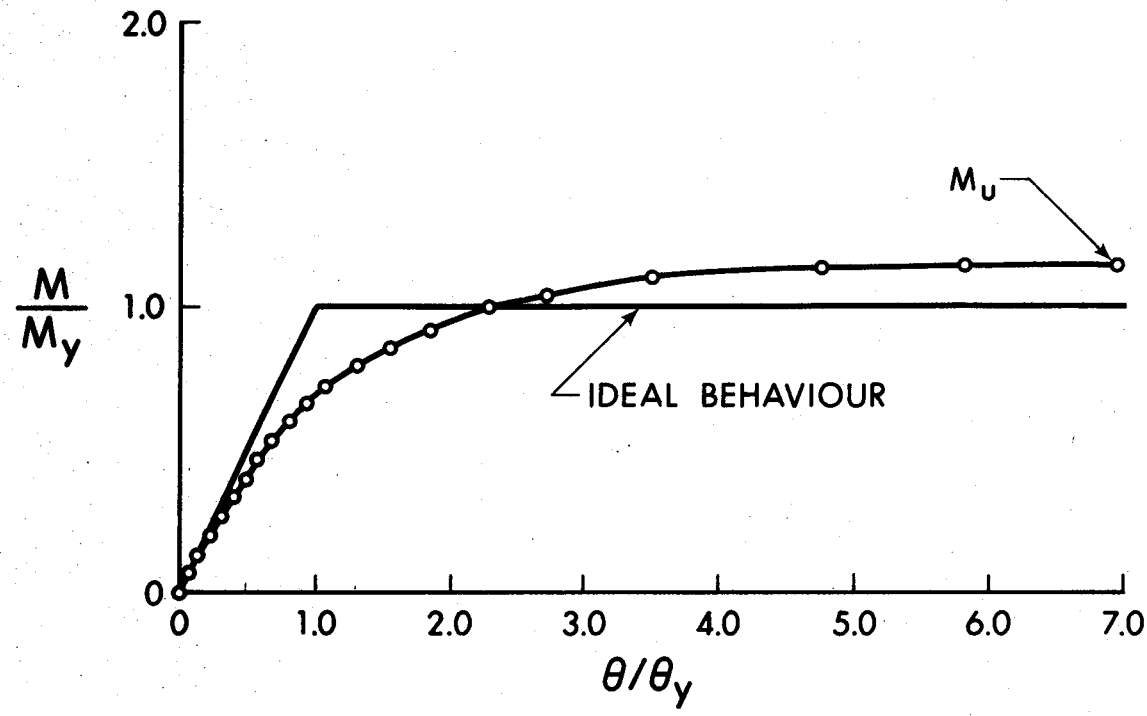

FIGURE 4.1(a)

MOMENT-ROTATION RELATIONSHIP - SPECIMEN 1

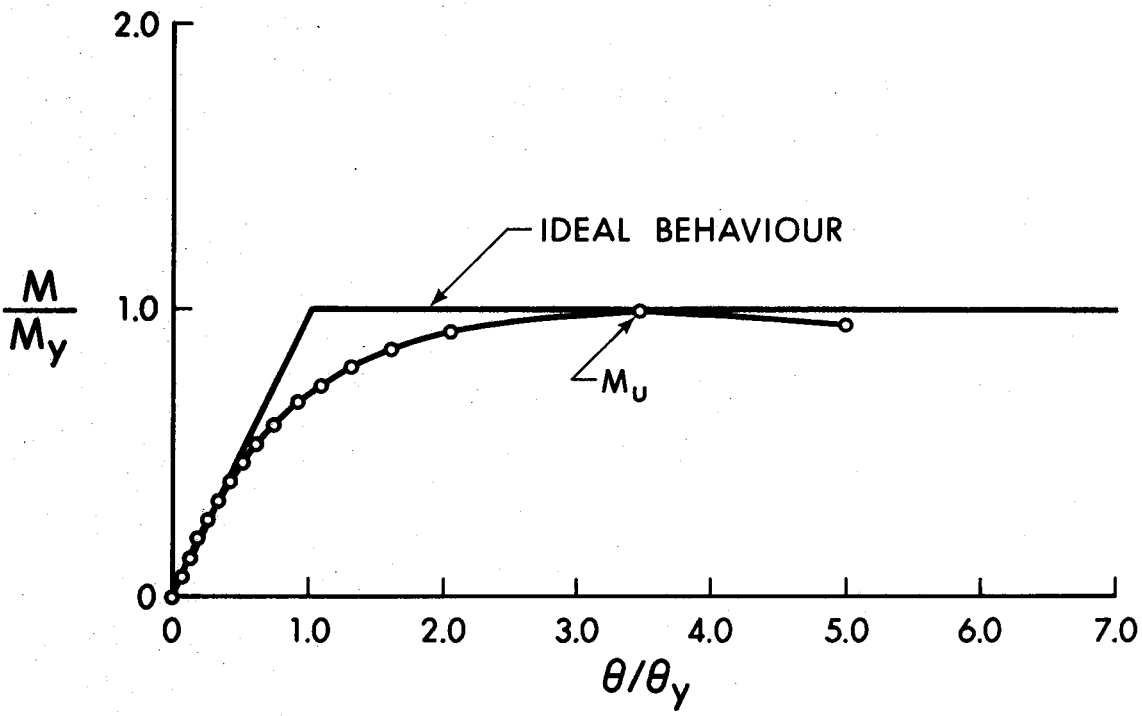

FIGURE 4.1(b)

MOMENT-ROTATION RELATIONSHIP - SPECIMEN 2

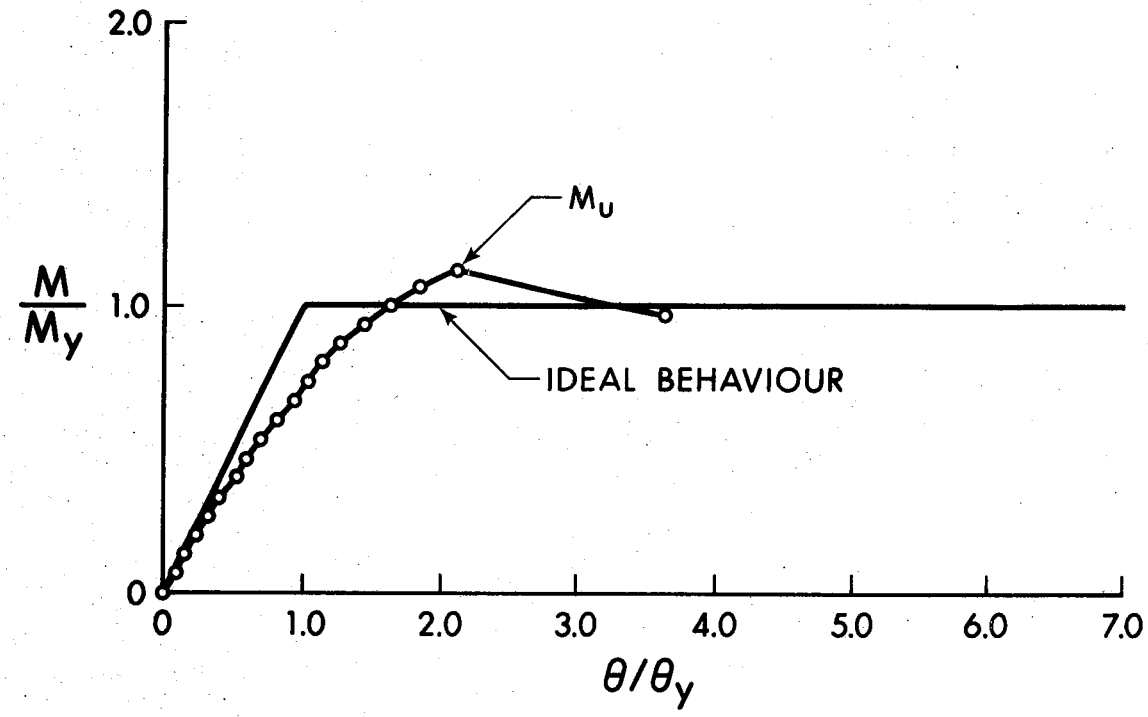

FIGURE 4.1(c)

MOMENT-ROTATION RELATIONSHIP - SPECIMEN 3

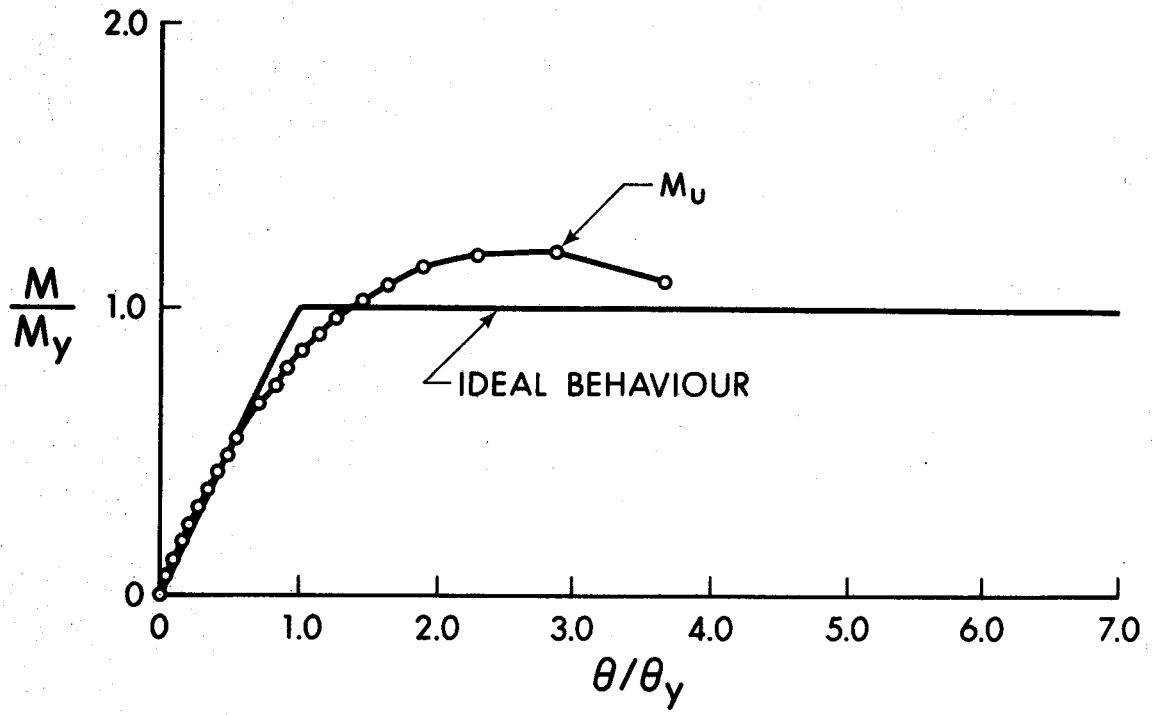

FIGURE 4.1(d)

MOMENT-ROTATION RELATIONSHIP - SPECIMEN 4

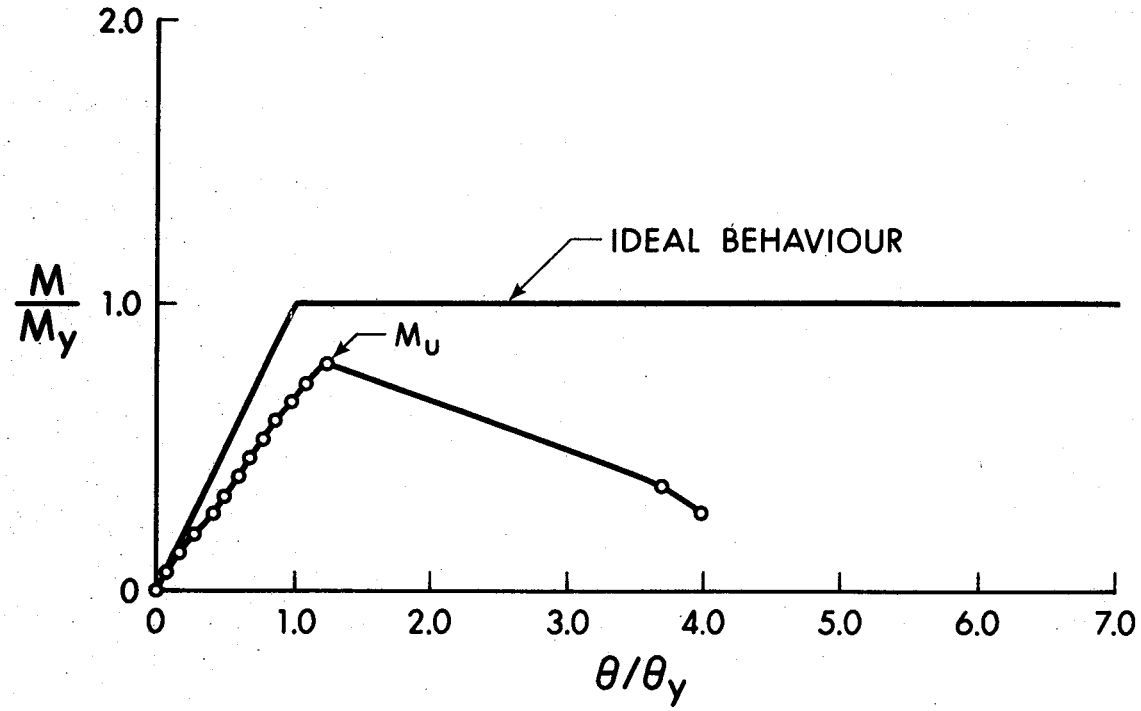

FIGURE 4.1(e)

MOMENT-ROTATION RELATIONSHIP - SPECIMEN 5

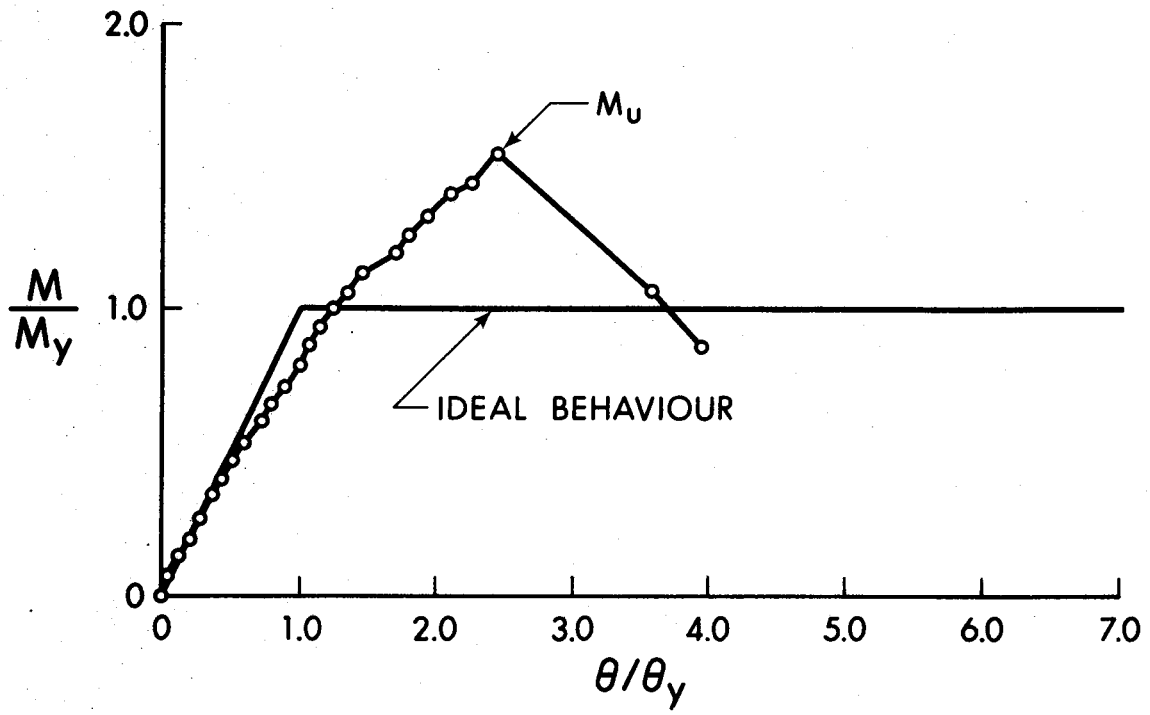

FIGURE 4.1(f)

MOMENT-ROTATION RELATIONSHIP - SPECIMEN 6

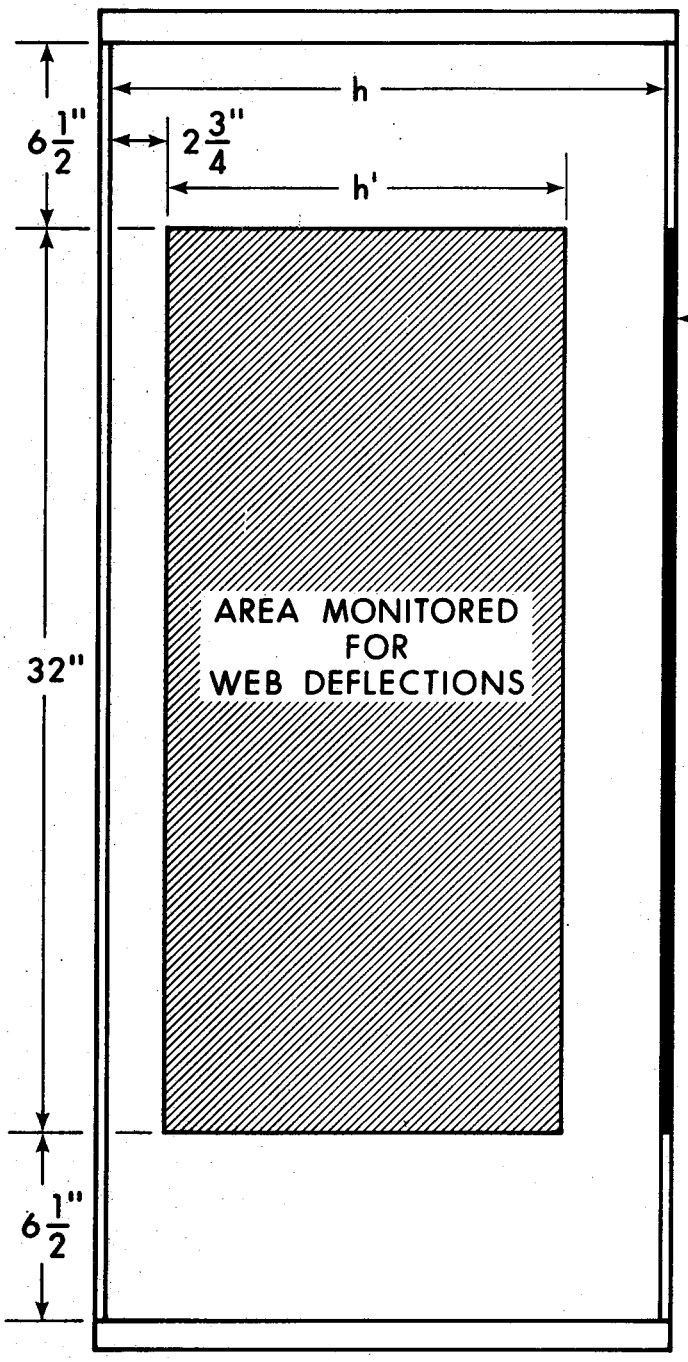

SPECIMEN	h (in)	h'(in)
1	24.01	16.00
2	20.06	12.00
3	22.18	14.00
4	18.33	12.00
5	18.82	12.00
6	15.06	8.00

FIGURE 4.2

PORTION OF SPECIMENS MONITORED FOR PLATE DEFLECTIONS

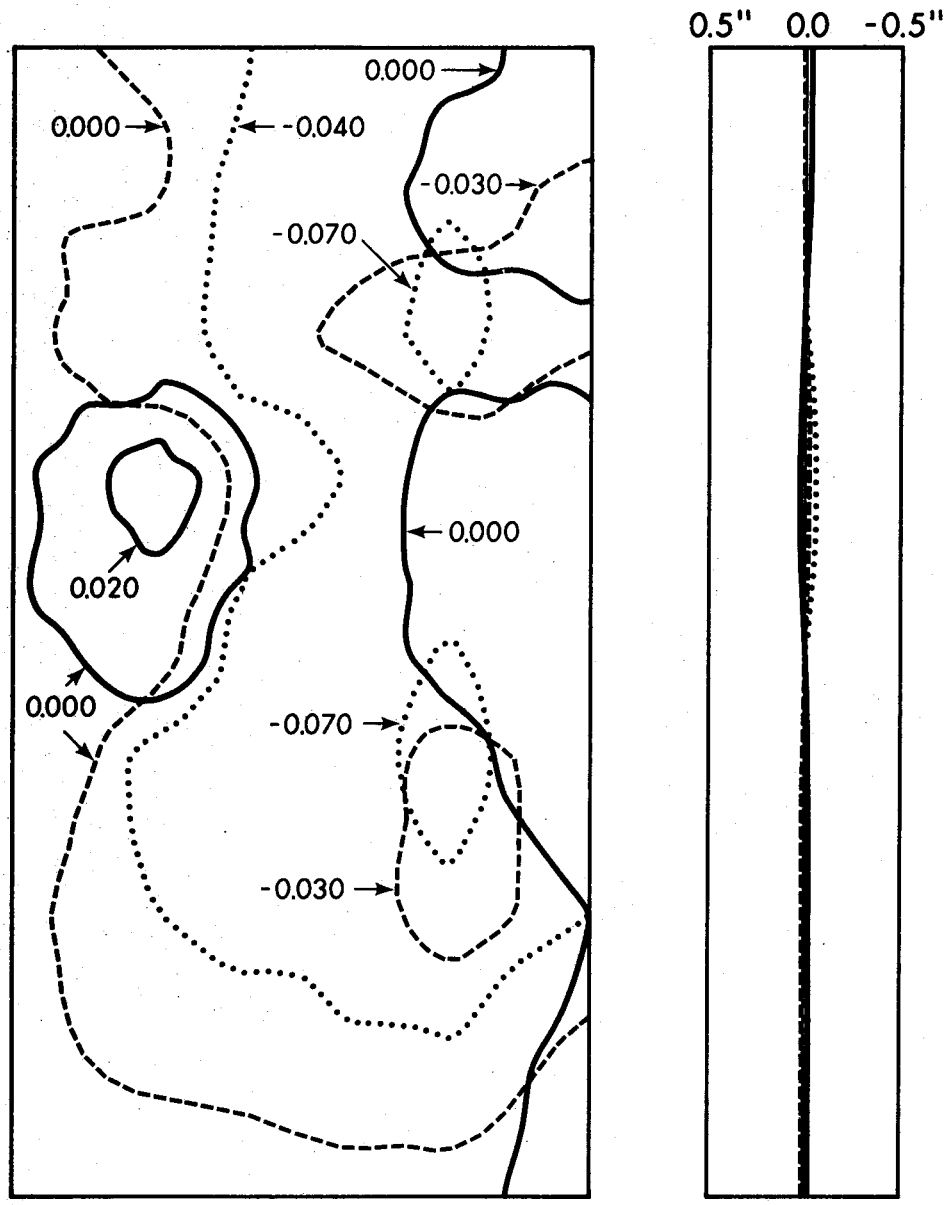

LINE	M (in-k)	P (k)
———	709	78
- - - - - - -	3260	78
.....	3555	78

FIGURE 4.3(a)

WEB AND FLANGE DEFLECTIONS - SPECIMEN 1

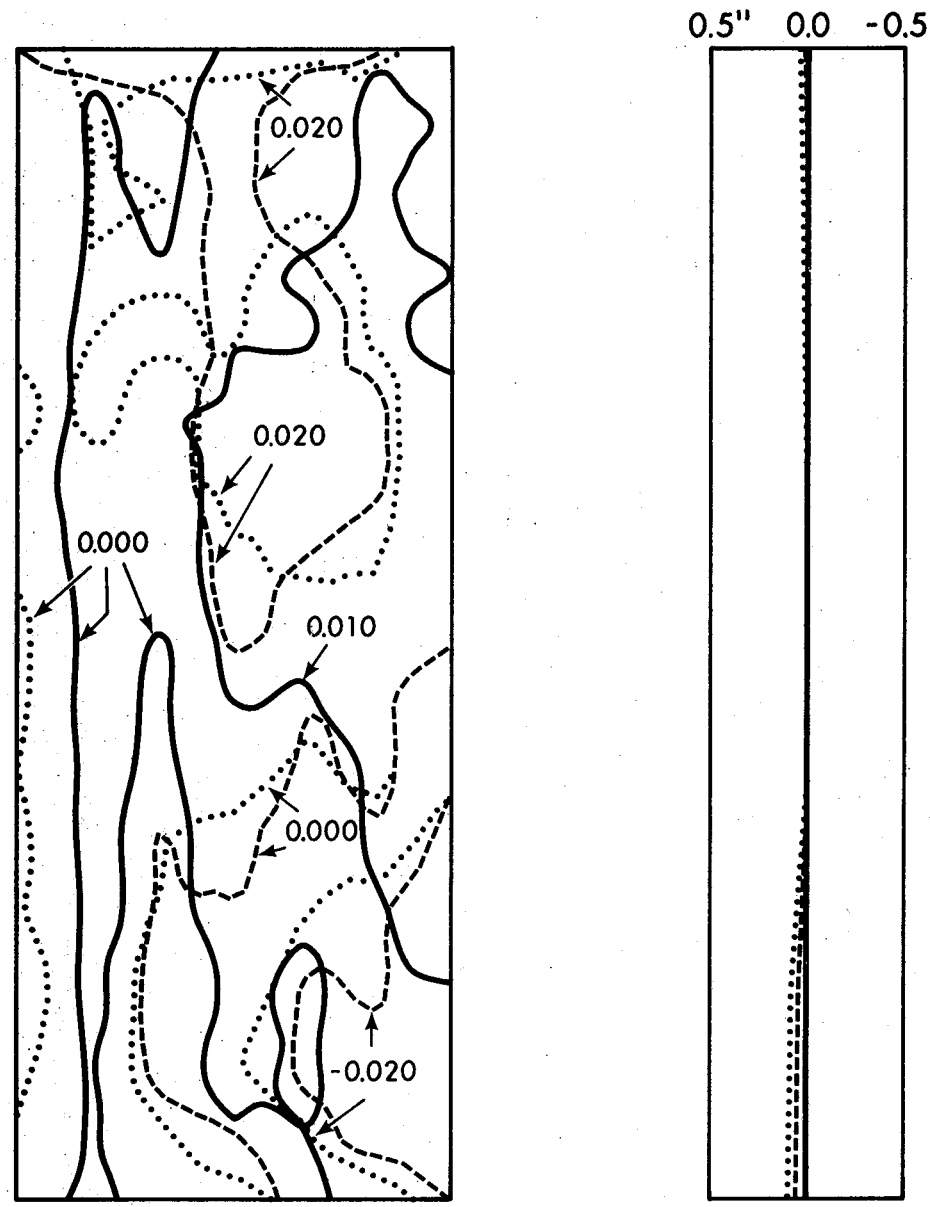

LINE	M (in-k)	P (k)
———	380	72
- - - - - - -	2446	72
.....	2622	72

FIGURE 4.3(b)

WEB AND FLANGE DEFLECTIONS - SPECIMEN 2

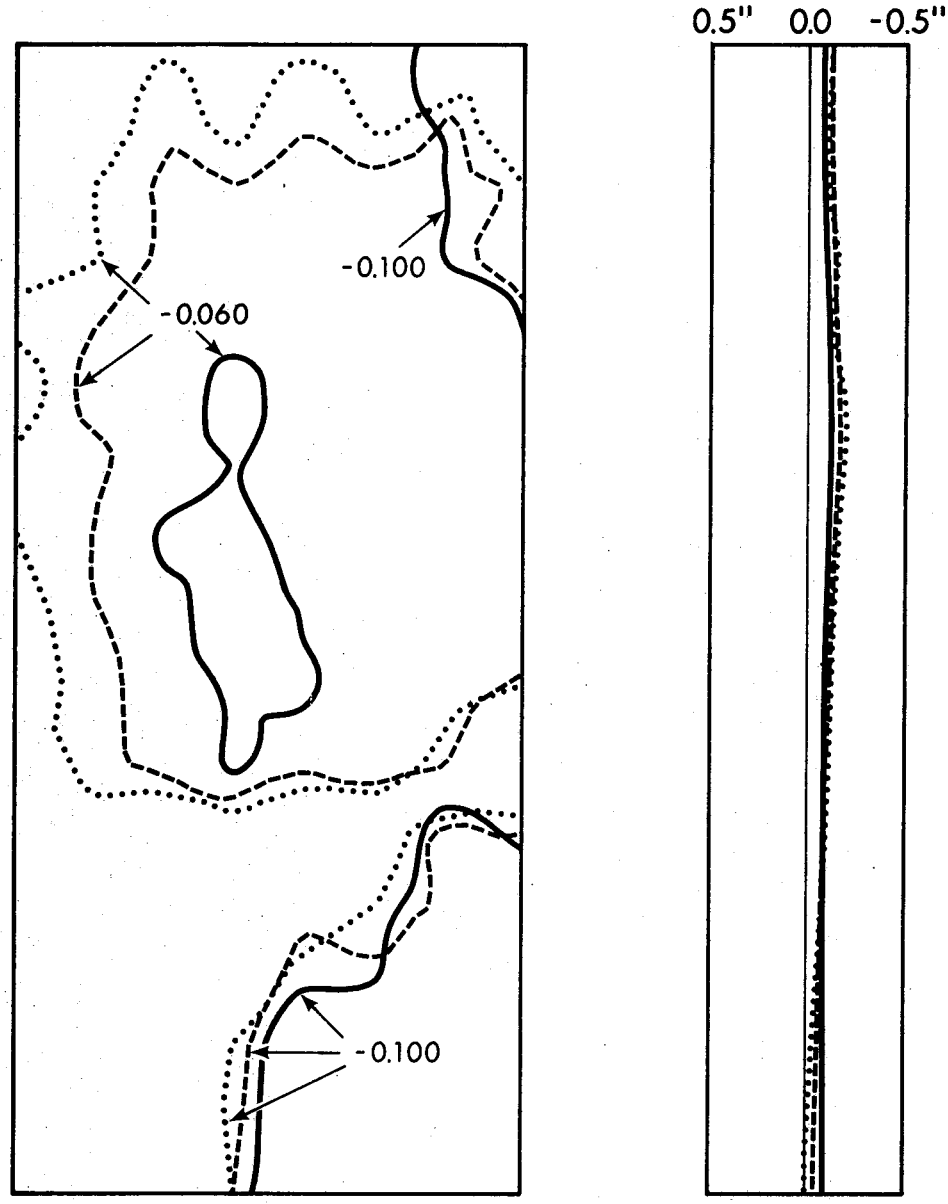

LINE	M (in-k)	P (k)
———	532	150
- - - - - - - -	2300	150
.....	2650	150

FIGURE 4.3(c)

WEB AND FLANGE DEFLECTIONS - SPECIMEN 3

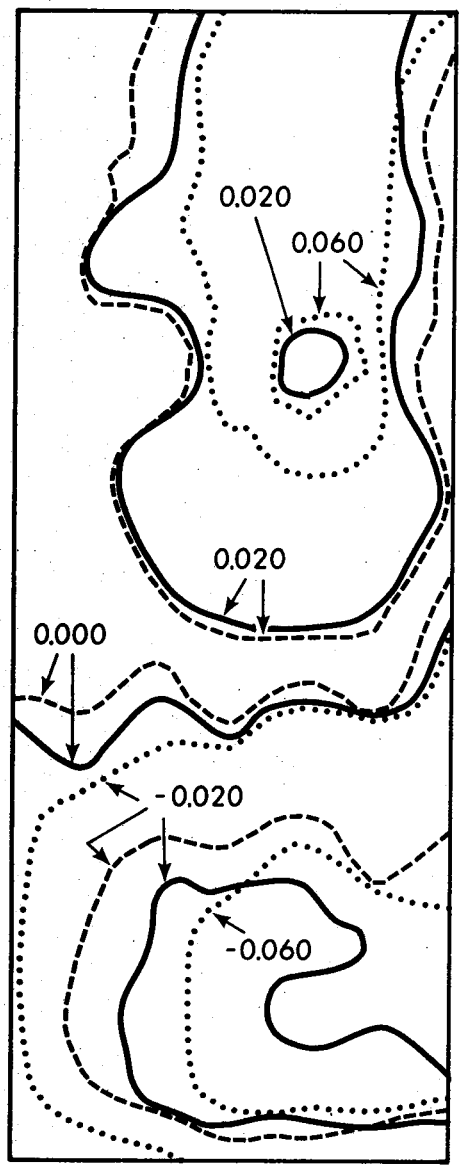

WEB CONTOURS

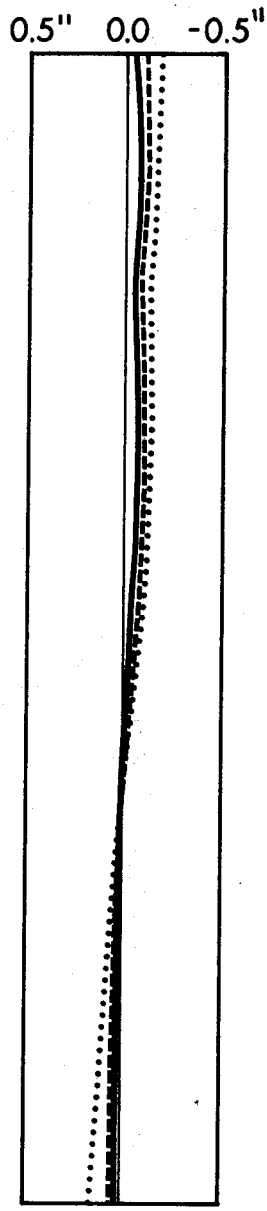

FLANGE DEFLECTIONS

LINE	M (in-k)	P (k)
———	2024	138
- - - - - - -	2268	138
.....	2488	138

FIGURE 4.3(d)

WEB AND FLANGE DEFLECTIONS - SPECIMEN 4

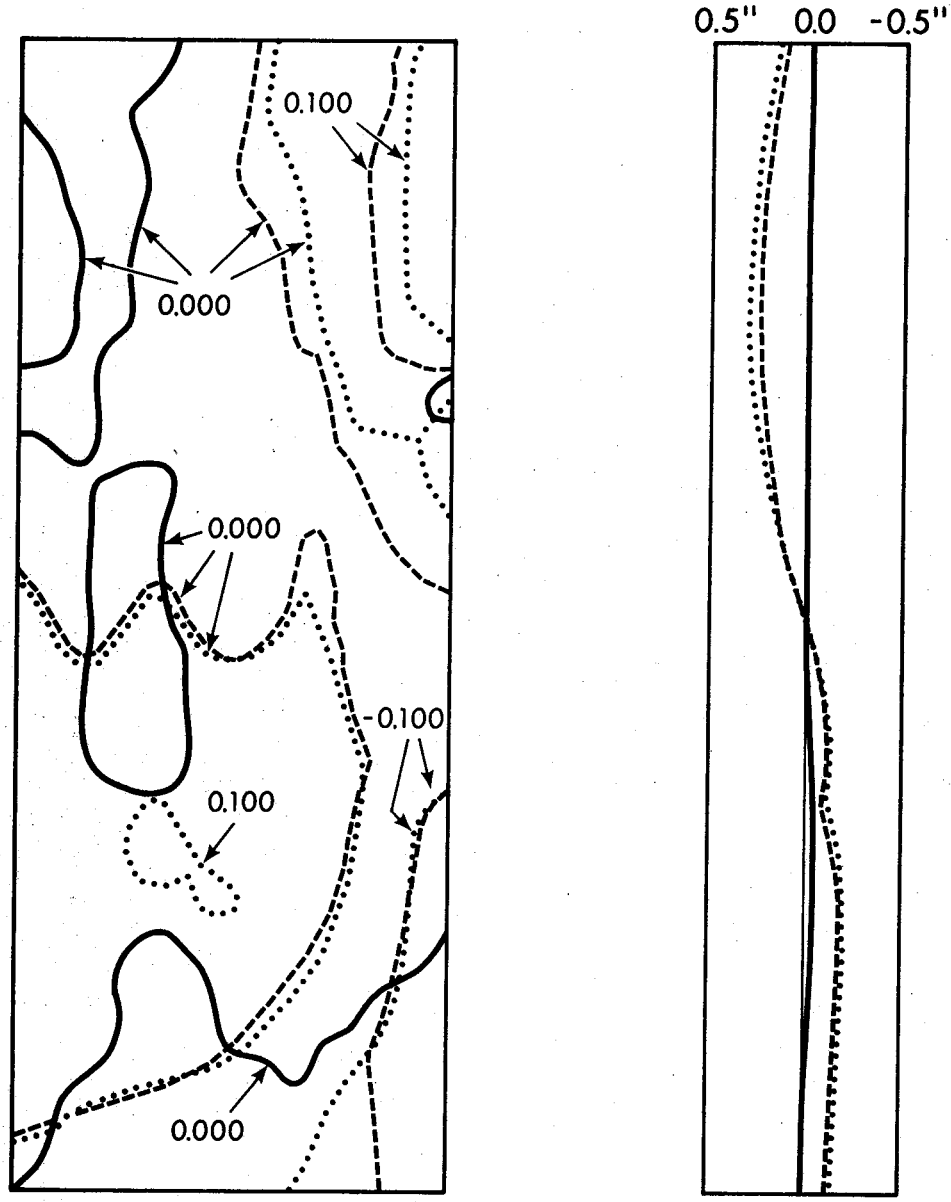

LINE	M (in-k)	P (k)
———	0	132
- - - - - - -	487	325
.....	668	325

FIGURE 4.3(e)

WEB AND FLANGE DEFLECTIONS - SPECIMEN 5

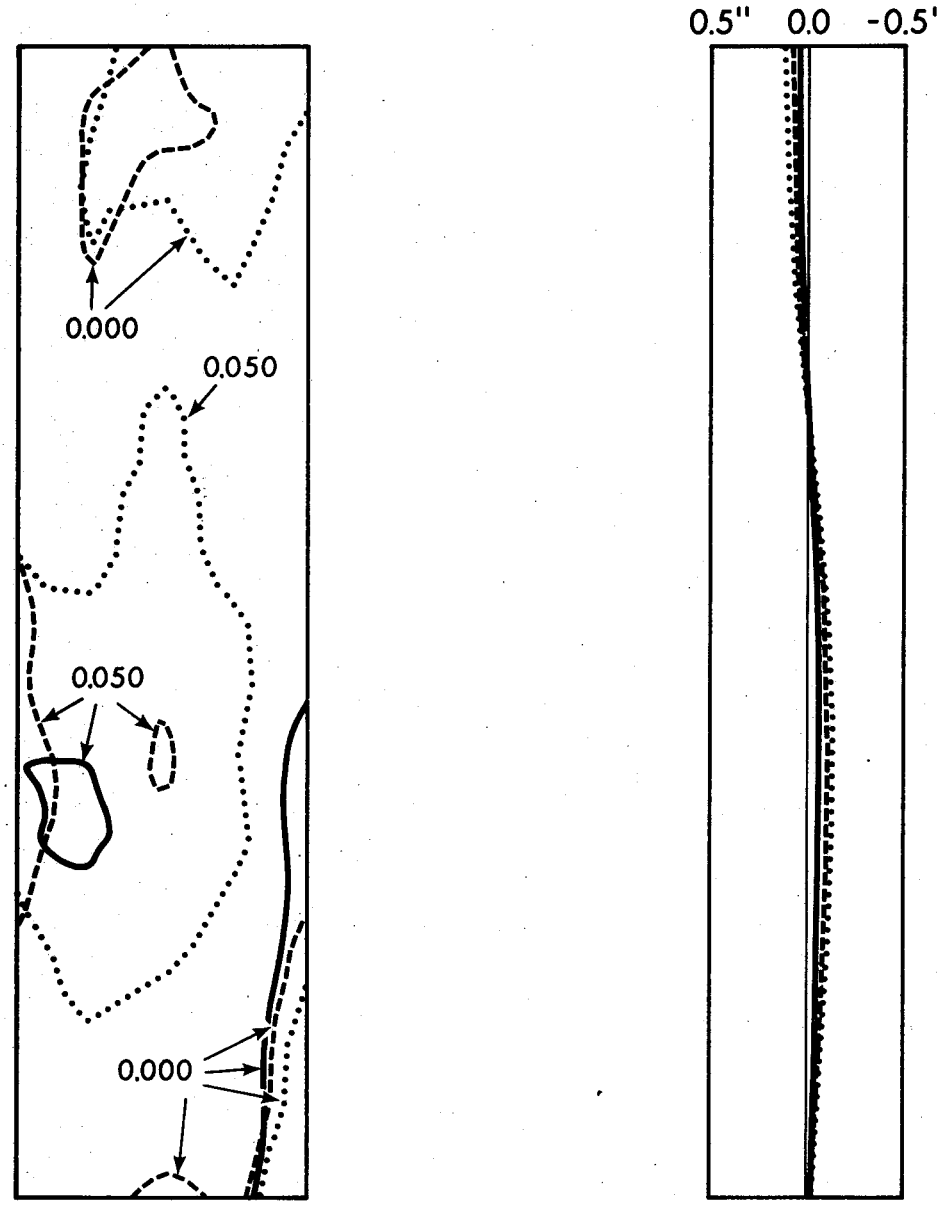

LINE	M (in-k)	P (k)
———	516	296
- - - - - - -	997	296
.....	1095	296

FIGURE 4.3(f)

WEB AND FLANGE DEFLECTIONS - SPECIMEN 6

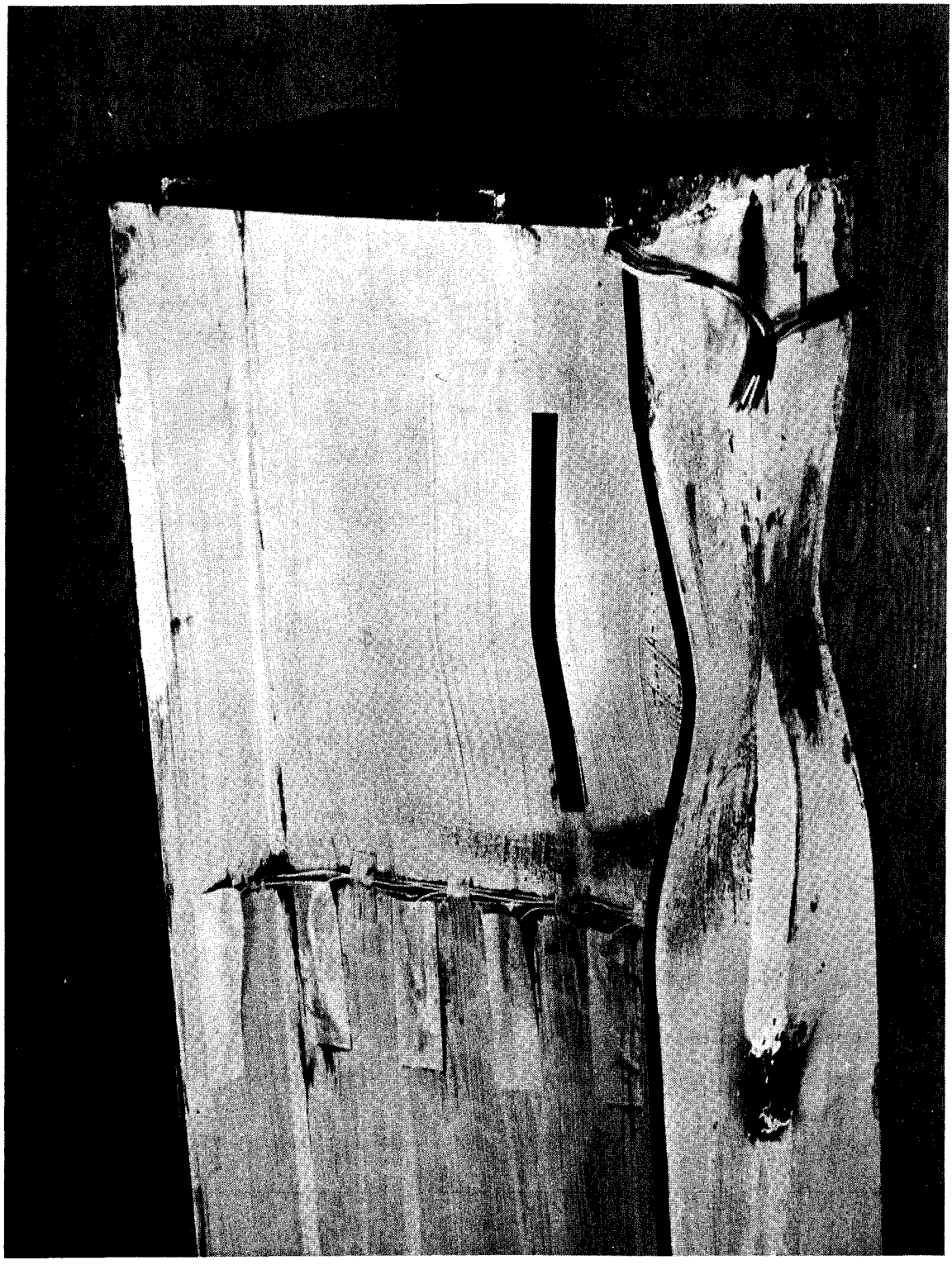

FIGURE 4.4

WEB AND FLANGE BUCKLE (SPECIMEN 6)

CHAPTER V

THEORETICAL ANALYSIS

5.1 Analysis of CSA S16-1969 Specification Requirements

The first major investigation into flange and web plate buckling was conducted by Haaijer[4]. In his investigation, Haaijer accounted for the possibility that web and flange plates may reach strain-hardening before buckling. His analysis was based on the following assumptions:

1. An idealized stress-strain diagram can be used for the analysis of the test results (Figure 5.1).
2. Yielding occurs in slip bands[15], so that the material is either in the elastic range or in the strain-hardening range.
3. The material is homogeneous and isotropic in the elastic range, and homogeneous and orthotropic in the strain-hardening range.
4. The rotation interaction between the web and flange plates can be accounted for by using a coefficient of restraint (β).
5. Yielding starts at the loaded edges of a column specimen and progresses inwards, or starts at the centre and progresses outwards

towards the loaded edges. (Haaijer uses this assumption to show that columns can buckle at stresses above the yield stress, then assumes that this also holds true for plates.)

6. An incremental stress strain relationship[16] can be applied to the analysis. Initial imperfections of the plate are accounted for by the introduction of effective moduli for the strain-hardening range.
7. No strain reversal occurs for a plate supported along all four edges when it deforms to its buckled shape from its non-buckled shape.

Once the possibility of column buckling at stresses above the yield stress was established, Haaijer developed a plate buckling equation for the strain-hardening range.

Assuming that buckling occurs without strain reversal, it is possible for a web plate element of orthotropic material to be in equilibrium in the deformed position when subjected to uniform edge compression (Figure 5.2). This can be expressed mathematically by the following fourth-order partial differential equation:

$$Dx\,\frac{\partial^4 u}{\partial x^4} + 2H\,\frac{\partial^4 u}{\partial x^2 \partial y^2} + Dy\,\frac{\partial^4 u}{\partial y^4} = -\frac{\sigma_{cr}\,w}{I}\,\frac{\partial^2 u}{\partial x^2} \qquad (5.1)$$

where:

$$Dx = \frac{Ex}{1 - \nu_x \nu_y}$$

$$Dy = \frac{Ey}{1 - \nu_x \nu_y}$$

$$Dxy = \frac{\nu_y Ex}{1 - \nu_x \nu_y}$$

$$Dyx = \frac{\nu_x Ey}{1 - \nu_x \nu_y}$$

$2H = Dxy + Dyx + 4Gt$

Gt = tangent shear modulus

u = deflection of plate at centre

w = plate thickness

σ_{cr} = critical buckling stress

$$I = \frac{w^3}{12}$$

Equation 5.1 is similar to Equation 2.1, the only difference being in the coefficients used to describe the material behaviour. Equation 2.1 deals with isotropic material which requires only two independent parameters to describe the material behaviour, while Equation 5.1 deals with orthotropic material which requires five such parameters to describe it.

The condition that the in-plane and deformed positions of the plate are in equilibrium at the instant of

buckling (the bifurcation point) can be expressed in terms of work. Any additional work done by the external forces in further bending the plate must equal the change in the internal energy of the plate. This yields the following integral equation:

$$\frac{\sigma_{cr}\, w}{I}\int\int \left(\frac{\partial u}{\partial x}\right)^2 dxdy = \int\int \left[Dx\left(\frac{\partial^2 u}{\partial x^2}\right)^2 + Dy\left(\frac{\partial^2 u}{\partial y^2}\right)^2 + (Dxy + Dyx)\left(\frac{\partial^2 u}{\partial x^2}\right)\left(\frac{\partial^2 u}{\partial y^2}\right) + 4\,Gt\left(\frac{\partial^2 u}{\partial x \partial y}\right)^2\right] dxdy \qquad (5.2)$$

This approximate work-energy approach was used because solutions to Equation 5.1 can be easily obtained only if $H^2 = DxDy$, an assumption made by Bleich[17]. This assumption, however, was found not to be valid for Haaijer's experimental results. If the following constraint on Equation 5.1 is considered:

$$2H = Dxy + Dyx + 4Gt$$

and if $H^2 = DxDy$ is substituted for H in the constraint equality, the equality is not satisfied using the values of the constants determined from Haaijer's experimental

results.

Equation 5.2 will give an approximate solution if an appropriate deflection surface is assumed. Although the degree of approximation depends upon the correctness of the assumed deflection surface, the result will be conservative in any case. For a rectangular plate supported along all four edges, with the loaded edges x = 0 and x = 1 being hinged, and the edges $y = \pm h/2$ having equal restraint against rotation (Figure 5.2), Haaijer used the deflected surface first proposed by Lundquist and Stowell[18]:

$$u = [B\pi((y/h)^2 - 0.25) + (A+B)\cos(\pi y/h)]\sin(\pi x/l) \qquad (5.3)$$

where:

A = constant

B = constant

$\beta = \frac{B}{A} = \frac{Mh}{2DyI}$ = coefficient of restraint against rotation

M = moment per unit length required for a unit rotation

h = width of plate

l = length of plate

Substituting Equation 5.3 into Equation 5.2 and integrating will give the critical buckling stress. In the limiting cases for a web plate subjected to uniform axial compression, when the unloaded edges $y = \pm h/2$ are hinged or

fixed, the minimum values of the critical buckling stress are:

(a) For $y = \pm h/2$, hinged, ($\beta=0$);

$$\sigma_{cr} = \frac{\pi^2}{12}\left(\frac{w}{h}\right)^2 [2\sqrt{DxDy} + Dxy + Dyx + 4\,Gt] \qquad (5.4)$$

(b) For $y = \pm h/2$, fixed, ($\beta=\infty$);

$$\sigma_{cr} = \frac{\pi^2}{12}\left(\frac{w}{h}\right)^2 [4.554\sqrt{DxDy} + 1.237\,(Dxy+Dyx) + 4.943\,Gt] \qquad (5.5)$$

By substituting the appropriate values of the constants Dx, Dy, Dxy, Dyx, and Gt for the strain-hardening range, Equations 5.4 and 5.5 can be used to give the critical buckling stress of plates subjected to strains greater than or equal to the strain at the start of strain-hardening, ε_{st} (Figure 5.1).

For the simplified stress-strain curve assumed, substitution of the elastic values of the constants in Equations 5.4 and 5.5 will give valid elastic buckling solutions for σ_{cr} less than σ_y. It is obvious that the lower critical buckling stress will occur for the case of the plate with all four edges hinged.

Haaijer conducted tests on wide-flange shapes of ASTM-A7 steel subjected to either pure bending or pure compression. He concluded that Equations 5.4 and 5.5

adequately described the test results. At the time, however, the behaviour of a web plate subjected to combined in-plane bending and uniform axial compression was not investigated.

Equations 5.4 and 5.5 pertain only to plate elements that are free of residual stresses, that is, annealed specimens. As-delivered specimens, however, generally contain residual stresses of a large enough magnitude to cause partial yielding to occur at an applied stress considerably less than the yield stress. The elastic solutions obtained from Equations 5.4 and 5.5 are valid only up to a limiting stress σ_p, where:

$$\sigma_p = \sigma_y - \sigma_r$$

in which σ_y = yield stress,

σ_r = residual stress.

A more realistic approach to the problem, for the range $\sigma_p < \sigma_{cr} < \sigma_y$, was proposed in 1958 by Haaijer and Thurlimann[8], when they suggested a plate buckling equation which took into account the effects of residual stresses. A plate buckling curve (similar to a column buckling curve) was developed which had an empirical transition curve to describe the buckling behaviour of a plate subjected to stresses between its proportional limit and its yield stress (Figure 2.1).

Dividing each side of Timoshenko's plate buckling relationship (Equation 2.2) by the yield stress results in:

$$\frac{\sigma_{cr}}{\sigma_y} = \frac{K\ \pi^2\ E}{12\ \sigma_y\ (1 - \nu^2)\ (h/w)^2} \tag{5.6}$$

Haaijer and Thurlimann defined:

$$\frac{1}{\alpha^2} = \frac{\sigma_{cr}}{\sigma_y} \tag{5.7}$$

to obtain:

$$\alpha = \frac{h}{\pi w}\sqrt{\frac{12\ \sigma_y\ (1 - \nu^2)}{K\ E}} \tag{5.8}$$

which is the same as Equation 2.3.

Equation 5.7 is valid for values of α greater than some limiting value α_p (Figure 2.1). This corresponds to stresses below the proportional limit and α_p corresponds to the non-dimensionalized limiting stress σ_p/σ_y. From the point given by (σ_p/σ_y, α_p), some transition curve must be followed as progressively more of the material reaches the strain-hardening range, to the point at which the buckling stress equals the yield stress ($\sigma_{cr}/\sigma_y = 1.0, \alpha_o$). A portion of a plate element reaching the latter point, has by

definition, all of its material yielded and has reached the strain-hardening range. Haaijer and Thurlimann proposed the following transition curve for $\alpha_o \leq \alpha \leq \alpha_p$:

$$\frac{\sigma_{cr}}{\sigma_y} = 1 - \left(1 - \frac{\sigma_p}{\sigma_y}\right)\left(\frac{\alpha - \alpha_o}{\alpha_p - \alpha_o}\right)^n \qquad (5.9)$$

where:

σ_{cr}= critical buckling stress for uniform compression

$\sigma_p = \sigma_y - \sigma_r$

σ_p = stress at proportional limit

σ_r = maximum value of the plate compression residual stresses

$n = \frac{2(\alpha_p - \alpha_o)}{\alpha_p(\alpha_p^2 - 1)}$

$\alpha_p = \sqrt{\sigma_y/\sigma_p}$

Haaijer and Thurlimann suggested values for α_o for three types of compression elements and showed that they are nearly independent of the amount of rotation restraint offered along the unloaded edges. For hinged webs, they found $\alpha_o = 0.579$, and for fixed webs, $\alpha_o = 0.588$. For simplicity, they suggested using $\alpha_o = 0.58$ for web plates supported along all four edges. By definition, then, when $\alpha_o = 0.58$, the web plate in a wide-flange member may be uniformly compressed up to strain-hardening without the occurrence of local buckling.

Knowing the maximum residual compressive stress in a specimen, σ_r, it is possible using Equation 5.9 to plot σ_{cr}/σ_y versus α. Using Equations 5.7 and 5.8, it is also possible to determine the limiting value of h/w for any value of σ_{cr}/σ_y. Haaijer did this for his test results and found that good correlation existed for webs and flanges subjected to pure compression. However no tests were conducted to determine the behaviour of web plates subjected to combined in-plane bending and axial compression.

Haaijer and Thurlimann realized the importance of extending the previous considerations to cases of plates subjected to combined bending and axial load. The web of a wide-flange section, subjected to an axial load P and a bending moment M, presents such a case. Depending upon the ratio of axial load to moment, the neutral axis may lie inside or outside of the web. For the case of combined in-plane bending and compression, they suggested that Equation 5.8 could still be used to describe the behaviour of a web plate if an appropriate plate buckling coefficient "K" could be determined. This is because α is a function of the maximum critical strain in the web and the web slenderness ratio h/w.

The minimum values for "K" for a stress distribution of a fully-plastified wide-flange section are shown in Figure 5.3. For any loading condition except pure compression, attaining the necessary stress distribution

would require that the ratio of the maximum compressive strain in the web to the yield strain be infinite. For the two limiting cases, pure bending is represented by $y_o/h = 0.5$, and pure compression by $y_o/h = 1.0$.

For an expedient solution to the determination of the values of α as a function of the ratio of the maximum strain to the yield strain in the web, Haaijer and Thurlimann plotted experimentally determined values of α as a function of the critical strain (ε_{cr}) for Haaijer's three pure compression tests failing by web buckling.

For a beam-column web, defining the maximum strain of the compression flange to be ε_m and assuming that the average strain over the compression zone in the web would be $\varepsilon_m/2$, it was graphically determined that for web plates:

For $\varepsilon_m/\varepsilon_y = 12$, $\alpha = 0.58$;

$\varepsilon_m/\varepsilon_y = 8$, $\alpha = 0.60$;

$\varepsilon_m/\varepsilon_y = 4$, $\alpha = 0.69$.

Using the assumptions stated in Chapter 2, web slenderness limits were proposed by Haaijer and Thurlimann[8]. These form the basis for the CSA S16-1969 web slenderness limitations. However, as has been noted, no tests on web plates subjected to combined axial load and moment were conducted for experimental verification.

Although good correlation was found to exist between Haaijer and Thurlimann's theory for plates in pure compression and their test results, in extending this same theory to apply to web plates subjected to combined axial load and moment, some assumptions of doubtful validity were used:

1. In determining the values of K for Equation 5.8 (Figure 5.3), a stress distribution corresponding to that of a fully-plastified wide-flange section was assumed. For all loading cases except pure compression, this would mean that the member would be required to deform until the condition $\varepsilon_m/\varepsilon_y = \infty$ had been reached.
2. The ratio of the maximum compression flange strain to the yield strain ($\varepsilon_m/\varepsilon_y$), would reach a value of four for members required to deform plastically.
3. It was also assumed that the maximum compressive strain in the compression flange would be ε_m and the average strain over the compression zone in the web would be taken as $\varepsilon_m/2$. This implies that the analysis is for a plate in uniform compression with a width equal to the depth of the compression zone of the web.

Since Perlynn and Kulak[5] were not able to satisfactorily correlate their test results for compact beam-columns with Haaijer and Thurlimann's web buckling theory, it was decided that this theory did not adequately describe beam-column behaviour. This was considered to be at least partly attributable to the assumptions used in the theory.

Based on their test results, and the test results from another investigation[9], Perlynn and Kulak recommended higher web slenderness ratios for both compact and non-compact beam-columns and these have been incorporated into the most recent CSA Standards[6,7].

5.2 Investigation Leading to Recent CSA Standard Revisions

Because of the proportions of their test specimens, Perlynn and Kulak[5] were able to closely establish experimentally the limit of web slenderness at which a compact member would have its compression flange and web buckle simultaneously (Figure 5.4). Having established this limit, they then developed two methods to predict the occurrence of web buckling.

Method I consisted of developing two relationships, one between the web slenderness h/w, and the ratio of the depth of the neutral axis to the web depth y/h,

and the other between P/Py and y/h. By equating the two relationships, h/w can be obtained as a function of P/Py. Since residual stresses were expected to affect the test results, they were taken into account.

By addition of the strain diagrams for axial load, moment and residual stresses, it is possible to determine the location of the neutral axis as represented by the y/h ratio (Figure 5.5). Since only one of the investigators quoted by Perlynn and Kulak determined the residual stress patterns in his test specimens[19], typical residual stress patterns for both rolled and welded members[20,21] for the other investigators' test results were assumed (Figure 5.6).

For their own test results, Perlynn and Kulak determined the y/h ratios by graphically determining the combined strain diagrams for each member at the applied load and ultimate moment. The resulting stress distributions were obtained from the superposition of the strain diagrams for axial load, ultimate moment (Mu), and the assumed residual stresses. They were able to show that at ultimate conditions, different assumed residual stress patterns do not greatly affect the resulting y/h ratio for a member, primarily because residual stress patterns possess symmetry and a certain degree of consistency in magnitude. In particular, the value of 15 ksi for the maximum compressive residual stress is considered to be typical for most deep rolled and welded wide-flange sections.

Perlynn and Kulak then plotted their test results, along with the test results of the three other investigations on a graph of y/h versus P/Py (Figure 5.7). It was noted that the resulting relationship was very nearly linear for P/Py < 0.8, and could be represented by:

$$\frac{y}{h} = 0.4463 \frac{P}{Py} + 0.607 \qquad (5.10)$$

When P/Py = 1.0, y/h is theoretically infinite. It is not obvious how the function behaves for $0.8 \leq P/Py \leq 1.0$. If a member that is loaded into the strain-hardening range (P/Py > 1.0) had a very small moment applied to its ends, the y/h ratio would quickly diminish from infinity. Hence Perlynn and Kulak assumed only that y/h starts to increase towards infinity for P/Py > 0.8.

For the second relationship, y/h versus h/w, test results were again plotted (Figure 5.8). This figure has been plotted as y/h vs $\frac{h}{w}\sqrt{Fy}$ so that the results of the present investigation could be plotted on the same graph. At this point, it was realized that two boundaries describing member failure were possible. One of these describes the web slenderness limits at which flange buckling ceases to be critical and web buckling becomes the mode of member failure. For web slenderness ratios that plot on this line, $M/Mpc \geq 1.0$. The other boundary (not plotted here) describes

the web slenderness limits at which a member would cease to reach M/Mpc = 1.0, irrespective of the mode of failure. These boundaries were determined primarily by observation of the types of failures of the specimens. Some judgement was required in determining these boundaries, although they are thought to be on the conservative side.

The boundary of interest is the one that describes the web slenderness limits when flange buckling ceases to be the mode of member failure because it yields the more conservative web slenderness ratio. Simultaneous flange and web plate buckling was found to occur at (Figure 5.8):

$$\frac{y}{h} = \frac{(8.20 - 0.100(h/w))^{(2.6)} + 61}{100} \qquad (5.11)$$

By combining Equations 5.10 and 5.11, Perlynn and Kulak determined that the boundary describing simultaneous web and flange plate buckling (and for which M/Mpc ≥ 1.0) was given by

$$\frac{P}{Py} = \frac{(8.20 - 0.100(h/w))^{(2.6)} + 0.3}{44.63} \qquad (5.12)$$

Equation 5.12 gave reasonably good correlation with the test results.

Method II consists of finding $\frac{h}{w}\sqrt{Fy}$ as a function of P/Py by using a revised form of Equation 2.3 (Equation 5.8). Using the results of four different experimental programs, they were able to find values of α for the various specimens by using Equations 5.7 and 5.8.

Knowing these α values, it is possible to calculate a modified K value using Equation 5.8, designated K'. This K' parameter was then plotted against $\frac{h}{w}\sqrt{Fy}$ to obtain a relationship between $\frac{h}{w}\sqrt{Fy}$ and K'. Substitution of h/w as a function K' into Equation 5.12 from Method I gives a relationship between K' and P/Py. This expression can then be substituted into Fquation 5.8 to find the relationship between $\frac{h}{w}\sqrt{Fy}$ and P/Py.

Although this method utilizes the results of Method I, it is in fact a different procedure, and is based directly on Haaijer and Thurlimann's buckling theory. Because the experimental test results were used for the determination of the relationships used in this development, it is expected that K' will reflect the inelastic plate buckling properties of the members tested.

In determining the α values from Equations 5.7 and 5.8, it is necessary to calculate $\sigma cr/\sigma y$ for the specimens. The maximum strain in the compression flange-to-web junction, at the ultimate moment, is determined from the experimental results. This is then converted to stress and

divided by the yield stress of the specimen to give the σ_{cr}/σ_y ratio.

Of the four experimental programs considered, only Haaijer's[4] had specimens where $\sigma_{cr}/\sigma_y > 1.0$. Although many tests in the other investigations showed that the yield strains in the compression flange-to-web junction were surpassed, none had attained strain-hardening. Since Haaijer and Thurlimann's transition curve, described by Equation 5.9, is not valid for σ_{cr}/σ_y ratios greater than 1.0, Perlynn and Kulak assumed that if σ_{cr}/σ_y was greater than 1.0, then $\sigma_{cr}/\sigma_y = 1.0$. This is because Equation 5.9 implies that once a member reaches $\sigma_{cr}/\sigma_y = 1.0$, it is in the strain-hardening range and Equation 5.9 is no longer applicable.

Perlynn and Kulak then plotted the various transition curves corresponding to the four investigations under consideration. They noted that the residual stress distribution caused the steels with the lower yield stresses to reach the proportional limit at a lower applied load than the higher yield strength steels. Hence the transition curves were not coincident for the investigations they considered.

In order to plot the transition curves, Perlynn and Kulak assumed $\alpha_o = 0.58$, a value suggested by Haaijer and Thurlimann. Using Equation 5.9, they then calculated the

corresponding value of α knowing σ_p, σ_y, σ_{cr}, α_o, and α_p. Since zero raised to a power greater than zero equals zero, they were able to prove that $\alpha = \alpha_o = 0.58$ when $\sigma_{cr}/\sigma_y = 1.0$. By doing this, it appeared that their specimens not failing by web buckling had $\alpha = \alpha_o = 0.58$. Since by definition, when $\alpha = \alpha_o$, the point of strain-hardening has been achieved, this in effect states that these particular specimens were able to reach strains greater than the yield strain before buckling occurred. Because the material yielded in slip-bands[15], some of the material reached strain-hardening. Perlynn and Kulak, on the other hand, state that none of their specimens reached the point of strain-hardening, meaning that the specimens as a whole did not reach strain-hardening, but some of the material did.

Perlynn and Kulak then solved for K' using Equation 5.8. Following this they obtained a linear approximation to the relationship of K' vs $\frac{h}{w}\sqrt{Fy}$ (Figure 5.9):

$$K' = \frac{0.48\ (h/w)\ \sqrt{Fy}}{\sqrt{Fy}} - 9.6 \qquad (5.13)$$

Next, K' was found as a function of P/Py. Referring to Method I, substituting Equation 5.12 into Equation 5.13 results in:

$$K' = 29.76 - 20.68\ (P/Py)^{(0.385)} \qquad (5.14)$$

Finally, substitution of K' in Equation 5.4 for K in Equation 5.8 results in an expression relating $\frac{h}{w}\sqrt{Fy}$ to P/Py:

$$\alpha = \frac{h}{100w}\sqrt{Fy}\sqrt{\frac{0.01241}{1 - 0.695\ (P/Py)^{0.385}}} \qquad (5.15)$$

where E = 30 X 10^6 psi and ν = 0.3.

From this, they assumed that since α = 0.58 appeared to be the limiting value from their test results, they substituted this value into Equation 5.15 to obtain an expression between $\frac{h}{w}\sqrt{Fy}$ and P/Py. This limit was set to ensure that the web component part of a member will reach the yield stress of the material, to a depth of about h/4 below the compression flange-to-web junction before web buckling will occur. This depth of h/4 corresponds to $\varepsilon_m/\varepsilon_y$ = 2.0 which is the maximum ratio of compressive web strain to yield strain recorded for their tests on compact beam-columns. The expression is:

$$\frac{h}{w}\sqrt{Fy} = 520\sqrt{1 - 0.695(P/Py)^{0.385}} \qquad (5.16)$$

which is the same as Equation 2.4. This expression is plotted in Figure 5.4.

This procedure was shown to give the same results as Method I, hence the usefulness of their results and procedures seems to be verified. Perhaps this is because uniform compression of a web plate up to strain-hardening (for which Haaijer and Thurlimann[8] recommended $\alpha = 0.58$) may be equivalent to combined axial load and bending moment up to the yield stress for an equivalent web depth of about h/4 (for which Perlynn and Kulak[5] used $\alpha = 0.58$). This could be rationalized by considering the extra rotational deformation, and hence the additional strain the compression part of the web must undergo when bending is present, as compared with pure compression.

5.3 Analysis of Present Investigation Test Results-Method I

As given here, Method I of predicting web buckling is analogous to the Method I used by Perlynn and Kulak[5] in their investigation of compact beam-columns. The y/h ratios for the specimens are first determined and then these are plotted as a function of P/Py in order to establish a relationship between y/h and P/Py. Then, y/h is plotted as a function of $\frac{h}{w}\sqrt{Fy}$ to find a relationship between y/h and $\frac{h}{w}\sqrt{Fy}$. The two relationships containing the y/h ratios are then equated to determine the allowable slenderness ratio $\frac{h}{w}\sqrt{Fy}$ for non-compact beam-columns as a function of P/Py. The procedure followed was then the same as that used by

Perlynn and Kulak as described in Section 5.2.

Once the neutral axis had been located in this way for all the specimens in this test series, and for the non-compact beams tested previously[9], the y/h values were plotted as a function of P/Py (Figure 5.7). These data are also tabulated in Table 5.1. The relationship shown in Figure 5.7 follows the same general trend as that observed earlier for compact beam-columns. From the plot, it was determined that the relationship for $P/Py < 0.8$ is:

$$\frac{y}{h} = 0.410 \frac{P}{Py} + 0.700 \qquad (5.17)$$

As was the case for compact beam-columns, it is not obvious how the function behaves for $P/Py > 0.8$. In theory, it is possible that it reaches infinity at $P/Py = 1.0$, and this is what has been indicated here.

In order to obtain the second relationship, y/h is plotted against the slenderness ratio $\frac{h}{w}\sqrt{Fy}$ (Figure 5.8). On this plot, the type of failures undergone by each specimen and their respective Mu/My ratios are also indicated. Judgement had to be used here to plot a reasonable curve for simultaneous web and flange buckling, as indicated by the failure mode of the specimens and their Mu/My ratios. The limiting web slenderness of interest is the one where the specimen will fail by simultaneous web and flange buckling

and for which Mu/My ≥ 1.0. Hence, the curve should pass between specimens 5 and 6 because specimen 5 failed by simultaneous web and flange buckling and specimen 6 failed by flange buckling. Moreover, the Mu/My ratios dictated than the curve pass somewhere near the mid-point between the two specimens, where linear interpolation indicated Mu/My = 1.0 should exist. A similar determination was made for specimens 3 and 4, and the curve was fitted to pass between the points representing these two specimens. The curve shown is probably conservative for P/Py > 0.2 because it indicates a less slender limit than the specimens which failed by simultaneous web and flange buckling and had Mu/My > 1.0 (Specimens 3 and 5). However for specimens 1 and 2, the curve appears to be unconservative because of both the Mu/My ratios and the mode of specimen failure. Because both specimens 1 and 2 failed by web buckling, the curve would normally be placed such that the expected maximum slenderness limit would be a lesser slenderness than specimen 2. However, because the Mu/My ratio was less for specimen 2 than specimen 1, the curve was placed near specimen 2 in the gap between specimens 1 and 2. This was done by judgement. Perlynn and Kulak's investigation offered some guidance as to the expected shape of the curve. From here, the curve was extended to reach approximately the mid-point of the gap between the beam specimens NC-1 and NC-2. The resulting curve is thought to be a conservative estimate of the limit of simultaneous web and flange failure

for non-compact members. Even though specimen 2 did not appear to fit the test results perfectly, it was felt that this had more to do with errors of unknown magnitude in the test procedure rather than the analysis, and so the curve was considered to be a conservative estimate. The equation describing the relationship between y/h and P/Py is:

$$\frac{y}{h} = 1.578 \times 10^{-7}\left(690 - \frac{h}{w}\sqrt{Fy}\right)^{2.6} + 0.70 \qquad (5.18)$$

Combining equations 5.17 and 5.18 results in a relationship between $\frac{h}{w}\sqrt{Fy}$ and P/Py. This estimate of the boundary of the failure limit due to simultaneous web and flange buckling is:

$$\frac{h}{w}\sqrt{Fy} = 690\left[1.0 - 0.425\ (P/Py)^{0.385}\right] \qquad (5.19)$$

This equation has been plotted in Figure 5.10, along with Perlynn and Kulak's theoretical prediction for compact members (Equation 5.16).

5.4 Analysis of Present Investigation Test Results-Method II

Analogous to Method I, Method II is similar to the second procedure used by Perlynn and Kulak[5] to determine the maximum web slenderness limits.

First, the values of α for the specimens (including the non-compact beams of Holtz and Kulak[9]) were calculated. For the beam-columns, this was done by calculating the average strain of the web strain gauge readings closest to the web to compression flange junction, and then converting this strain to stress using E = 29600 ksi. If the strain was greater than the yield strain, α was taken to be equal to 0.58. For the specimens where this averaged strain was less than the yield strain, the appropriate value of α was calculated using either Equation 5.7 or 5.8. It was felt that these strain readings would not be adversely affected by the presence of residual strains, because the assumed residual strain distribution is small where these two strain gauges were located on the web. For the beams, the values of α were calculated by choosing the maximum compressive stress in the web as obtained by adding up the total stress due to the sum of the assumed residual stress, the stress due to the moment, and the stress due to the axial load. Once the maximum stress in the web was determined, it was substituted into Equation 5.7 and the α value was calculated. These data are also tabulated in Table 5.1, and are plotted in Figure 5.11.

After the values of α were calculated, they were substituted into Equation 5.8 and a new value of K, called K', was calculated for each specimen. This K' parameter was then plotted against $\frac{h}{w}\sqrt{Fy}$, to obtain a relationship between these parameters. This relationship is also plotted in Figure 5.9. In this figure, the solid line represents the results of the present investigation (E = 29600 ksi), and the dotted line represents the test results considered by Perlynn and Kulak which did not fail by web buckling (E = 30000 ksi). The points plotted which are not near the curves are the four specimens considered in this investigation which buckled in the web. The remaining four specimens are plotted on the curve.

From this plot, it is possible to conclude two things. The first conclusion is that the plots for K' versus $\frac{h}{w}\sqrt{Fy}$ from the separate investigations are coincident within experimental error. This indicates that K' is not a function of the cross-sectional proportions of the specimens involved. Indeed, Perlynn and Kulak originally used the results from three other testing programs as well as their own to obtain the curve. The second thing of note is that any specimen which failed by web buckling plots above the curve. It is, for example, reasonable to assume that specimen 2 buckled in the web, because it is considerably above the curve. Perlynn and Kulak represented their test results with Equation 5.13, which is a linear approximation

to the curved line they obtained by plotting the points corresponding to the specimens they were considering which did not fail by web buckling. A better representation of the curve, using a parabolic approximation, is:

$$K' = 0.000111 \left(\frac{h}{w} \sqrt{Fy}\right)^2 \qquad (5.20)$$

It is considered that this curve represents a reasonable approximation to the maximum web slenderness which a specimen may have (in terms of K') before a specimen will fail by web buckling.

Next, substitution of the results of Method I (Equation 5.19) into Equation 5.20 will give a relationship between K' and P/Py:

$$K' = 0.000111 \left[690 - 293.1 \, (P/Py)^{0.385}\right]^2 \qquad (5.21)$$

Substitution of Equation 5.21 into Equation 5.8 should result in another expression to determine the maximum limit of web slenderness, provided a suitable value for α can be chosen. Perlynn and Kulak had $\alpha = 0.58$ for all their specimens not failing by web buckling. For the present investigation, however, α varies, although it is equal to

0.58 for all the specimens not failing by web buckling. Hence, it was decided to use $\alpha = 0.58$, and see if the results would be meaningful. Assuming $\alpha = 0.58$, E = 29600 ksi, and $\nu = 0.3$, this results in:

$$\frac{h}{w}\sqrt{Fy} = 690\,[1.0 - 0.425(P/Py)^{0.385}] \qquad (5.22)$$

Note that this equation is identical to Equation 5.19, and both methods therefore yield the same result. This expression is thought to be a reasonable estimate of maximum web slenderness for non-compact beam-columns. The plot of this expression along with the test specimens is shown in Figure 5.12.

5.5 Discussion of Analytical Results

In spite of the difficulty of reducing the data obtained from specimen 2, which had a difficult failure mechanism to interpret, the analyses did indicate a reasonable prediction of the expected limit of simultaneous web and flange buckling.

Because the curve for K' vs $\frac{h}{w}\sqrt{Fy}$ corresponded to that of Perlynn and Kulak's[5], which in itself utilized data from four separate investigations, it was safe to

assume that any points which plotted above this line failed by web buckling. This aided the analysis especially with regard to specimen 2, and substantiated the opinion that this specimen failed by web buckling.

Since the expressions for maximum web slenderness turned out to be identical using the two methods of analysis, it appears that a choice of $\alpha = 0.58$ in Method II for specimens not failing by web buckling is justified. Indeed, if Equation 5.20 is substituted into Equation 5.8 with $\alpha = 0.58$, $\nu = 0.3$, and $E = 29600$ ksi, Equation 5.8 reduces to the trivial identity $0 = 0$. Hence the results of Method I will always be the solution of Method II, provided $\alpha = 0.58$. Therefore Perlynn and Kulak's conclusion that web buckling invariably occurs before flange buckling or simultaneous web and flange buckling if α is greater than 0.58 seems to be extendable to the case of non-compact beam-columns.

It should be noted that the curve determined by the analyses (Figure 5.12) appears to be slightly non-conservative in the region of $P/Py = 0.15$. In particular, it appears as if the curve indicating the limit for simultaneous web and flange failure lies above a specimen known to have failed by web buckling. This is due to the shape of the curve used to predict simultaneous web and flange buckling (Figure 5.8). In this figure, the curve of expected simultaneous web and flange failure is on the

unconservative side of specimen 2. Since both methods of analysis utilized the results of this plot, and its associated relationship (Equation 5.18), the results of the theoretical analyses will also appear unconservative in the region near specimen 2. A recommended design approximation should then be reduced slightly in this region to take care of this inconsistency.

The two methods used in the analysis portion of this investigation yield what appears to be identical results. Although Method II appears to be similar to Method I and utilizes the results from Method I, it is essentially based upon Haaijer and Thurlimann's web buckling theory.

During the tests, it was noted that the greatest value of the ratio of the averaged maximum strain to the yield strain ($\varepsilon_m/\varepsilon_y$) at the web to compression flange junction was 2.5 (Specimen 6). It appears as if the compression flanges strained approximately the same amounts as those in Perlynn and Kulak's investigation. Since α is a function of the critical strain (ε_{cr}), and the amount of straining is reasonably consistent in both investigations, it appears as if using $\alpha = 0.58$ can be justified by this consideration for this investigation, as it was used successfully by Perlynn and Kulak to predict the web slenderness limit for compact members.

It appears as though Haaijer and Thurlimann's[8] recommendation of $\alpha = 0.58$ for uniform compression of web plates up to strain-hardening is also applicable to the case of compact and non-compact beam-columns subjected to axial load and moment which did not fail by web buckling. This is due to the behaviour of the material, because it yields in slip-bands[15]. Since the material cannot be at strains between the yield strain ε_y, and the strain at the start of strain-hardening ε_{st} (Figure 5.1), $\alpha = 0.58$ appears to apply to any web where the yield strains have been surpassed.

The maximum value of the strain ratio ($\varepsilon_m/\varepsilon_y$) at approximately h/4 of the web was 0.81 (Specimen 6). Hence the supposition that the y/h ratio would not be substantially affected if the effects of the yield stress having been attained at some location in the web were ignored seems to be justified. This is because, for the worst case, the web has not reached the yield stress closer than 0.4h to the point where the total stress is zero. It also appears as if the web in non-compact beam-columns does not have to be stocky enough to prevent failure until the yield stress has been surpassed to a depth of h/4, but rather to a depth of h/6 or h/8.

At this point, it is useful to compare the analytical results with those expected when the specimen design was done. In Appendix I, the specimens were expected

to have a value of α of approximately 0.8, while in the analysis, the limit of web slenderness was shown to be $\alpha = \alpha_o = 0.58$. This can be resolved by taking a closer look at the equations used for these calculations. In general, the equations have the following form:

$$\frac{h}{w}\sqrt{Fy} = C\,[1.0 - D(P/Py)^{0.385}]^{x} \qquad (5.23)$$

where x = 0.5 if Perlynn and Kulak's approximation for K' vs $\frac{h}{w}\sqrt{Fy}$ is used (Equation 5.13), and x = 1.0 if Equation 5.20 is used.

When the specimen design was done, Perlynn and Kulak's equation was used, where C = 690 and 750, D = 0.695, and x = 0.5. This value of D led to the prediction of α being approximately equal to 0.8.

The analysis, however, indicates that a close approximation to the same curve can be generated by using different values of α and D, for a given value of x. Therefore, the apparent change in values of α between that expected and that obtained can be explained by noting that the value of D in Equation 5.23 varies for the two investigations, for a consistent use of either Equation 5.13 or 5.20.

It is useful to note that the differences in slenderness ratio between P/Py = 0 and P/Py = 1 is approximately the same for both compact and non-compact beam-columns (Figure 5.10). This difference is approximately 280 and can be expressed mathematically by:

$$CD = 280 \tag{5.24}$$

The constants C and D are thus related and seem to be reasonably independent of flange slenderness.

Hence, it appears possible that any flange cross-section (plastic design, compact, non-compact, or other) can have the appropriate web slenderness limit calculated by using Equation 5.23, provided the value of C has been established from an appropriate beam test, and D has been obtained from Equation 5.24. Therefore, once the flange slenderness has been chosen on the basis of the desired amount of rotation, it should be possible to predict any beam-column web slenderness limit by this procedure.

SPECIMEN	P/Py	Mu/My	y/h	σ_{cr}/σ_y	α	K'	$\frac{h}{w}\sqrt{Fy}$	FAILURE
1	0.15	1.16	0.74	0.98	0.76	26.46	639.4	W
2	0.15	0.99	0.76	0.96	0.82	15.87	534.2	W
3	0.30	1.12	0.82	1.00	0.58	38.77	590.7	W&F
4	0.30	1.20	0.81	1.00	0.58	26.48	488.2	F
5	0.70	0.79	0.97	1.00	0.58	27.91	501.2	W&F
6	0.70	1.53	0.95	1.00	0.58	17.87	401.1	F
NC-1•	0.00	1.04	0.70	0.75	1.13	13.33	674.8	W
NC-2•	0.00	1.02	0.70	0.74	1.14	15.41	732.0	W

•From Holtz and Kulak[9]

TABLE 5.1

SPECIMEN TEST DATA

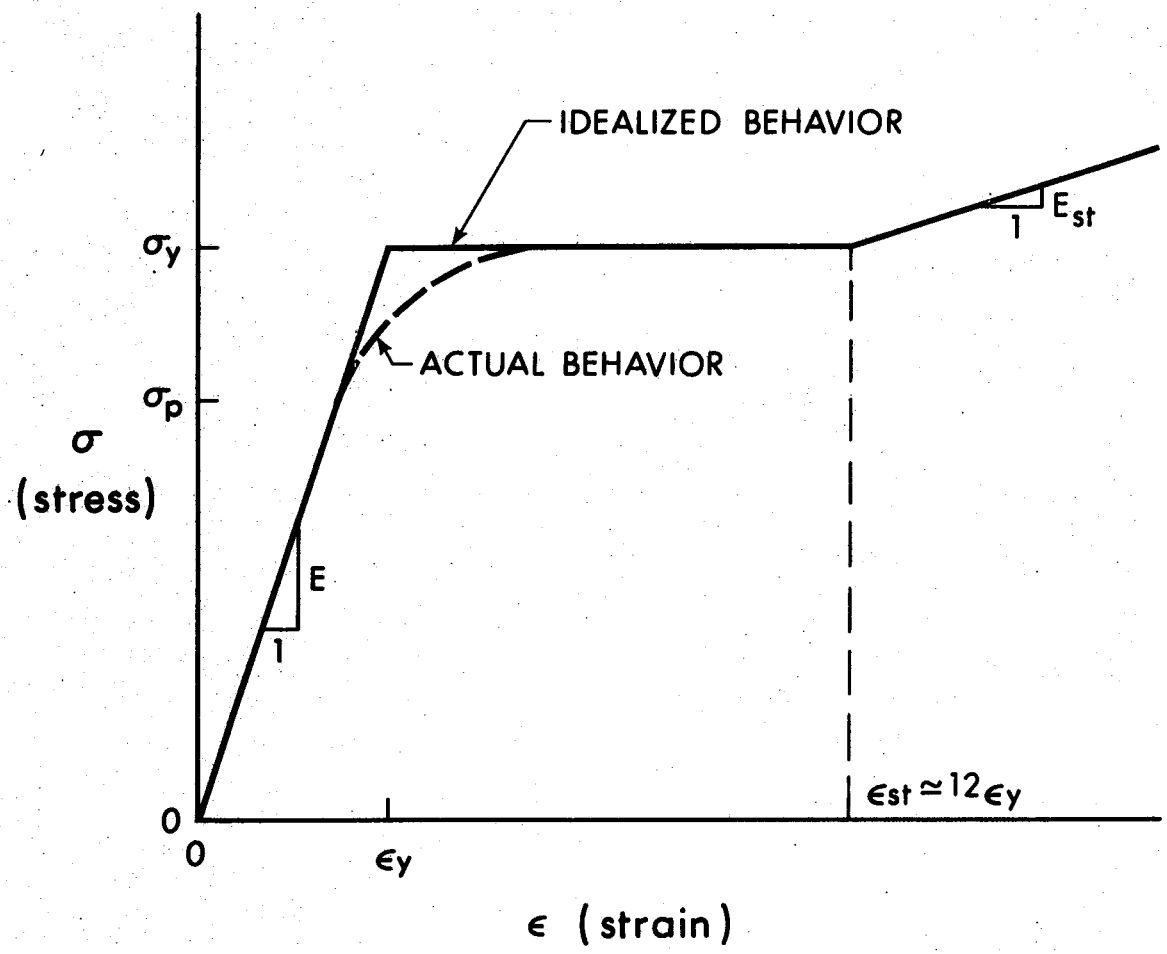

FIGURE 5.1

IDEALIZED STRESS-STRAIN DIAGRAM

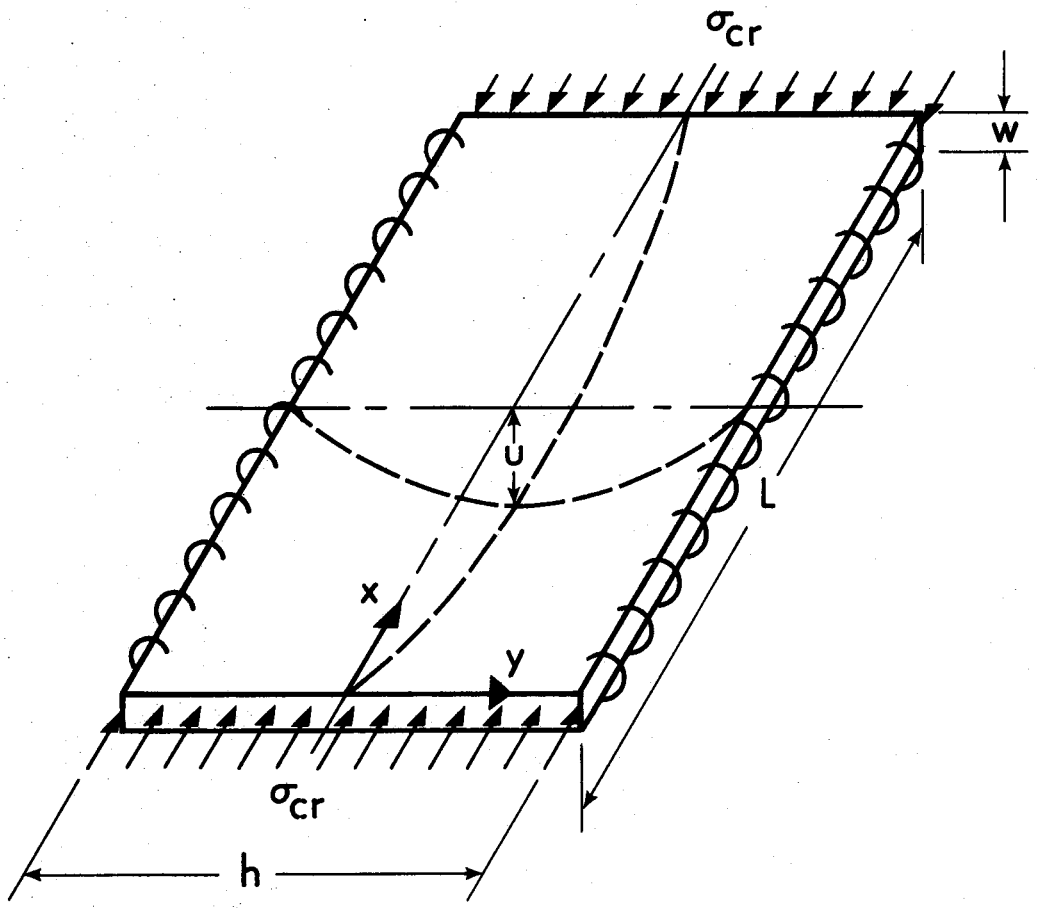

FIGURE 5.2

PLATE BUCKLING MODEL

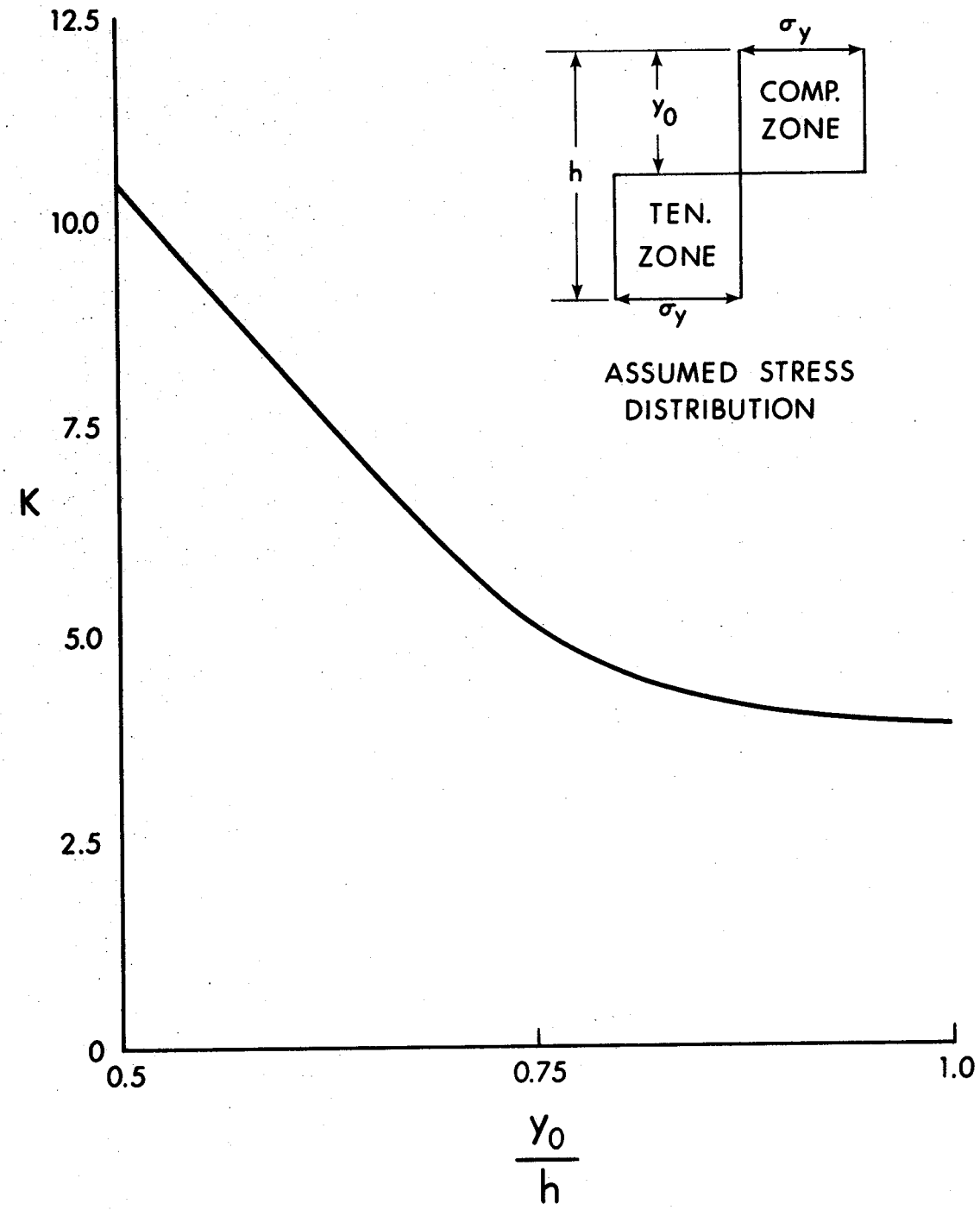

FIGURE 5.3

PLATE COEFFICIENT FOR FULLY PLASTIFIED WIDE-FLANGE SECTIONS UNDER AXIAL LOAD AND MOMENT

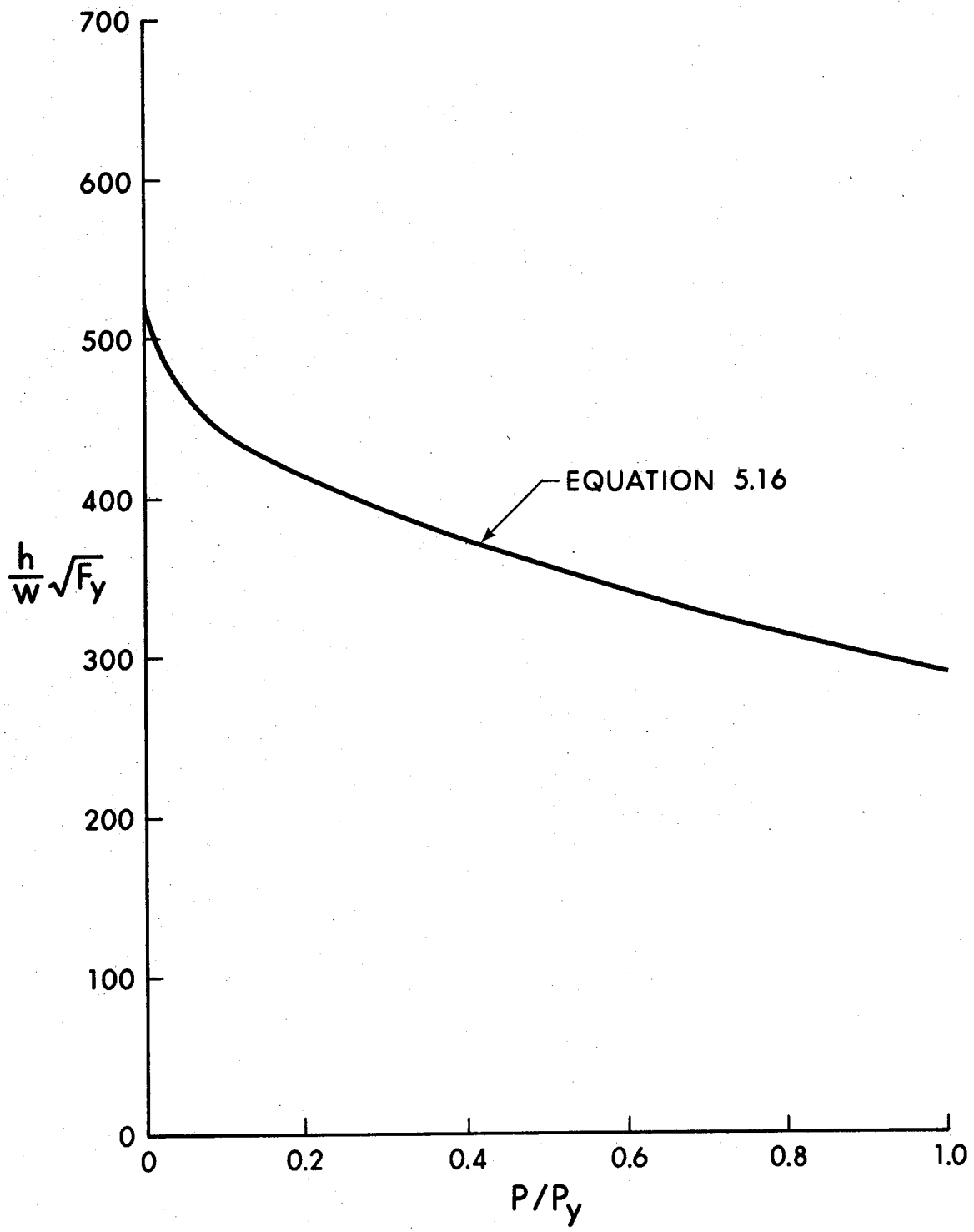

FIGURE 5.4

THEORETICAL LIMIT OF WEB SLENDERNESS FOR COMPACT MEMBERS

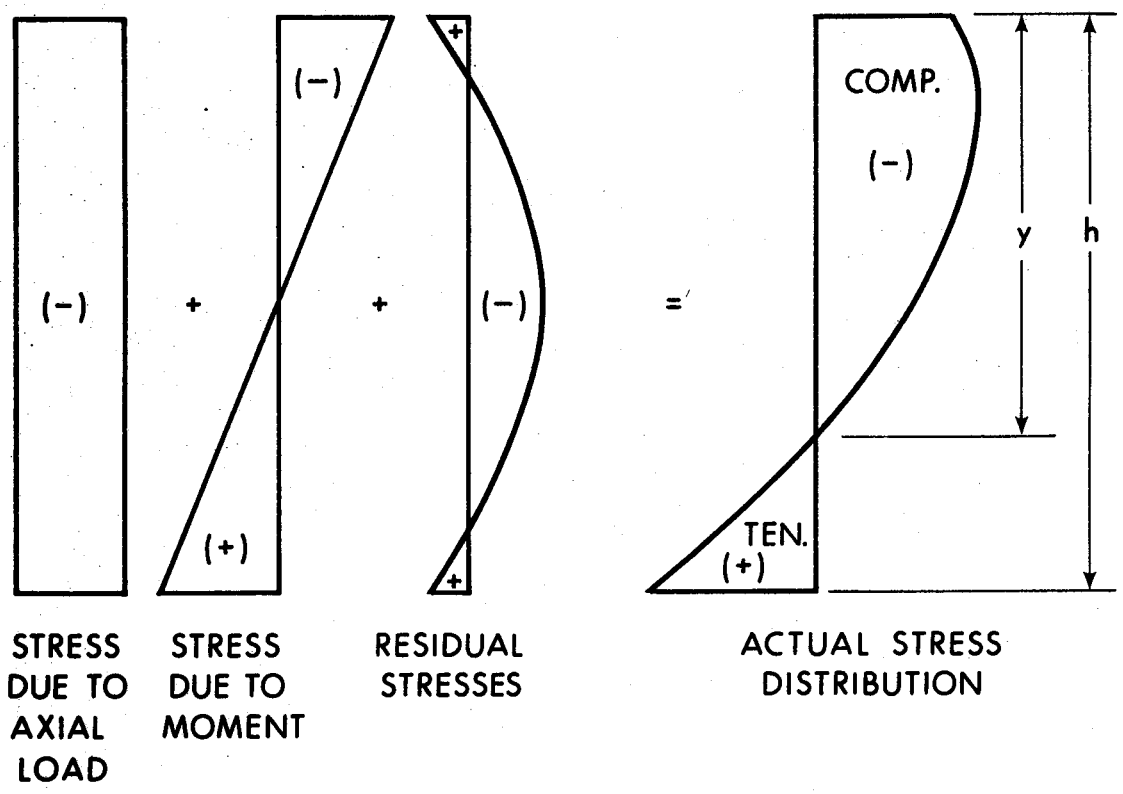

FIGURE 5.5

ACTUAL STRESS DISTRIBUTION INCLUDING RESIDUAL STRESSES

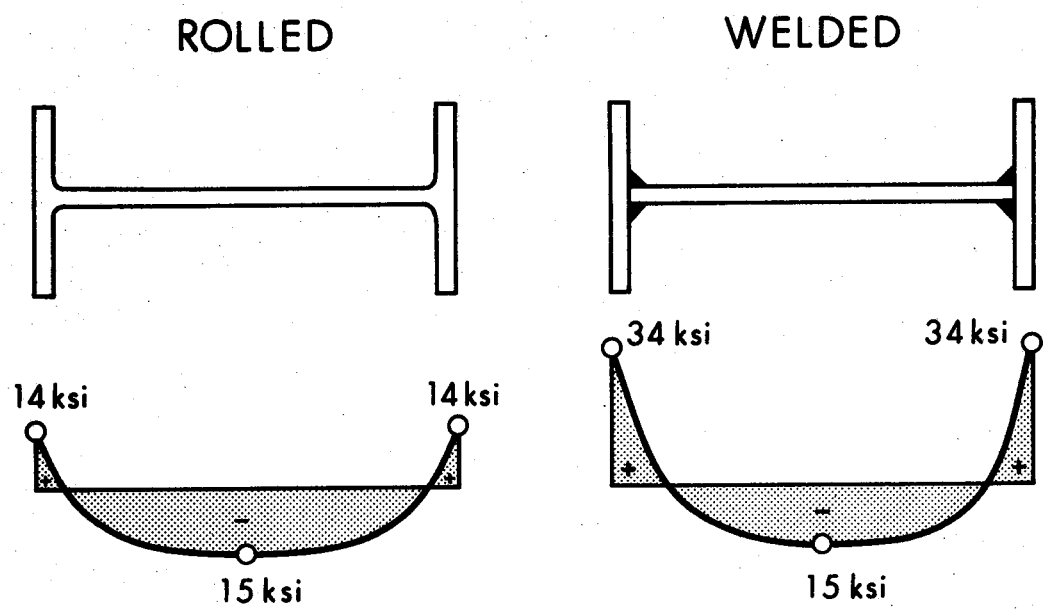

FIGURE 5.6

TYPICAL RESIDUAL STRESSES FOR ROLLED AND WELDED MEMBERS

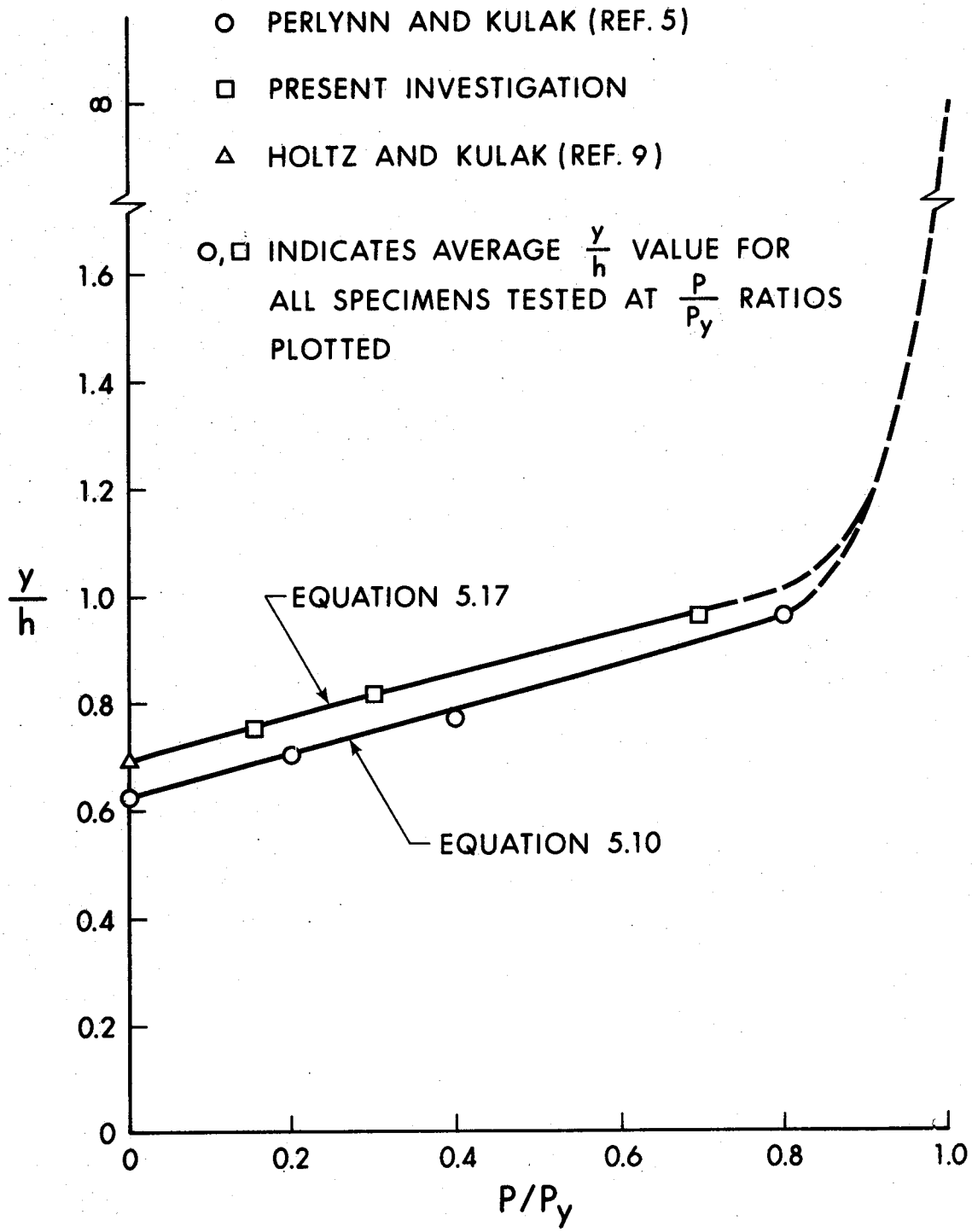

FIGURE 5.7

y/h AS A FUNCTION OF P/Py (COMPACT AND NON-COMPACT)

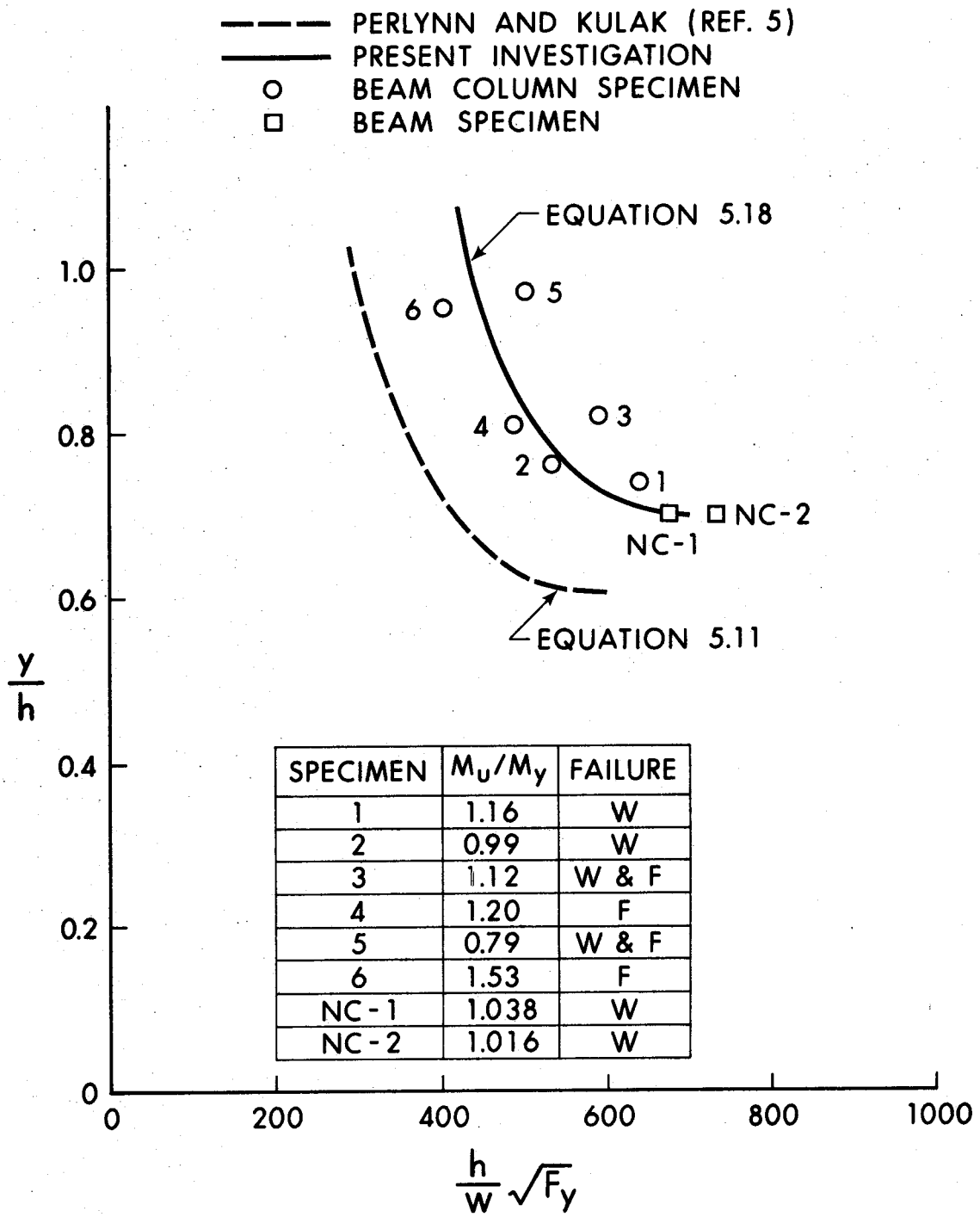

SPECIMEN	M_u/M_y	FAILURE
1	1.16	W
2	0.99	W
3	1.12	W & F
4	1.20	F
5	0.79	W & F
6	1.53	F
NC-1	1.038	W
NC-2	1.016	W

FIGURE 5.8

y/h AS A FUNCTION OF $\frac{h}{w}\sqrt{Fy}$ (COMPACT AND NON-COMPACT)

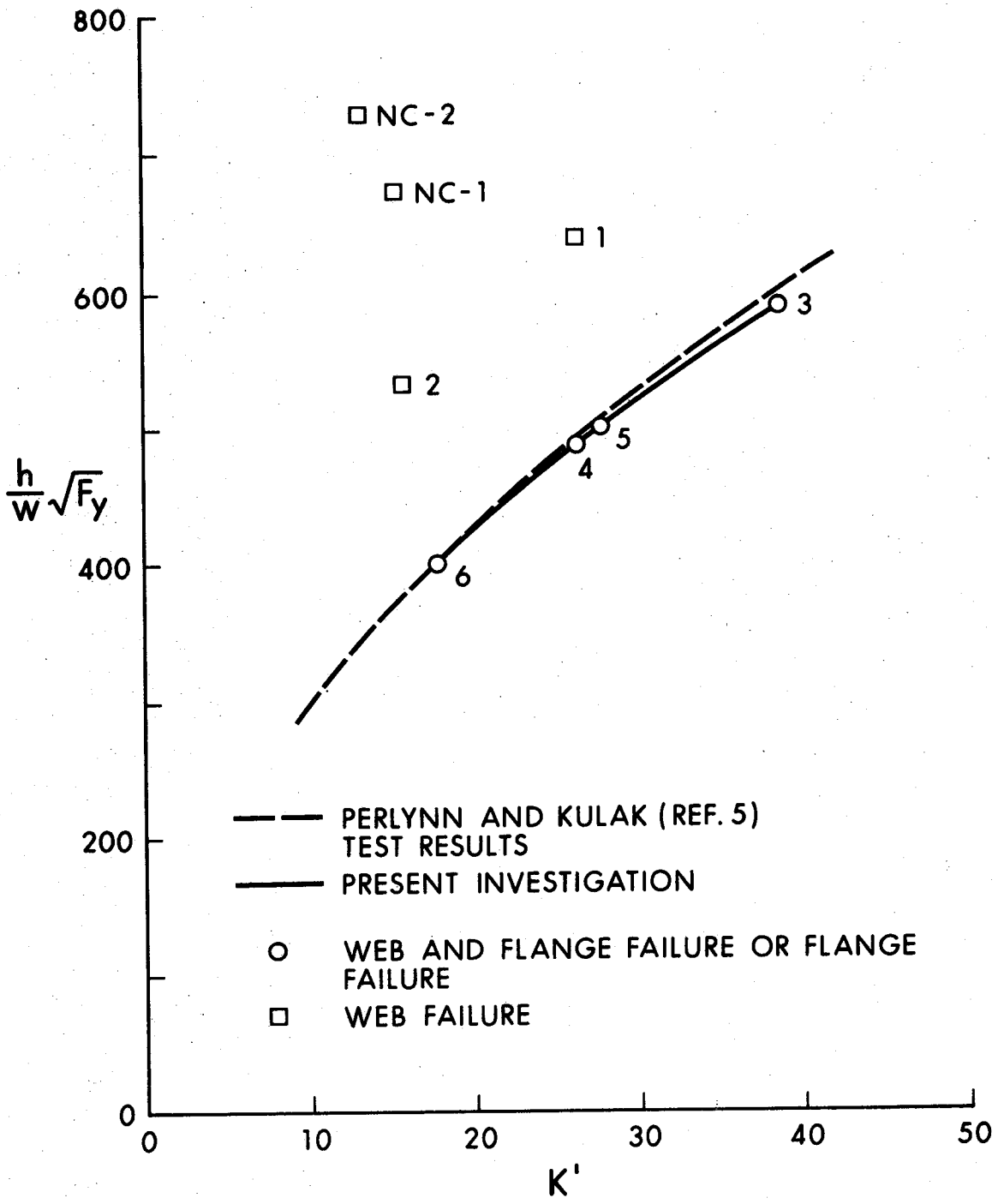

FIGURE 5.9

K' AS A FUNCTION OF $\frac{h\sqrt{Fy}}{w}$ (COMPACT AND NON-COMPACT)

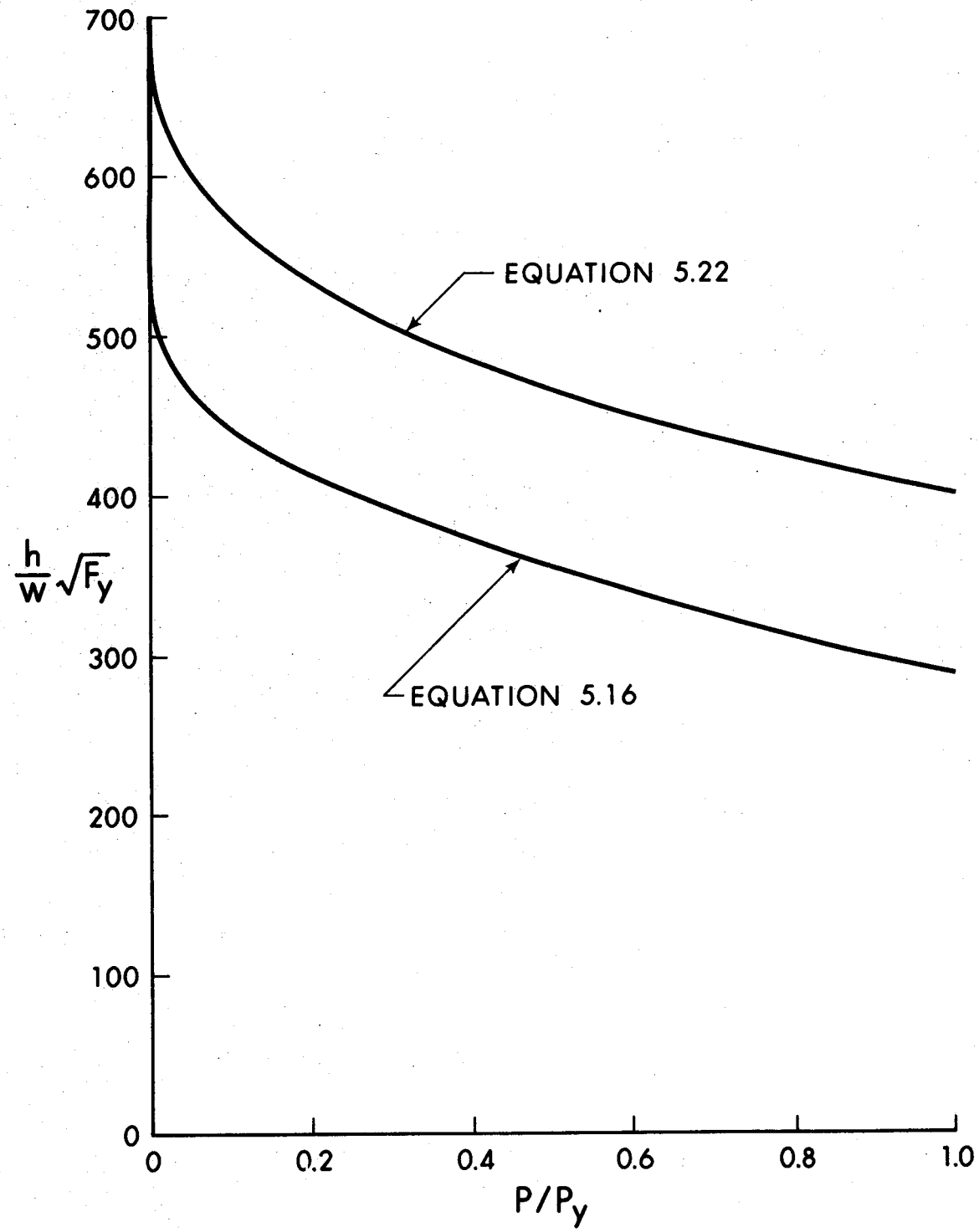

FIGURE 5.10

THEORETICAL COMPACT AND NON-COMPACT

BEAM-COLUMN WEB SLENDERNESS LIMITATIONS

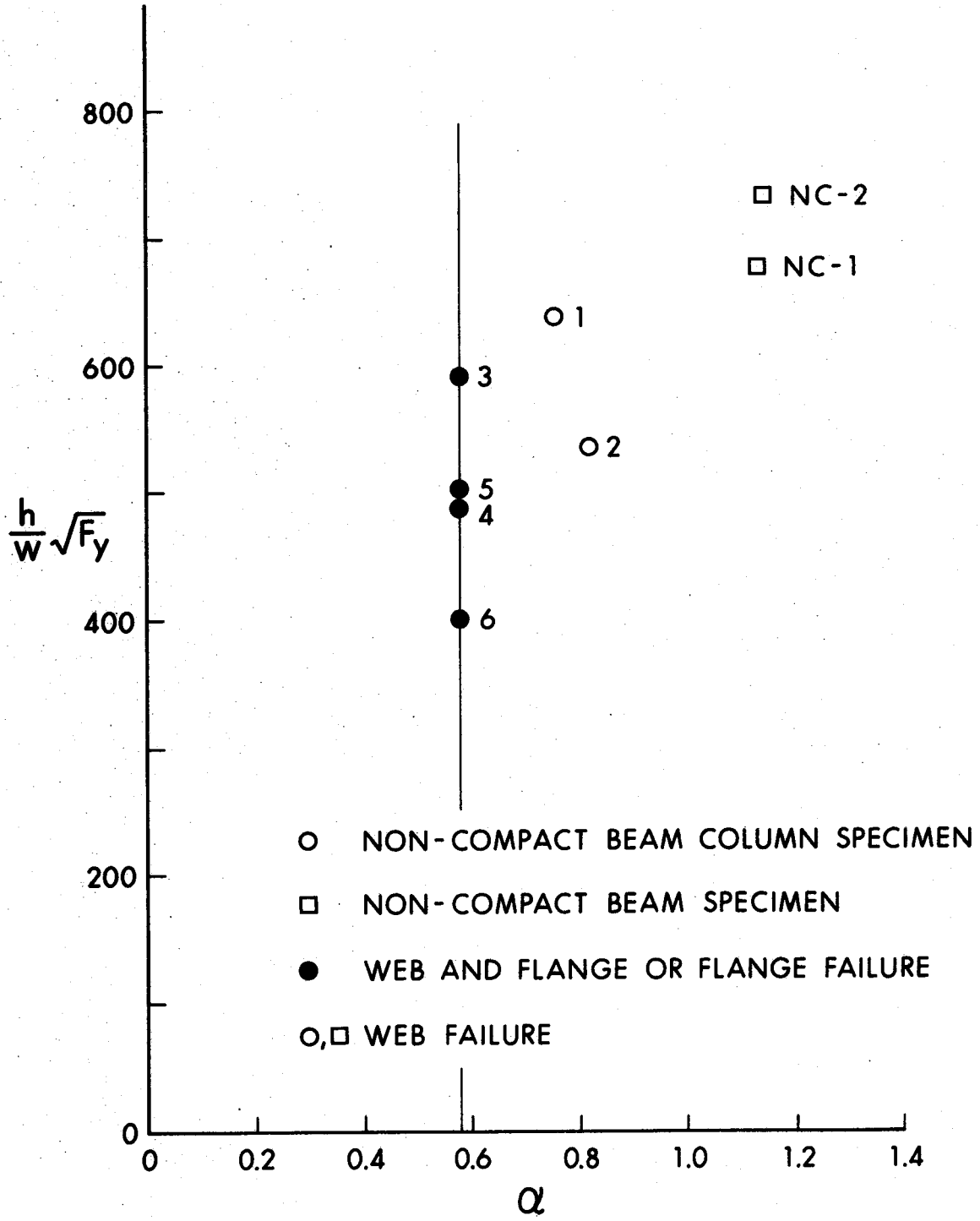

FIGURE 5.11

ALPHA AS A FUNCTION OF $\frac{h}{w}\sqrt{Fy}$

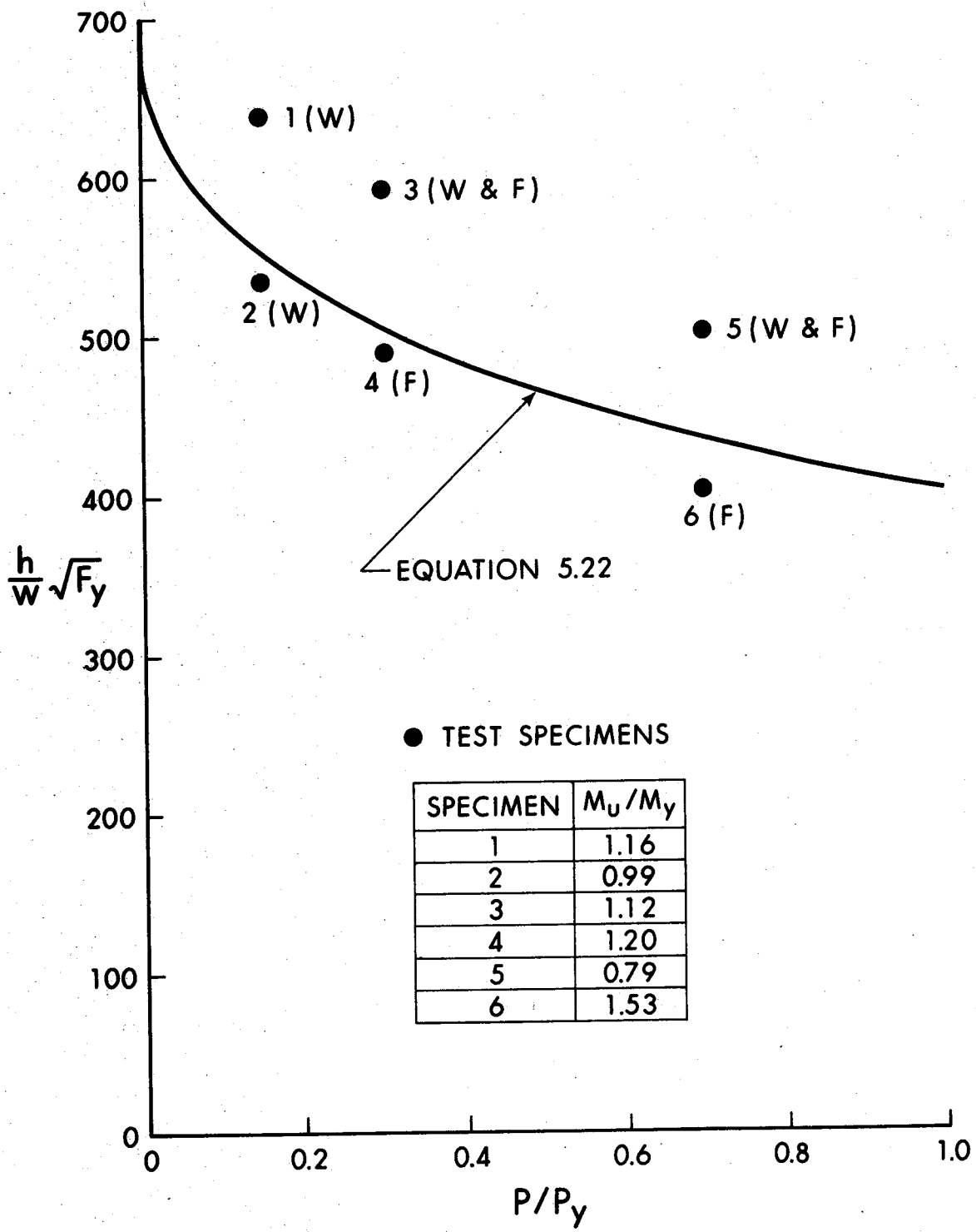

SPECIMEN	M_u/M_y
1	1.16
2	0.99
3	1.12
4	1.20
5	0.79
6	1.53

FIGURE 5.12

TEST SPECIMENS AND

THE NON-COMPACT WEB SLENDERNESS LIMITATION

CHAPTER VI

SUMMARY, CONCLUSIONS, AND RECOMMENDATIONS

6.1 Summary

In order to determine whether or not the web slenderness limits for non-compact beam-columns could be revised upwards, a total of six specimens were tested. All of the specimens had flanges proportioned such that the CSA Standard S16-1969 specification for non-compact flanges was just satisfied, and had webs that were more slender than permitted by the current S16.1 and S16.2 standards. Two tests were conducted at each of three P/Py ratios, to encompass a wide range of beam-column design.

The deflections, rotations, loads, and strain gauge readings were all taken by a minicomputer serving as a data acquisition device. These data were then used to evaluate the specimen behaviour, including the determination of which plate element of the specimens buckled first, causing specimen failure.

The specimens failed by web buckling, flange buckling, or a combination of both. Failure itself is caused by the first plate to deflect significantly with resultant unloading of the member.

In two of the three test series at the different P/Py ratios, the more slender specimen of the two failed at

a lower Mu/My ratio than did the stockier section. However, for the specimens tested at P/Py = 0.15, the more slender specimen failed at a higher Mu/My ratio than the stockier section. This discrepancy has not been resolved.

The two web buckling theories previously presented for compact beam-columns[5] were re-developed, using the results of the present investigation. The theories, allowing for the differences between compact and non-compact members, adequately describe both types of beam-column behaviour. Furthermore, some of the conclusions previously postulated for compact members were extended to non-compact members.

A generalized web buckling theory has been developed which makes it possible to determine any beam-column web slenderness limit, provided the maximum web slenderness is known for a beam with the same flange proportions.

6.2 Conclusions

The main conclusion that this investigation has brought forward is that the web slenderness of non-compact beam-columns may be relaxed significantly. Hence, non-compact members will be used more efficiently in the future.

An important theoretical conclusion relates to the earlier work of Perlynn and Kulak in which it was noted that, for compact beam-columns, if α, the plate buckling modulus, is greater than 0.58, web buckling will invariably occur before flange buckling or simultaneous web and flange buckling. This investigation has shown that this conclusion is also valid for non-compact members. Extending this conclusion, if a specimen has not failed by local buckling when the strain (including the residual strain) at any point in the web has reached the yield strain, it appears that it will not fail by web buckling. This is equivalent to defining α_o as the value of α at the first occurrence of yielding.

Another conclusion of interest is the apparent lack of effect the specimen's proportions have on the revised plate buckling coefficient, K'. Six separate studies, four of which were considered by Perlynn and Kulak, and the other two in this investigation, all indicated that specimens failing by web buckling plotted erratically above a smooth curve formed by joining the points plotted for the specimens failing by simultaneous web and flange buckling or flange buckling. This smooth curve is another representation of the straight line corresponding to $\alpha = 0.58$ in Figure 5.11.

6.3 Recommendations

Since it has been determined that the web slenderness limits of non-compact beam-columns may be increased, it remains to present the theoretical result, (Equation 5.22), such that it may be easily used for design purposes. This equation is repeated here:

$$\frac{h}{w}\sqrt{Fy} = 690\,[1 - 0.425\,(P/Py)^{0.385}] \qquad (6.1)$$

As previously noted, it is considered that this curve is slightly unconservative in the region of specimen 2. This will be taken into account in proposing a limitation suitable for design use.

To maintain continuity between this investigation and the previous design approximations, a bi-linear design approximation will be proposed. This approximation is:

For $0 \leq P/Py \leq 0.15$,

$$\frac{h}{w}\sqrt{Fy} = 690\,[1 - 1.69\,(P/Py)] \qquad (6.2)$$

For $0.15 \leq P/Py \leq 1.0$,

$$\frac{h}{w}\sqrt{Fy} = 535\,[1 - 0.28\,(P/Py)] \qquad (6.3)$$

It is hoped that equations of this kind, based on this investigation, will be incorporated into future building standards. These equations, along with the theoretical limit, (Equation 6.1), and the present web slenderness limitations for non-compact beam-columns are shown in Figure 6.1.

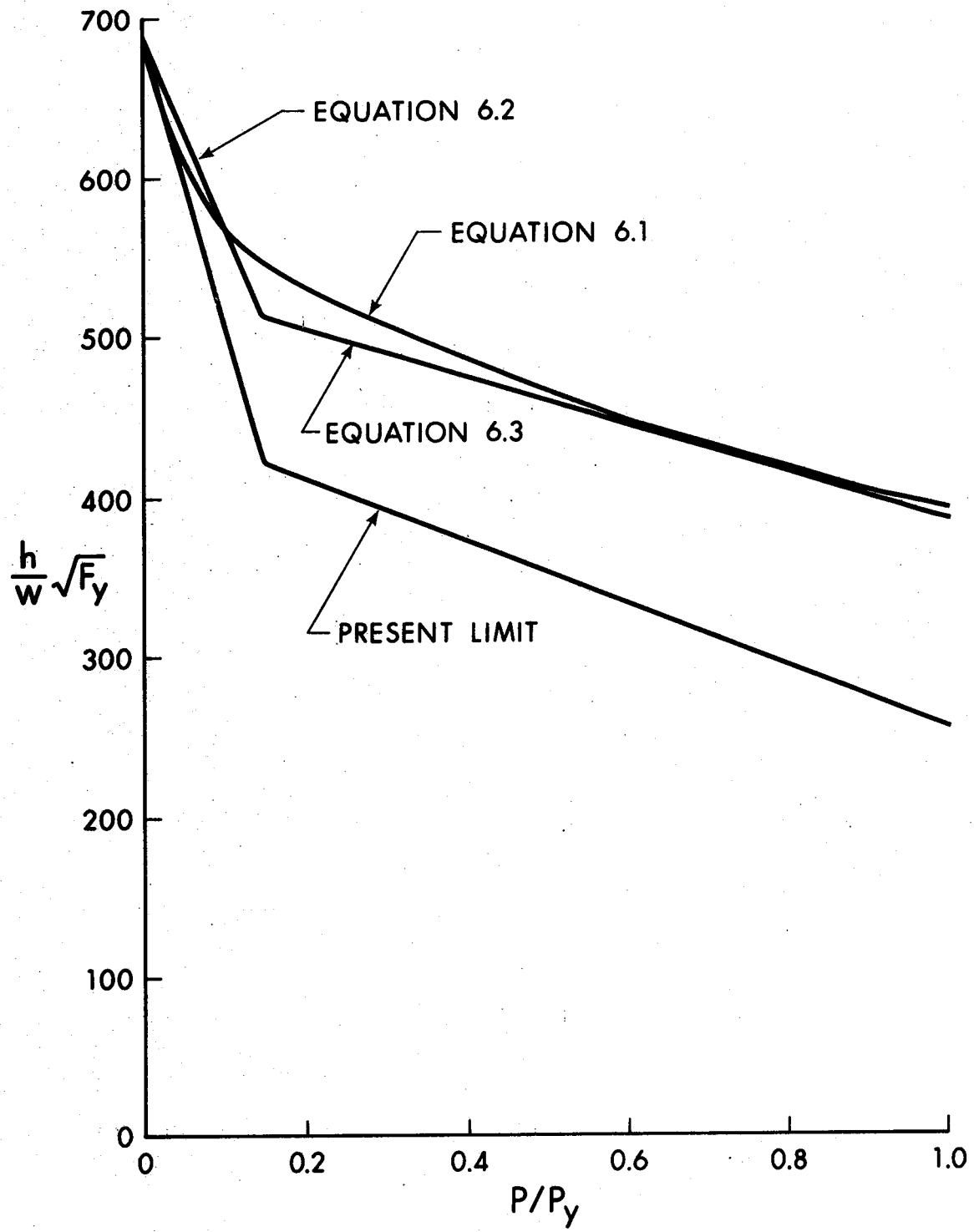

FIGURE 6.1

THE BI-LINEAR DESIGN APPROXIMATION

NOMENCLATURE

A = constant

A = total specimen area

Aw = specimen web area

b = width of flange

B = constant

C = constant

C = maximum beam web slenderness for a given flange slenderness

D = constant

D = $EI/(1 - \nu^2)$ for idealized plate buckling model

Dx = $Ex/(1 - \nu_x\nu_y)$

Dy = $Ey/(1 - \nu_x\nu_y)$

Dxy = $\nu_y Dx$

Dyx = $\nu_x Dy$

e = eccentricity of eccentric load (P_2)

E = Young's Modulus = 30000 ksi for Perlynn and Kulak[5]

E = Young's Modulus = 29600 ksi for present investigation

Ex = Young's Modulus in x-direction

Ey = Young's Modulus in y-direction

Fy = 44.33 ksi = yield stress of web material

Gt = tangent shear modulus

h = width of plate in plate buckling model

h = height of web

h_t = total height of specimen = 2t + h

H = (Dx + Dy + 4Gt)/2

I = moment of inertia

K = Timoshenko's[2] plate buckling coefficient

K = Haaijer and Thurlimann's[8] plate buckling coefficient for a fully-plastified wide-flange section

K' = modified plate buckling coefficient taken from beam-column tests

l = length of plate in plate buckling model

M = moment per unit length required for a unit rotation for plate buckling model

M = applied moment = P_2 X e

Mpc = plastic moment (reduced for axial load)

My = yield moment (reduced for axial load)

Mu = ultimate moment held by specimen

n = $2(\alpha p - \alpha o)/(\alpha p(\alpha p^2 - 1))$

P = applied axial load = $P_1 + P_2$

P_1 = concentric load applied by testing machine

P_2 = eccentric load applied by eccentric load jack

Py = Fy X A = specimen yield load

t = thickness of flange

u = plate mid-point deflection in plate buckling model

w = thickness of plate in plate buckling model

w = thickness of specimen webs

x = constant

x = Cartesian coordinate

y = Cartesian coordinate

y = distance to neutral axis from compression side of web

yo = distance to neutral axis of fully-plastified

wide-flange section from compression edge of web

α = plate buckling modulus

α_o = 0.58 = alpha at the first occurrence of yielding

α_o = alpha at the point of strain-hardening

$\alpha_p = \sqrt{\sigma_y/\sigma_p}$ = alpha at the proportional limit

β = B/A = Mh/2DyI = coefficient of restraint against rotation

δ = maximum initial web deflection

Δ = maximum strong-axis deflection of specimen at Mu

ε_{cr} = maximum strain in web when the ultimate moment is reached

ε_m = maximum compressive strain in web

ε_m = maximum compressive strain in flange

ε_{st} = strain at the beginning of the strain-hardening range as known on a stress-strain diagram

ε_y = yield strain of web plate material

σ_{cr} = maximum stress in web when ultimate moment is reached (not greater than σ_y)

$\sigma_p = \sigma_y - \sigma_r$ = stress at proportional limit

σ_r = 15 ksi = maximum compressive residual stress in web

σ_x = uniform compressive stress applied to edge of plate elastically restrained against rotation along the unloaded edges

σ_y = 44.33 ksi = Fy

ν = 0.3 = Poisson's ratio for steel

ν_x = Poisson's ratio in the x-direction

ν_y = Poisson's ratio in the y-direction

REFERENCES

1. "CSA S16-1969 Steel Structures for Buildings", Canadian Standards Association, Rexdale, Ontario, 1969.

2. Timoshenko, S., and Gere, J., "Theory of Elastic Stability", Second Edition, McGraw-Hill Book Co. Inc., New York, N. Y., 1961.

3. "Specification for the Design, Fabrication and Erection of Structural Steel for Buildings", American Institute of Steel Construction, New York, N. Y., 1969.

4. Haaijer, G., "Plate Buckling in the Strain-Hardening Range", Journal of the Engineering Mechanics Division, ASCE, Volume 83, No. EM2, April 1957.

5. Perlynn, M. J., and Kulak, G. L., "Web Slenderness Limits for Compact Beam-Columns", Structural Engineering Report No. 50, Department of Civil Engineering, University of Alberta, September 1974.

6. "CSA S16.1-1975 Steel Structures for Buildings - Limit States Design", Canadian Standards Association, Rexdale, Ontario, 1975.

7. "CSA S16.2-1975 Steel Structures for Buildings - Working Stress Design", Canadian Standards Association, Rexdale, Ontario, 1975.

8. Haaijer, G., and Thurlimann, B., "On Inelastic Buckling in Steel", Proceedings, ASCE, Volume 84, No. EM2, April 1958.

9. Holtz, N. M., and Kulak, G. L., "Web Slenderness Limits for Non-Compact Beams", Structural Engineering Report No. 51, Department of Civil Engineering, University of Alberta, August 1975.

10. "CSA G40.21-1973 Structural Quality Steels", Canadian Standards Association, Rexdale, Ontario, 1973.

11. American Society for Testing and Materials, "Standard Specification for Structural Steel-Designation A36-67", Philadelphia, Pa., 1967.

12. Yarimci, E., Yura, J. A., and Lu, L. W., "Techniques for Testing Structures Permitted to Sway", Fritz Engineering Lab Report No. 273.40, Lehigh University, Bethlehem Pa., 1966.

13. American Society for Testing and Materials, "Test Methods for Compression Members", ASTM Special Technical Publication No. 419, August 1967.

14. "CSA W59.1-1970 General Specification for Welding of Steel Structures (Metal-Arc Welding)", Canadian Standards Association, Rexdale, Ontario, 1969.

15. Nadai, A., "Theory of Flow and Fracture of Solids", McGraw-Hill Book Co., Inc., New York, N. Y., 1950.

16. Handelman, G. H., and Prager, W., "Plastic Buckling of a Rectangular Plate Under Edge Thrusts", National Advisory Committee for Aeronautics, Technical Note No. 1530, August, 1948.

17. Bleich, F., "Buckling Strength of Metal Structures", McGraw-Hill Book Co., Inc., New York, N. Y., 1952.

18. Lundquist, E. E., and Stowell, E. Z., "Critical Compressive Stress for Flat Rectangular Plates Supported along all Edges and Elastically Restrained against Rotation along the Unloaded Edges", National Advisory Committee for Aeronautics, Technical Report No. 733, 1942.

19. Lukey, A. F., and Adams, P. F., "Rotation Capacity of Wide-flange Beams under Moment Gradient", Structural Engineering Report No. 1, Department of Civil Engineering, University of Alberta, May 1967.

20. McGuire, W., "Steel Structures", Prentice-Hall Inc., Englewood Cliffs, N. J., 1968.

21. Brockenbrough, R. L., and Johnston B. G., "United States Steel Design Manual", United States Steel Corporation, ADUSS 27-3400-02, November 1968.

APPENDIX I

DESIGN OF THE TEST SPECIMENS

It was decided, that because of the availability of test results for compact beam-columns[5], and test results for non-compact beams[9], testing two specimens at each of three different P/Py ratios would be sufficient to closely determine the maximum web slenderness limits for non-compact beam-columns.

The test results for the non-compact beams provided a means for estimating the maximum web slenderness ratio. This was done by determining the value of α from Perlynn and Kulak's[5] Equation 5.16 corresponding to the non-compact beam results. This equation is:

$$\alpha = \frac{h}{100w}\sqrt{Fy}\sqrt{\frac{0.01241}{1 - 0.695(P/Py)^{0.3846}}} \qquad (A1.1)$$

For P/Py = 0, Equation A1.1 becomes:

$$\alpha = 0.001114\ \frac{h}{w}\sqrt{Fy} \qquad (A1.2)$$

Substituting Holtz and Kulak's test result for non-compact beams of $\frac{h}{w}\sqrt{Fy} = 690$ in Equation A1.2 yields

α = 0.77. This is the same value recommended by Haaijer and Thurlimann[8] to guarantee that web buckling will not occur for plates uniformly compressed up to the yield stress.

Having this value gives a reasonable indication of where the limit of web buckling might be. However, it was expected that the value of α would be somewhat higher than this for the case of non-compact beam-columns because of the effects of residual stresses, and the fact that not all the web is subjected to the yield stress. Somewhat arbitrarily, a value of $\frac{h}{w}\sqrt{Fy}$ = 750 was chosen for P/Py = 0 to obtain a second value of α. Using the same procedure as before results in α = 0.84.

By back-substituting the value of α in Equation A1.1, a unique relationship can be obtained for web slenderness as a function of P/Py. Figure A1.1 shows the two boundaries which are obtained by this procedure.

It was considered that it would be useful to incorporate the compact beam-column test results into the specimen design, if possible[5]. An inspection of those test specimens indicated that specimen BC-9 failed at M/Mpc = 0.9, or at about the yield moment. While the flanges of their specimens were compact, and so the test result could not be used directly for this investigation, this specimen was still of some interest because it failed by web buckling, and its slenderness was only slightly below that

of the curve corresponding to α = 0.77 at P/Py = 0.8. Hence it was decided to design three of the specimens to be below the curve α = 0.77 by the same amount as specimen BC-9 was at P/Py = 0.8. Similarly, the other three specimens were designed to be this amount above the curve corresponding to α = 0.84. Ratios of P/Py of 0.15, 0.30, and 0.70 were used to obtain results useful for a large range of beam-column design. The location of these test specimens is also shown in Figure A1.1.

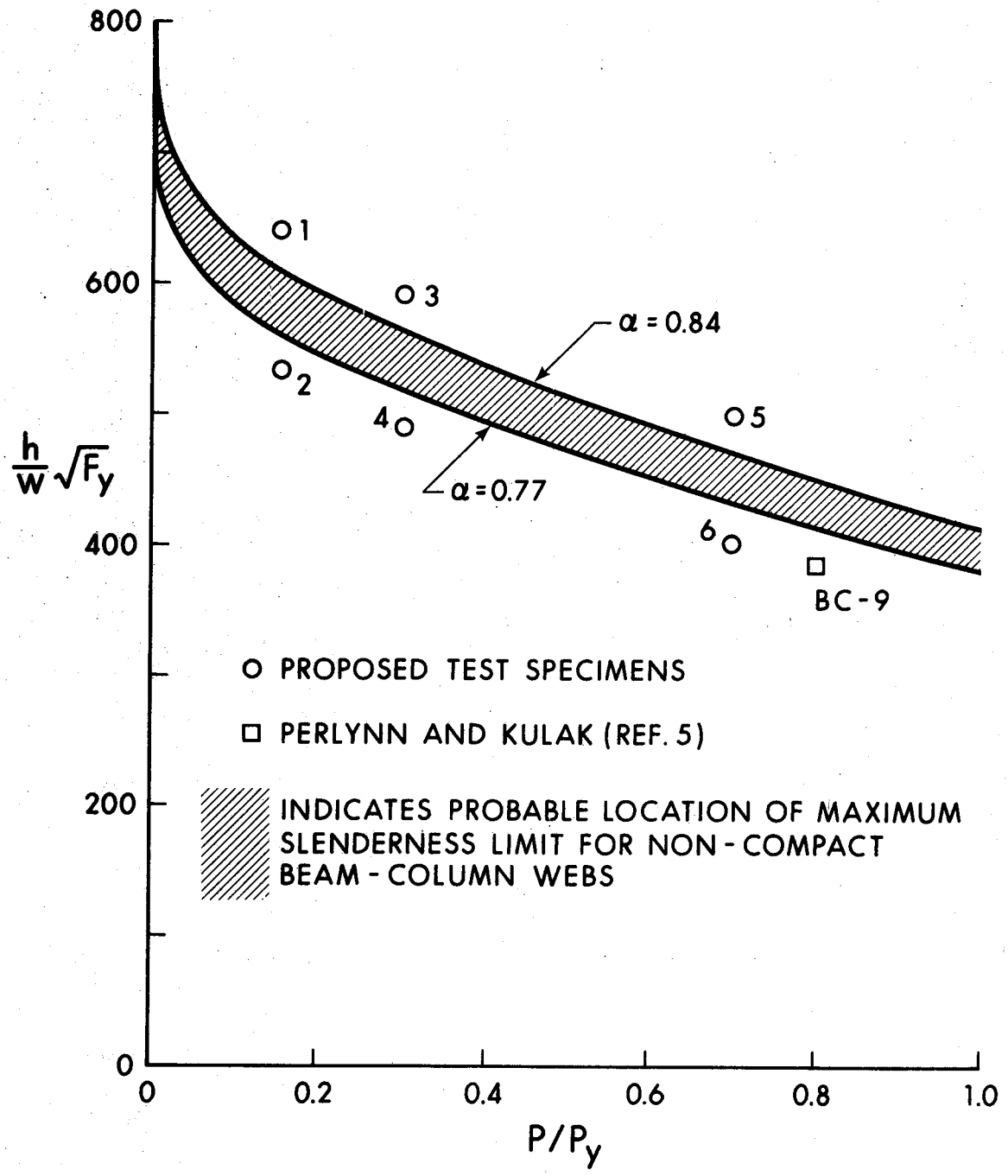

FIGURE A1.1

LOCATION OF THE TEST SPECIMENS

APPENDIX II

THE DEFLECTION MEASURING APPARATUS

A2.1 Introduction

This device made it possible to record many deflection readings over a short period of time and store them for later processing. As a result, it was possible to plot accurate deflections of the web and the compression flange for a number of load increments. This in turn made the process of determining which plate element buckled first easier to do, and minimized the possibility of data misinterpretation.

A2.2 The Trolley

The apparatus itself was moved up and down by a motorized trolley (Figure 3.6). The trolley travelled about one inch per second, and was designed to follow the edge of the specimen's tension flange in such a way that the tension flange could be considered as datum for the positions of the grid points of the web. Because the tension flange was used as datum, this also provided a means for measuring compression flange deflections. The trolley was moved by a motor powering a drive gear along a gear rack which was fastened to the ends of the tension flange by two special clamps.

In order to record the vertical position of the trolley, it was fitted with a ten-turn potentiometer which was attached to one of the wheels running along the edge of the flange (Figure 3.6). The voltage across the potentiometer changed as the trolley moved, and the resulting analog signal was used by the minicomputer to sense where the trolley was, and, hence, when it was correctly positioned to take a reading. The trolley was also equipped with microswitches at both ends which touched spring loaded bumpers mounted on the tension flange clamps and prevented the apparatus from running off the ends of the specimen.

The trolley carried the side-rack on which the deflection measuring apparatus was mounted. After one vertical set of readings, the apparatus was moved over to the next position manually and the next vertical string of readings taken. After measurement of the web was completed, the apparatus was turned 90° on a bracket mounted on the side rack and the compression flange readings were taken (Figure 3.7).

A2.3 The Apparatus

The apparatus itself operates on an optical feedback system. A light powered by a well-filtered power supply is housed along with a photocell in a container at

the end of a flexible tube containing many strands of fiber optics. The light is positioned such that about 85% of the strands are able to transmit the light. The other 15% of the strands are used for the photocell.

The principle of operation is to shine a light via the fiber optics onto the surface being measured. Depending upon the reflectivity of the surface and on the angle between the probe and the surface, some light is reflected back up the tube in the 15% of the fiber optics connected to the photocell. The output of the photocell varies as the amount of light which strikes it varies. This output is amplified and modified by an electronic circuit to control the motor of the apparatus. The motor operates so as to correct for the reading of the photocell in such a way that an initial predetermined analog signal is maintained (Figure A2.1). This predetermined reading takes the form of deciding on a suitable distance for the probe to run above the surface it is measuring before any readings are taken. The correction is automatically made by means of a motor moving the probe either closer or farther away from the surface being measured. Hence the probe keeps the same distance between it and the surface it is monitoring.

The portion of the flexible tubing doing the actual movement over the deflected surface is housed in a small pipe to make it rigid. The shaft of the motor is connected so as to both move the probe and turn a

potentiometer over which a regulated voltage is maintained. This potentiometer acts as a voltage divider and the resulting change in voltage from it was used to determine the deflections.

The initial probe height, and hence the initial photocell reading, was adjusted beforehand, along with the damping of the probe and its sensitivity. Because flat white paint proved to be ideal for making these adjustments, and for reflecting a reasonable but not excessive amount of light, the specimens were painted on the side the measurements were taken before the tests were performed. All readings were read into storage by the minicomputer for later processing.

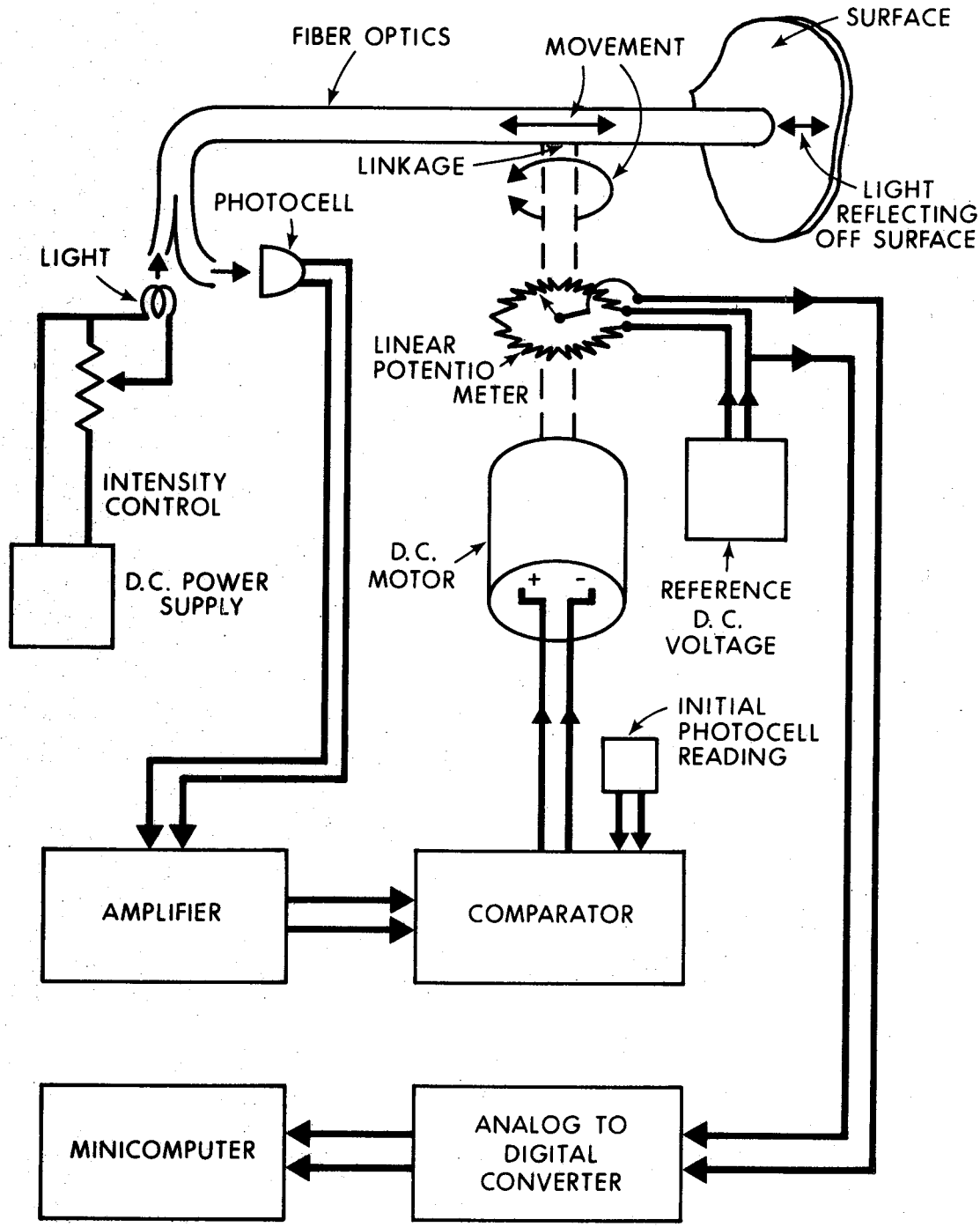

FIGURE A2.1

BLOCK DIAGRAM OF DEFLECTION MEASURING DEVICE